Electrospinning of in situ synthesized silica-based and calcium phosphate bioceramics for applications in bone tissue engineering: A review

Léa Dejob, Bérangère Toury, Solene Tadier, Laurent Gremillard, Claire Gaillard, Vincent Salles

Version of Record: https://www.sciencedirect.com/science/article/pii/S1742706120307467
Manuscript_5b278698f108ba7c2d94879475644c41

Title: **Electrospinning of in situ synthesized silica-based and calcium phosphate bioceramics for applications in bone tissue engineering: a review**

Type of article: **Review**

Léa Dejob[a,b], Bérangère Toury[a], Solène Tadier[b], Laurent Grémillard[b], Claire Gaillard[b], Vincent Salles[a,*]

[a] Laboratoire des Multimatériaux et Interfaces, UMR CNRS 5615, Univ Lyon, Université Claude Bernard Lyon 1, F-69622 Villeurbanne, France.

[b] Univ Lyon, INSA-Lyon, CNRS, MATEIS UMR 5510, F-69621, Villeurbanne, France.

[*] Corresponding author:

Vincent Salles
Laboratoire des Multimatériaux et Interfaces
Bâtiment Chevreul (2e étage)
6 rue Victor Grignard
69622 Villeurbanne Cedex
Tel: +33 4 72 43 16 08
vincent.salles@univ-lyon1.fr

ELECTROSPINNING OF *IN SITU* SYNTHESISED SILICA-BASED AND CALCIUM PHOSPHATE BIOCERAMICS FOR APPLICATIONS IN BONE TISSUE ENGINEERING: A REVIEW

ABSTRACT

The field of bone tissue engineering (BTE) focuses on the repair of bone defects that are too large to be restored by the natural healing process. To that purpose, synthetic materials mimicking the natural bone extracellular matrix (ECM) are widely studied and many combinations of compositions and architectures are possible. In particular, the electrospinning process can reproduce the fibrillar structure of bone ECM by stretching a viscoelastic solution under an electrical field. With this method, nano/micrometer-sized fibres can be produced, with an adjustable chemical composition. Therefore, by shaping bioactive ceramics such as silica, bioactive glasses and calcium phosphates through electrospinning, promising properties for their use in BTE can be obtained. This review focuses on the *in situ* synthesis and simultaneous electrospinning of bioceramic-based fibres while the reasons for using each material are correlated with its bioactivity. Theoretical and practical considerations for the synthesis and electrospinning of these materials are developed. Finally, investigations into the *in vitro* and *in vivo* bioactivity of different systems using such inorganic fibres are exposed.

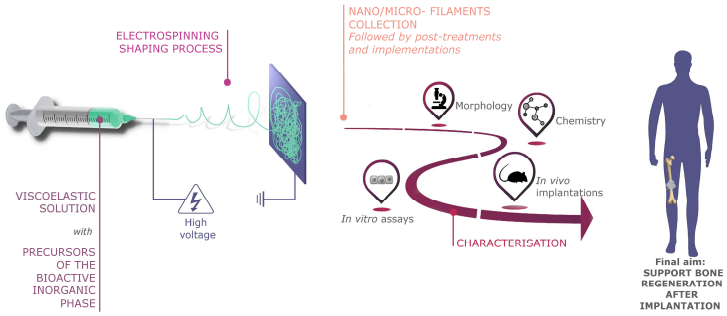

Graphical abstract

KEYWORDS

In situ electrospinning; sol-gel synthesis; bioactive glass; calcium phosphate; bone tissue engineering

INTRODUCTION

Different events can deteriorate bone tissue such as bone loss and bone fractures, which can result from injuries via traumatisms, infections and diseases like osteoporosis. Even though the bone is able to heal itself through a combination of biological mechanisms, this healing process can be insufficient when the bone defect is too large. While bone grafts can be clinically implanted to resolve this issue, there are different drawbacks associated with their use as they imply donor site morbidity for autologous grafts, but also infections or a shortage in allograft materials [1].

For these reasons, researches have started to explore a new route using synthetic materials in order to meet all the ideal bone grafts features: high osteoinductive and angiogenic potentials, biological safety, low patient morbidity, no size restrictions, ready access to surgeons, long shelf life, reasonable cost and good reproducibility [1]. Many different materials have been investigated to create such synthetic implants for the purpose of so called “Bone Tissue Engineering” (BTE). They are either polymeric, inorganic or a combination of both. Loading with cells, proteins or drugs was also reported [2]. Besides its

composition, the morphology of the material can be controlled via shaping procedures, including lithographic methods [3], 3D bioprinting [4] or electrospinning for example. Electrospinning is widely used indeed and the reasons for its usefulness can be explained by the natural bone structure.

Bone is a specialised form of connective tissue composed of both an inorganic and an organic matrix, the latter consisting largely of collagen with some hyaluronic acid and chondroitin sulfate [5]. Fibrillar collagen serves as a mechanical framework in the bone extracellular matrix. Nevertheless, the use of natural collagen to create biomaterials is limited. First of all, the incomplete removal of antigens during decellularisation can induce severe inflammation and rejection of the implant. Also, the extraction procedure and conditions of usage (for instance temperature and solvents) can lead to collagen protein denaturation as well as architecture degradation [6,7]. In this context, electrospinning reveals itself as a promising method of reproducing the fibrous morphology of the collagen network, whose natural fibril diameter is of around 500 nm and assembles into fibres of around 5 µm [8]. As a result, electrospinning can provide cells with a structure similar to the organic part of bone. Also, porosity created between fibres can help deliver nutrients to bone cells. This role is especially fulfilled by blood vessels and canaliculi in healthy bones [9].

Electrospinning is a powerful approach for obtaining nano- and micro- metric sized fibres. In this method, sketched in *Figure 1*, a polymeric solution with appropriate viscoelastic properties is extruded through a syringe needle. An electric field between the solution and the fibre collector is created by applying a high voltage to the needle and an oppositely charged one to the collector. Alternatively, the latter can also be grounded. Under this electric field, the solution is charged with either positive or negative charges. As these charges have the same polarity, they repel each other, resulting in stretching the solution in the form of a filament. This filament is attracted by the collector due to the potential difference. During its flight to the collector, the filament dries and experiences instabilities resulting in fibre jet deviation. As a result, mats with random fibre orientation are collected on the collector. So as to prevent the jet from breaking up and maintain the continuity of the electrospun filament [10], the solutions are loaded with polymers with long macromolecular chains that can entangle together. It should be noted that this process is also compatible with the stretching of melted polymers [11].

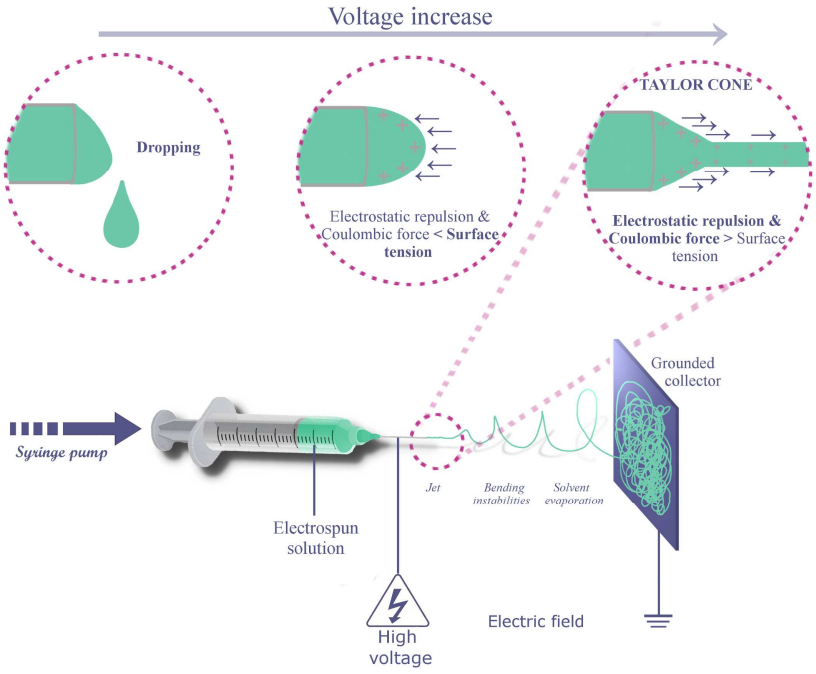

Figure 1. Electrospinning setup and influence of the electric field strength

As previously mentioned, inorganic species also enter the composition of bone. This mineral matrix is mostly made up of calcium phosphate crystals in the form of hydroxyapatite orientated along the collagen molecules of the bone organic matrix [12]. It is noteworthy that the calcium concentration

reaches 34.8 wt.% of the bone and that the one of phosphorus reaches 15.2 wt.%. Carbonates are also found in the bone (7.4 wt.%) as well as trace quantities of sodium, magnesium, potassium, fluoride and chloride salts [13]. While many researches focus on the synthesis of calcium phosphate materials in the field of bone or dental applications [14,15], other types of ceramics have been suggested and include well-known bioactive glasses [16]. These materials and their mechanisms of bioactivity will be further described in the review. The most commonly reported strategy for electrospinning these ceramics implies the dispersion of pre-synthesised nanoparticles into a polymeric solution that is simultaneously electrospun. Besides well-known calcium phosphates and bioactive glasses, other ceramics have been similarly electrospun using a dispersion of nanoparticles: including not only $CaCO_3$ [17–19], Si-doped $CaCO_3$ [20–26] but also Mg-based ceramics such as forsterite Mg_2SiO_4 [27–29], magnesium oxide MgO [30] and amorphous magnesium phosphate [31]. Finally, clays - laponite [32], montmorillonite [33], halloysite [34] - were also marginally investigated for their potential applications in bone tissue engineering.
Nevertheless, all of these mats were prepared by blending either a commercially or upstream prepared powder of ceramic into a polymer solution before electrospinning. In this review, the choice was made to focus on the *in situ* reactions of the ceramic phase within the electrospun solution. It is important to specify to what the term "*in situ*" refers. In the systems described throughout this review, sol-gel reactions start from the solution preparation and they continue all through the whole process: from the mixing of the precursors in the solution prior to syringe loading, during the electrospinning itself and they can also go on with subsequent thermal treatments. The term "*in situ*" thus encompasses the filaments fabrication process in its entirety. When the ceramic material is synthesised that way, better spatial distribution, stronger interactions between the organic and the inorganic phases and consequently superior mechanical and biological properties are expected, as will be discussed in section I.1.1.1. Besides well-known bioactive glasses and calcium phosphates, silica, which presents bioactivity as well as a high stiffness [35], is the only electrospun material intended to be used for bone applications obtained from an *in situ* reaction.

This review gives an insight into the *in situ* synthesis and electrospinning of bioactive ceramics materials whose intended application is related to bone tissue engineering. This review is organised in two chapters: the first one focuses on silicon-based materials and separately discusses their synthesis, their electrospinning and reported bone tissue engineering applications in the literature. Shaping considerations of such fibres and effects of processing parameters on the fibrous morphology were reviewed by Nagrath *et al.* [36]. Even though these aspects are mentioned in this article because they are inextricably linked to the features of the final fibres, they are less detailed. Here, importance is given to the chemistry of the sol-gel synthesis. Also, choices about system composition and shaping of the materials are justified as far as possible by results from biological studies. The second chapter is dedicated to calcium phosphate materials.

I. SILICON-BASED ELECTROSPUN FIBRES

I.1. SYNTHESIS OF Si-BASED SOLS ENTERING THE COMPOSITION OF ELECTROSPUN SOLUTIONS

Sol-gel synthesis is the method selected to create silicon-based materials via *in situ* reaction and subsequent electrospinning. Sol-gel synthesis is a chemical process in which an alkoxide solution is slowly hydrolysed and condensed to form a sol that is a colloidal suspension. Colloidal particles grow and create discrete particles or interconnected networks of polymeric chains in which solvent molecules are trapped; this system is defined as a gel. This method is highly adaptable and allows for the possibility of tailoring the final material properties and morphology by adjusting the solution composition and process parameters. Information that is detailed in the next paragraphs about the method for preparing spinnable solutions is gathered and summarised in *Figure 2*. This section I.1 specifically deals with the "Inorganic Si-based network" orange block in the figure.

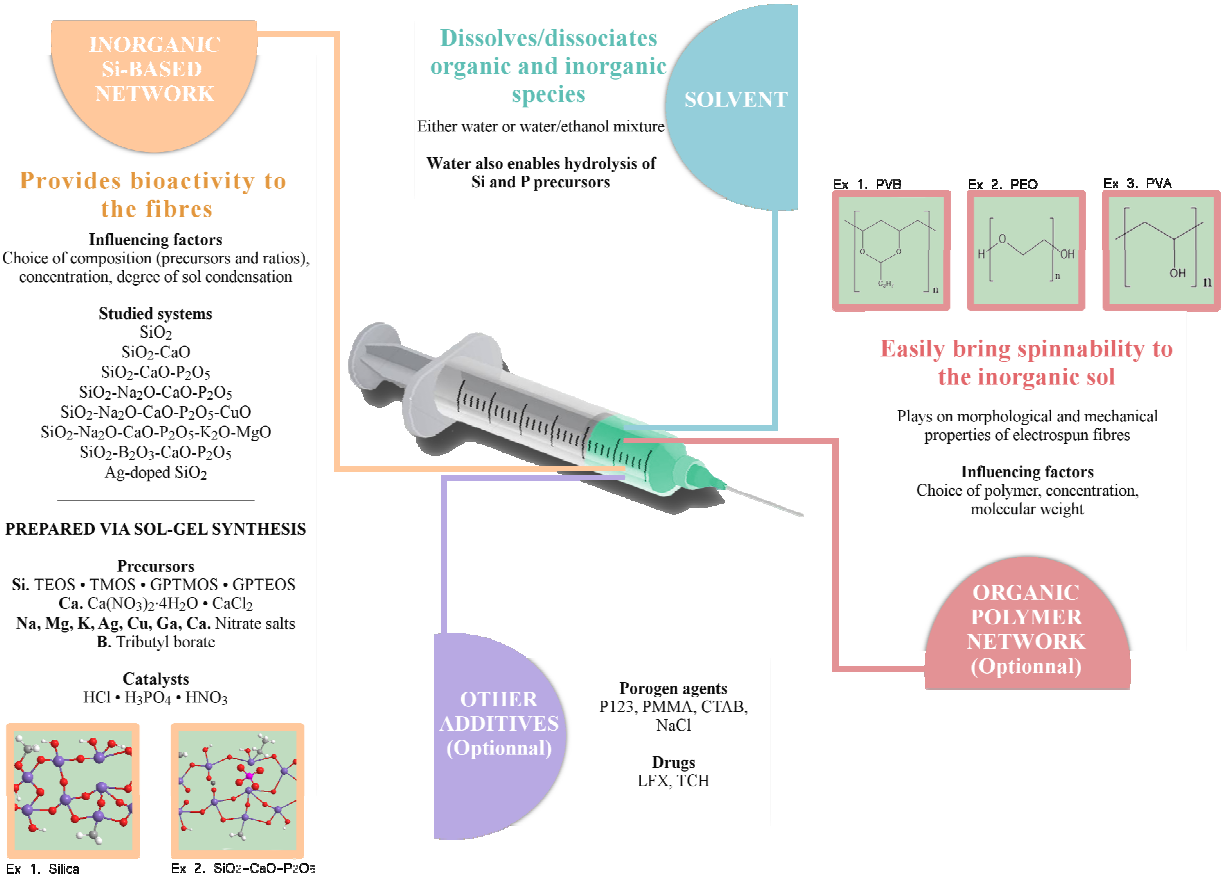

Figure 2. Considerations for the preparation of spinnable Si-based bioceramics with adequate bioactive properties

I.1.1. Silica

I.1.1.1. Justified use of silica fibres for Bone Tissue Engineering

Silica is the general term given to minerals composed of both silicon and oxygen. Although silica like silicon dioxide (SiO_2) and silicones (polymeric compounds with a Si-O-Si backbone) is insoluble in water, it can release small but significant amounts of ortho-silicic acid (H_4SiO_4) [37]. This acid is water soluble and as a result biologically available. The exact action mechanisms of silicon in bone health have not been clearly elucidated yet. However, its positive effects on collagen I synthesis, matrix mineralisation and osteoblast differentiation have been reported many times over the last few decades [20,38,39].

The earliest SBF (Simulated Body Fluid)-bioactive silica spun fibres were obtained via a dry spinning process in 2000 [40,41]. In this process, a pushing gas was used to extrude the spinning solution through microscale holes, without using an electric field. As a result, the fibre diameter was quite large (14-82 µm). Six years later, Sakai *et al.* reported on a cellular study on electrospun silica fibres [42] for the first time, to the author's knowledge. Osteoblastic cells elongated along these thin fibres - whose diameters ranged from several hundreds of nanometres to several micrometres - in the early stages of cell culture. Subsequently, they proliferated and filled the space between fibres.

The benefits from an *in situ* synthesis of silica were evaluated by Yaping Ding *et al.* [43], who compared this method with the dispersion of fumed silica nanoparticles into a polymer solution. After electrospinning, sol-gel derived fibres displayed a stiffness two times higher and a tensile strength 32 % greater. This was due to a more uniform distribution of the inorganic phase in the polymeric matrix, as well as higher interfacial adhesion strength between the inorganic and organic phases. On the contrary, blended nanoparticles could agglomerate in the polymer matrix and cause shear stress concentrations weakening the fibres. On a biological point of view, both materials showed good MG-63 cell adhesion and

proliferation, but only sol-gel derived silica-containing fibres promoted ALP (Alkaline Phosphatase) activity after 2 weeks of incubation [43]. ALP is an enzyme and biochemical marker of bone formation. As reported by the authors, this improved bioactivity could be due to the enhanced stiffness obtained by the sol-gel based approach, but also to the easier release of silicon ions during sol-gel phase degradation compared with the more stable fumed silica nanoparticles. About those analyses, it is important to note that MG-63 are human osteoblast-like cells that have been used as an *in vitro* standard model to study bone-implant interactions and biocompatibility (adhesion and proliferation of cells). They present the advantage of a rapid and endless proliferation, and they retain a differentiated phenotype under culturing conditions. Nonetheless, these are osteosarcoma-derived cells and in some experimental conditions, they behave differently than primary cells in response to biomaterials. A first investigation of material's biocompatibility with MG-63 should therefore be further confirmed with primary and target cells. Also, it is noteworthy that performing alkaline phosphatase testing on MG-63 as reported in the last cited study [43] and many others in the literature is controversial, because these cells already possess an osteoblastic phenotype.

I.1.1.2. Sol-gel synthesis of silica

All studies reporting the *in situ* synthesis of silica networks involve a sol-gel technique in which an organosilane is hydrolysed and condensed. During the hydrolysis process, Si-OR groups react to form Si-OH and the latter condense together into Si-O-Si groups during condensation step. In most cases, TEOS (tetraethyl orthosilicate) or TMOS (tetramethoxysilane) are employed. But other silica precursors are marginally used, such as 3-glycidyloxypropyltriethoxysilane (GPTEOS) [44] and 3-Glycidyloxypropyltrimethoxysilane (GPTMOS, also GPTMS) [45] for their ability to bond both organic and inorganic components through their organic and inorganic functionalities, leading to hybrid materials. Addition of GPTEOS to TEOS was also reported, by Toskas *et al.,* to increase sol-gel solution stability upon gelation [44].

Acid- and base-catalysis are efficient at accelerating the hydrolysis and condensation of sol-gel derived silica. Under acidic conditions, silica tends to form linear molecules, while highly branched clusters of silica behaving as discrete species are obtained under basic conditions [46]. All of the sol-gel *in situ* syntheses of electrospun silica for BTE are acid-catalysed, either with HCl [35,42,47–49], H_3PO_4 [50] or HNO_3 [44]. *Figure 3* displays reaction mechanisms of acid-catalysed hydrolysis and condensation of organosilanes. It is suggested that an acid catalysis is preferred over a basic one, as the latter induces the formation of spherical particles that can grow, agglomerate and precipitate, thus creating uneven distribution within the fibres [51]. This irregular distribution can lead to shear stress concentrations weakening the fibres, and we can also imagine that the fibrous structure of the material wouldn't be kept after polymer calcination if the silica phase is not continuous.

Silicon-containing materials can also refer to compositions where the silicon oxide network is modified by the incorporation of metallic cations. When they possess bioactive properties, these materials are referred to as "bioactive glasses". In the research area combining *in situ* reaction and electrospinning for BTE field, they have been studied more closely than pure silica fibres.

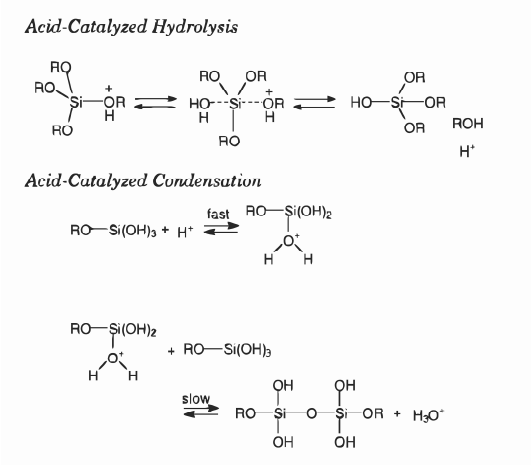

Figure 3. Reaction mechanisms of acid-catalysed hydrolysis and condensation of organosilanes. Reproduced from [46]

I.1.2. Silicon-containing bioactive glasses

In 2016, Xiu-Rui Zhang *et al*. demonstrated that the delivery of soluble ions arising from the dissolution of bioactive glasses was not the only factor influencing the behaviour of rat BMMSC (Bone Marrow Mesenchymal Stem Cells). Their osteogenic differentiation was indeed more pronounced when the cells were cultured directly on the surface of the materials rather than in a transwell chamber. Also, the formation of carbonated hydroxyapatite while soaking a bioactive glass in SBF was found to be faster when the glass displayed a fibrous structure rather than a flat surface [52]. Besides, when rat BMMSC (Bone Marrow Mesenchymal Stem Cells) were cultured on these surfaces for 5 or 10 days, a higher ALP expression was observed on the fibrous morphology [52]. Such research justifies the global strategy of electrospinning bioactive glasses that are prone to dissolution. Therefore, this section I.1.2 gathers significant information to be considered for the preparation of such materials.

I.1.2.1. Introduction – Structure of bioactive glasses and link with their bioactivity

Bioactive glasses and glass-ceramics are interesting materials for bone tissue engineering applications as they enhance osteoblast adhesion and the differentiation of mesenchymal stem cells as well as progenitor cells, and revascularization [53]. While bioactive glasses exhibit an amorphous structure, "glass-ceramics" is a widely-used term in the literature to refer to materials that consist of crystalline phases embedded into an amorphous glassy matrix. Glass-ceramics thus belong to a material class between glasses and polycrystalline ceramics [54]. Both the mechanical and biological properties of the glass-ceramics can be significantly different from those of their parent glass phase [53].

Being amorphous, bioactive glasses do not show any long-range order. However, atoms do possess a short-range arrangement within the glass. Specifically in silicate and phosphosilicate glasses, silicon and phosphorus atoms are surrounded by oxygen atoms, themselves potentially belonging to another silicon or phosphorus tetrahedra. Covalent bonds of ≡Si-O-Si≡ (and sparse ≡P-O-P≡) are formed and these are called bridging oxygen atoms. They are responsible for network connectivity as they link different tetrahedral units together [55]. Therefore, silicon and phosphorus (as well as boron) are called network formers. Also, although it has been proved that P-O-Si bonds may be detected by NMR or using molecular dynamics simulations, phosphorus is mainly present in the form of orthophosphate ions charge-balanced by modifier ions [17,55,56]. For instance, sodium, calcium, magnesium, copper and potassium ions are considered as network modifiers. As orthophosphate units are barely polymerised to the silica network, they are rapidly lost from the glass when exposed to aqueous environments and so act directly in the biological media to trigger apatite formation. However, no study comparing the biological activity of silicate and phosphosilicate glasses in the form of electrospun fibres could be found to support this idea.

When network modifiers such as alkali or alkaline earth oxides are added to a phosphate or silicate glass, bridging oxygen atoms are turned into non-bridging oxygen atoms by the formation of ionic bridges (≡Si-O^{-} $^{+}$M or ≡P-O^{-} $^{+}$M). Increasing network modifier content therefore decreases connectivity and polymerisation of the glass. While vitreous silica is chemically very stable, the addition of modifiers of the silica network decreases its stability and as such increases its dissolution and bioactivity. The bioactivity mechanism of these glasses is based on solution-mediated dissolution. Through ion exchanges between such dissolved species and the ones originally present in the solution (body fluid or simulated body fluid), a carbonated hydroxyapatite (either referred to as CHA or HCA [58]) layer is formed on the bioactive glass surface. This CHA layer is then able to bond with proteins on which cells can attach and are subjected to differentiation and production of the bone matrix. Nonetheless, the mechanism is not fully understood yet. For more details on bioactive glass bioactivity, readers are directed to the relevant literature [16,55,59]. When taking into account the criteria that define the scope of this review (*i.e. in situ* synthesis in the solution used for electrospinning), addition of calcium into a silicate glass has been associated with an improvement in apatite formation after soaking the fibres in SBF [60], but also to a better osteoconductivity and bone regeneration ability when the filaments were implanted in *vivo* in rabbit calvarial bone defects.

Bioactive glasses can be prepared either by using a melt-quenching (involving temperatures above 1300 °C) or a sol-gel method. Although an *in situ* synthesis during electrospinning is not compatible with the melt-quenching technique, different silicate- and phosphosilicate-glass systems have been studied to produce fibres from sol-gel *in situ* synthesis and simultaneous electrospinning.

I.1.2.2. Sol-Gel chemistry and resorption rates of bioactive glasses

Optimising the sol gel synthesis involves the choice of inorganic precursors, solvent and catalyst, along with their mutual ratios. Regarding calcium-containing silicate glasses, TEOS was the main organosilane used as a silicon source, but the use of GPTMS as a coupling agent was also suggested [61]. Calcium nitrate [62] and calcium chloride [63,64] were the two reported calcium precursors for this system, which was always acid-catalysed with hydrochloric acid. For the tertiary phosphosilicate glass system composed of SiO_2, CaO and P_2O_5, the most commonly used precursors are TEOS, calcium nitrate tetrahydrate $Ca(NO_3)_2.4H_2O$ and triethylphosphate (TEP) for the silicon, calcium and phosphorus sources, respectively [52,61,65–86]. Also, in order to avoid the incorporation of toxic nitrates in the material, calcium chloride has also been used as a calcium precursor [87,88], which removes the need for the calcination step required for nitrate elimination.

Furthermore, controlling the ratios between precursors during the synthesis helps in adjusting the bioactivity of the fibres. It was found that if the total amount of glass was kept constant between different glass-containing electrospun fibres, mineralisation in SBF and the growth of MC3T3-E1 cells were slowed down when the SiO_2 amount was increased in the glass composition (*i.e.* from 68S to 86S, compositions with respectively 70 and 90 mol% of SiO_2), due to its greater stability [68]. Cell morphologies after culture on the materials followed the same trend as higher cell density and larger spreading area were found in the case of 68S-containing carbon fibres. These results raise awareness of the importance of choosing adequate ratios between the oxides constituting the glass. Ideally, the chemical composition of the sol-gel has to be adjusted to fabricate bioactive glass fibres with a resorption rate of the scaffold which matches with the new bone regeneration speed.

Common issues can disrupt the formation of fibres with desired compositions. A loss of phosphorus in the nanofibers has been reported, even though it was inserted in the initial sol-gel system before electrospinning. This loss was attributed to the vaporisation of incompletely hydrolysed TEP during the electrospinning process [89]. However, the phosphorus content is rarely analysed in published researches, and deeper investigations need to be performed. In particular, a solution to overcome this loss has to be put forward to maintain the desired glass composition after electrospinning. Another issue is the difficulty in obtaining uniform calcium distribution in the electrospun fibres and the necessity to calcine them at high temperature when calcium nitrates are used as precursors. These issues have been

addressed using calcium chloride as a precursor, and drying the fibres in a controlled humidity environment and in a container limiting the evaporation of solvents [88].

I.2. PREPARATION OF SILICONE-BASED SPINNABLE SOLUTIONS

I.2.1. Sol-gel and polymer solution mixture

Once prepared, silica or bioactive glasses sols are commonly mixed with a polymer solution that ease the electrospinning process by controlling the solution properties - mainly viscoelasticity, conductivity and surface tension. *Figure 2* displays the main considerations regarding polymer and solvent addition to the sol-gel system (respectively red and blue blocs in the figure). As will be discussed later in this review, the addition of a polymer is not the only method to make a silica sol spinnable under an electric field, but it is the simplest one.

Polymers are introduced into the sol to provide it with suitable properties for electrospinning. For instance, attempts at electrospinning a TEOS/GPTEOS sol with a viscosity of 11 mPa.s led to the formation of droplets [90] (*Figure 4.A*). Fibres could only be obtained when a minimum viscosity of 50 mPa.s was reached through the addition of PEO (*Figure 4.B*). The same authors evidenced that electrospraying occurred instead of electrospinning when PEO was replaced by chitosan with a concentration of the same order of magnitude [44]. Indeed, in addition to polymer concentration, its molecular weight also influences its ability to be electrospun. In section I.3.2.2, the effect of polymer concentration on the structure of electrospun fibres will be presented.

A major requirement in selecting the carrying polymer is its non-cytotoxicity and biocompatibility when it is kept in the final fibres, as well as its ability to provide good mechanical properties to the final material. When the polymer is intended to be calcined after the electrospinning process, its thermal behaviour and ease of electrospinning are the main properties to take into account. In the case of silicon-based ceramics, the most commonly used polymers are polyvinyl butyral PVB [52,69,71,81,82,91,92], polyethylene oxide PEO [44,45,90] and polyvinyl alcohol PVA [47,50,85]. But studies with polycaprolactone PCL [43,88], poly(vinyl butyral-co-vinyl alcohol-co-vinyl acetate) [72,83], gelatine [61], polyvinylpyrrolidone PVP [49], poly (L-lactic acid) PLLA [35], polylactic acid PLA [67] or a combination of PCL and PHB [87] have also been published. Natural polymers such as chitosan [44], which has the particularity of being bioactive and antibacterial, can also be used.

On top of these requirements, a suitable solvent for polymer dissolution has to be selected and most of the syntheses reported in the literature are water or water and ethanol-based systems. Water is also necessary for the hydrolysis of silicon and phosphorus precursors and thus for a successful sol-gel synthesis and glass formation. This condition implies that to enable the use of hydrophobic biodegradable polymers, the water content has to be limited but not suppressed. In the PCL/phosphosilicate bioactive glass system for example, methyletylketone (MEK) is used as a co-solvent for both PCL and inorganic precursors [88]. The water to TEOS ratio was reduced to 8, while the water to MEK (v/v) ratio was kept under the value of 1. Indeed, at lower ratios, hydrolysis reaction was too slow. Conversely, for higher ratios the polymer phase started to separate from the sol as water limits the solubility of PCL in the inorganic sol. Water content can also influence the morphology of electrospun fibres, as it modifies the hydrolysis rate of glass precursors and thus the viscosity of the solution. As a result, the fibre diameter was found to increase with an increasing water/TEOS ratio [80].

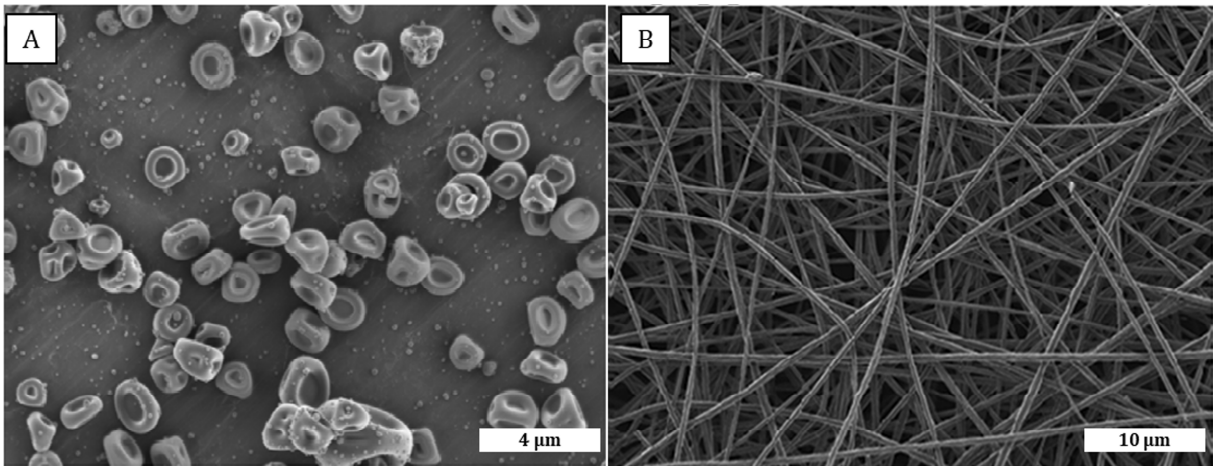

Figure 4. Electrosprayed and electrospun silica solutions. (A) TEOS/GPTEOS solution with a viscosity of 11 mPa.s and (B) PEO/TEOS/GPTEOS solution with a viscosity of 50 mPa.s. Adapted from [90]

I.2.2. Polymer-free sol-gel solutions

Several researchers have also studied the electrospinning of polymer-free sols. In this case, an accurate control of the rheological properties of the sol gel solution is necessary to make it viscous and elastic enough so as to enable its stretching and thus avoid spraying. Although this is a very challenging operation, this technique offers the advantage of not bringing any polymers into the electrospun fibres. Therefore, there is no need to perform any subsequent thermal treatment to eliminate the polymer chains.

In the sparse concerned studies of polymer-free electrospinning, the synthesis protocol was very similar: for silica sols, a mixture of TEOS and ethanol was acidified using diluted hydrochloric acid. Acidic catalysis is expected to form long linear molecules in order to provide the viscoelastic properties that are necessary to stretch the jet without breaking it into droplets (role fulfilled by the polymer in the inorganic-polymer systems). Experimentally, molar ratios of TEOS:EtOH:H_2O:HCl were set to 1:2:2:0.01 [42,93–95], 1:3.8:2:0.08 [48], 1:1:2:0.01 [96] or 1:1:4:0.02 [97]. Regarding Ca-containing silicate glasses (composition 70S30C: 70 mol.% SiO_2 and 30 mol.% CaO), calcium was incorporated in the system using calcium nitrate [62] or calcium chloride dihydrate precursors [63,64]. Molar ratios of TEOS:EtOH:H_2O:HCl:$Ca(NO_3)_2$ were set to 1:2:2.2:0.01:0.3 [62] and molar ratios of TEOS:EtOH:H_2O:HCl:$CaCl_2{\cdot}2H_20$ were of 1:1:2:0.02:0.1 [63,64]. For both silica and SiO_2-CaO systems, heating the sol to around 70-80 °C was necessary to increase the viscosity and for linear crosslinking of the inorganic chains, both resulting from solvent evaporation and subsequently a higher probability of species meeting and reacting in a more concentrated solution [93]. In addition, the evaporation of ethanol generates a displacement of the reaction equilibrium [62]. Varying the duration of ageing time at 60-80 °C is also a way of controlling the final viscosity of the solution [93,98].

Viscosity of the sol plays a major role in its ability to be electrospun. In the case of 70S30C glass, short fibres, long fibres or agglomerates were obtained for viscosity values of 250 mPa.s, 560-950 mPa.s and above 2.77 Pa.s respectively (*Figure 5)* [62]. For comparison, in the Ca-free (100% SiO_2) composition, the optimal viscosity for getting continuous fibres was found to be between 290 and 560 mPa.s. In another study, the exact same composition of the silica sol was used (TEOS:EtOH:H_2O:HCl = 1:2:2:0.1) but with a slightly different ageing procedure. In that case, bead-free fibres could be obtained for viscosities higher than 110 mPa.s (*Figure 6*) [93], and the most stable jet was achieved for viscosities between 130 and 160 mPa.s. However in such optimised cases, instabilities started to appear after 3 to 5 min. After that, cleaning the solidified solution at the needle tip was necessary to make the electrospinning start again.

Actually, there is no threshold value of viscosity for which any sol of any composition can be electrospun because the viscosity of the solution is not the only parameter involved in its spinnability. Indeed, its elasticity is another criterion for the rheological properties to be optimal: it should be high enough to withstand the stretching of the jet under the electrical field. Although this phenomenon has

been reported for polymer-only solutions [99], this feature hasn't been studied for these types of sol-gel systems.

Ideally, avoiding the use of a polymer has the advantage of limiting the temperature of the heat treatment that is usually performed to eliminate organic species (more details will be provided in section I.3.3), but that can also lead to glass crystallisation and thus modified bioactivity. Both the silica and SiO_2-CaO fibres were treated at a temperature as low as 60 °C [42,62]. Also, it was demonstrated that apatite formation in SBF was prevented by increasing the calcination temperature (up to 800 °C) of polymer-free silica fibres [94]. In fact, thermal treatment gradually eliminates Si-OH silanol groups that act as nucleation sites for apatite. In both this study and also a second one from the same authors [95], cellular tests were performed on fibres which were either non calcined [95], treated at 200 °C [94] or treated at 500 °C [95]; but the choice was made not to present the results here due to the lack of controls for the biological tests. Also, it is noteworthy that in the calcium nitrate-containing systems, high temperature would be required anyway to remove toxic nitrates before using the fibres *in vitro*.

On a biological point of view, silica fibres obtained via polymer-free electrospinning were shown to support MC3T3-E1 osteoblast-like cells proliferation better than tissue culture plate positive control [96]. In another study from the same research group however, cell attachment and proliferation were reduced on the silica fibrous constructs compared to tissue culture plates [97]. Even so, the expression of markers of MC3T3-E1 cell differentiation was stronger when the cells were cultured on the fibrous scaffolds. Also, a first investigation on the *in vivo* activity of these materials four weeks after their implantation in rabbit calvarial defect evidenced new bone formation without engaging soft tissue between the fibres and the new bone. This result supports the potential use of such fibres to promote bone regeneration. However, the lack of mechanical properties of these pure inorganic scaffolds was evidenced during compressive mechanical testing: fibres are broken as a result of their brittleness and cannot get back to their initial shape after unloading [62].

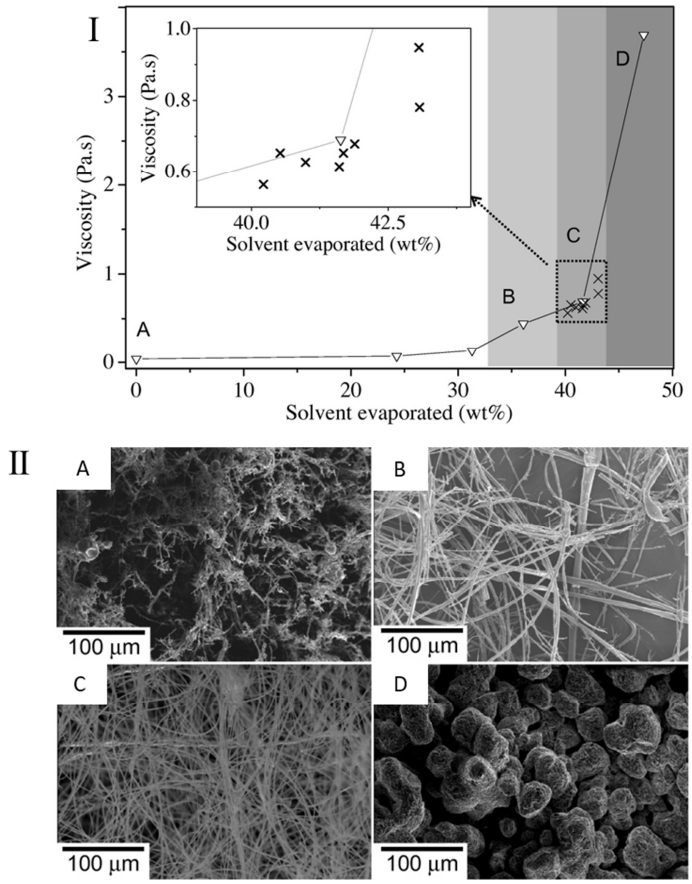

Figure 5. Change in morphology of electrospun Ca-containing SiO_2 bioactive glass with the evolution in solution's viscosity resulting from solvent evaporation. SEM images (II) are named after the A to D domains of graph I, which gives viscosity values of electrospun solutions. Reproduced from [62]

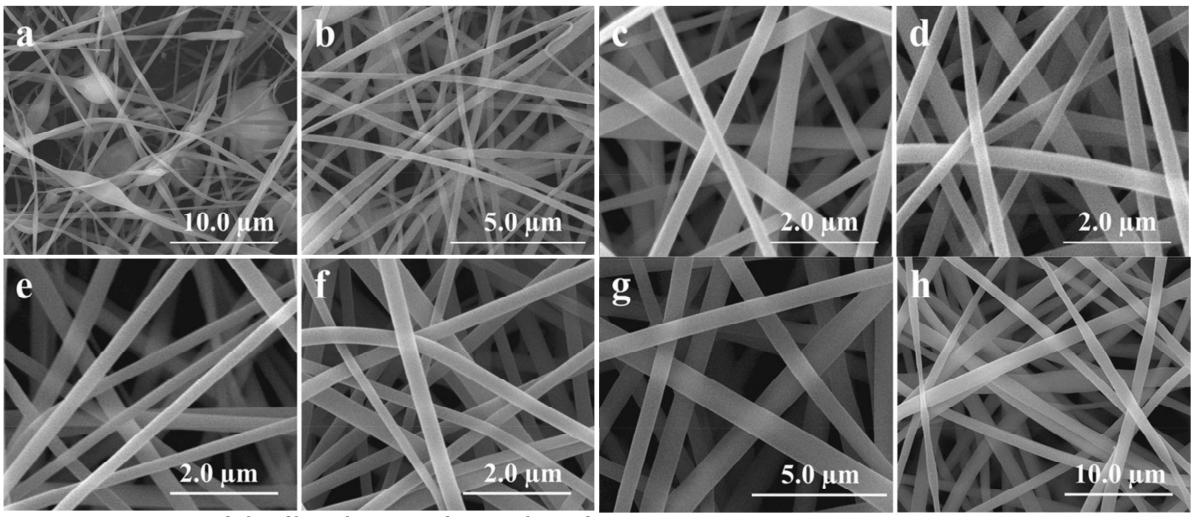

Figure 6. SEM images of silica fibres electrospun from a polymer-free solution. Viscosity values of the sol are a) 65 mPa.s, b) 102 mPa.s, c) 110 mPa.s, d) 125 mPa.s, e) 145 mPa.s, f) 198 mPa.s, g) 398 mPa.s and h) 981 mPa.s. Reproduced from [93]

I.3. PROCESS PARAMETERS AFFECTING THE FIBRE STRUCTURE

As seen in the first sections, electrospinning of a silicon-containing sol or a sol/polymer hybrid is achievable by controlling the properties of the electrospun solution. Besides, the electrospinning parameters must be adapted too to produce the filaments. During the entire process leading to the

formation of ready-to-use fibres, many different parameters including both chemical composition of the spinnable solution and electrospinning setup control affect the final structures of the filaments.

I.3.1. Influence of the electrospinning parameters

During electrospinning, the choice of parameters is directly related to the properties of the solution – its rheological behaviour, electric conductivity and surface tension. Indeed, an electric field high enough to overcome the surface tension of the solution is required in order to initiate jet production (*Figure 1*). The stretching of the jet is also dependent on the solution's ability to carry charges, thus its electrical conductivity [10]. Nagrath *et al.* reviewed the effects of these parameters on the morphology of bioactive glass fibres resulting from *in situ* synthesis in greater detail [36]. For this reason, only general trends are given here and readers are referred to that article for more information. As literature is lacking on this subject in the case of silica, optimisation of the electrospinning process is discussed below regarding mainly bioactive glasses.

When the electric field strength was increased from 1.6 to 1.8 kV/cm for a PVP+P123/bioactive glass system [84], fibre diameters decreased from 110 to about 85 nm. Also, the fibre diameter was not significantly changed when the electric field was increased to 2.0 kV/cm. In fact, when the voltage is increased, a higher amount of charges is present on the fibre surface. The self-repulsion of these charges leads to the increase of elongation forces applied to the jet, and as a result the fibre diameter becomes smaller. When the amount of charge is too high, instabilities appear and the jet can break. Taking these parameters into consideration, average diameters of 58S fibres (mol%: 58.0% SiO_2-26.3% CaO-15.7% P_2O_5) can be obtained in the range from 85 to more than 400 nm by varying the polymer (PVP only or PVP and P123 mixture) concentrations and electric field value [84]. It is also necessary to find a good compromise between the values of voltage and needle-to-collector distance. Indeed, so as to get smooth fibres, this distance needs to be increased for higher voltage values [85]. It is therefore more meaningful to consider electric field (kV/cm) and not only high voltage (kV). When the working distance is too short, solvent evaporation is incomplete and leads to interconnected structures of the mats [100]. Finally, the feeding rate is another parameter to control during the electrospinning process as it influences the diameter of the obtained fibres. Also, if the feeding rate is too low, the collected fibres are not continuous [100]. No studies analysing the effects of environmental factors such as temperature and humidity, known to play a role in the electrospinning process [10], could be found for the electrospinning of *in situ* synthesised Si-based materials. In conclusion, many factors can influence the homogeneity of the obtained fibres. Controlling these parameters represents a tool to tailor the final characteristics of the resulting fibres and to make them correspond with expected features.

I.3.2. Effect of the characteristics of the spinnable solution

I.3.2.1. Effect of sol ageing time

An important point is that the inorganic sol that is part of the electrospun solution is also reactive and evolves with time. Hydrolysis and condensation phenomena imply at least an increase in viscosity which is usually not proportional to time. ^{29}Si NMR results showed that amount of Q_4 species increased with duration of ageing time of a 58S sol, which resulted in the formation of a 3D crosslinked Si network structure and thus an increase of the sol viscosity [66]. Indeed, increasing the ageing time of the solution was found to result in the same effect as an increase in PVA concentration: an enhancement of viscosity and conductivity and reduced pH [50]. Fibres diameters were also impacted, ranging from less than 0.5 µm with no ageing time to about 2.0 µm after 5 hours of ageing for the solution containing 4.5 wt.% of PVA. The time period studied was as short as 5 hours, demonstrating the rapidity of rheological changes. However, it is not specified how long the sol can be electrospun before being unspinnable due to overextended ageing time. As sol-gel chemistry is very sensitive to many parameters such as solution composition as well as external factors like temperature, reaction time and others, it is quite difficult to compare studies to each other as many processing parameters are not kept constant. For instance, Shu-

Hui Xia *et al.* were able to electrospin a similar solution of hydrolysed TEOS and PVA in water after 2 days of ageing [47]. In that case, higher PVA concentration (8 wt.%), lower TEOS/PVA ratio (2.5 against 5.9 to 10.6 wt.% in the previous study), as well as different electrospinning parameters were used. All these parameters minimise the effect of the rheology changes due to gelling.

These evolving properties of the bioactive glass sol can also affect the homogeneity of the sol/polymer mixture. In particular, for the first 4 days of ageing of a 58S glass sol, small synthesised particles could easily be dispersed in a PAN solution [66]. On the contrary, after 7 days of ageing, compact aggregates formed and could hardly be dispersed in the polymeric solution, leading to an irregular distribution of particles along the fibres after electrospinning. Also, an uneven distribution of Si and Ca along the fibres was noticed. Crystallisation of the glass after heat treatment at 1000 °C was also favoured when the ageing time reached 4 days or more, with a higher crystallinity for a 7-day ageing time.

Sol-gel reaction thus needs to be accurately controlled so as to obtain homogenous solutions with appropriate properties that will allow them to be electrospun and to form glass with adequate characteristics.

I.3.2.2. Effect of sol/polymer ratio

Adjusting the ratio between the polymer solution and the silica xerogel or bioactive glass sol influences the electrospun fibre morphology. While keeping constant the final concentration (11 wt.%) of PLLA in the electrospun mixtures, a reduction in fibre diameter was noticed when the silica content was increased [35]. While the average fibre diameter of pure PLLA was (1330 ± 220) nm, it was substantially decreased to (280 ± 60) nm, (210 ± 40) nm and (140 ± 50) nm for 20, 40 and 60 wt.% silica xerogel content, respectively. Besides, the addition of PVP polymer to a bioactive glass sol resulted in the increase of the viscosity and conductivity, and a decrease in the surface tension of the solution [84]. These last two phenomena explain the decrease in fibre diameter until a certain value of PVP concentration was reached – 0.20 g/mL – leading to an average fibre diameter of around 125 nm. At higher PVP concentrations, the effect of viscosity dominates and the average diameter of the fibres increased again (around 425 nm at a PVP concentration of 0.30 g/mL).

Another interesting result is related to the core-shell structures obtained by varying this polymer/silica xerogel solutions ratio in PEO-silica xerogel hybrid fibres [90]. Indeed, when the PEO/silica xerogel weight ratio was 10 wt.% or lower, a core-shell structure with PEO as the core and silica xerogel as the shell was obtained. Following the same principle, hollow fibres of silica [101,102] and 70S30C [100] were created by electrospinning a mixture of glass precursors and PVP or PVB polymers, respectively. According to the authors, this phase separation would be caused both by solvent evaporation during electrospinning and by a low affinity between glass precursors and polymer. As discussed later (section I.4.2), hollow fibres have been studies for drug delivery applications.

I.3.2.3. Effect of supplementation with a porogen agent

Another advantage of polymer addition in the solution is linked to the creation of porosity inside and at the fibre surface. This is an interesting way of improving the bioactivity of the materials by enhancing their surface area, the amount of bioactive glass available at the surface of the fibres and consequently their dissolution rate. A system combining bioactive glass (58S) and PAN was used, but poly(methyl methacrylate) PMMA was added in the system as a porogen polymer [76]. This polymer underwent a phase separation when mixed with PAN. As its degradation temperature is lower than that of PAN, it was eliminated during heat treatment at 1000 °C in N_2 while PAN was transformed into carbon fibres. For a PAN/PMMA weight ratio of 4/3, the fibres displayed grooves and pores at their surface, creating an open porous structure. The pore size was of about 22 nm and the surface area of 35.0 m^2/g. As a result of the increased surface area, biomineralisation, cell proliferation and osteogenic differentiation were favoured [76]. Similarly, Ravichandran *et al.* inserted shaping agent P123 into silica fibres to create mesoporosity in the fibres after their calcination [49,103].

I.3.3. Role of treatments on as-spun fibres

Biodegradable polymers can be used for electrospinning purpose and then be kept in the fibres to be degraded little by little and to gradually expose the inorganic materials to the biological media and cells. For this purpose, biodegradable polycaprolactone (PCL) was used on its own with the bioactive sol [88], but also in combination with polyhydroxybutyrate (PHB) [87]. As in the last cited example, combined properties from two polymers exhibiting distinctive features can be granted to the final fibres [87]. Indeed, another positive effect of the polymer, before it is dissolved, is its contribution to the mechanical properties of the final fibres [87]. As such, PCL and PHB were selected for their flexibility and stiffness, respectively. But most commonly, fibres are subjected to treatments once electrospun so as to increase the condensation of the silica network or to get rid of organic species and of salt precursor counter ions.

First of all, the drying and/or ageing of as-spun fibres are commonly reported right after the electrospinning process. They are pivotal steps because they are meant to evaporate solvent residues and to further condense the silica network respectively. Both the silica xerogels and bioactive glass fibres, either containing a polymer or not, were treated at temperatures ranging from room temperature to 110 °C. It was reported in section I.3.2.1 that polycondensation of silicon networks could also be improved by varying the ageing duration of the gel before electrospinning. Another suggested way of doing this is to use an acid stream treatment [67]. After electrospinning, fibre mats were placed above HCl solutions at 40 °C for 24 hours. However, no chemical analysis was performed to prove the enhanced degree of polycondensation of the resulting fibres in that case. Also, crosslinking of silica xerogel/PVA hybrid fibres after electrospinning with glutaraldehyde was reported so that the fibres can maintain their fibrous morphology during *in vitro* or *in vivo* studies [47]. In fact it was shown that, without cross-linking, the fibres fused into a dense, non-fibrous membrane.

Secondly, embedding the biological ceramic into a polymer matrix that does not present bioactive features can limit the bioactivity of the fibres. Therefore a calcination step can be carried out after electrospinning (and drying/ageing if any) with the aim of exposing all the ceramic content to the biological medium. This enables the elimination of the polymer and results in the obtaining of pure inorganic fibres. The processing temperature needs to exceed the degradation temperature of the polymer. For instance, typical pyrolysis temperatures used for silica fibres are 500-550 °C so as to ensure polymer decomposition [49,50,103]. In such cases, the silica content should be high enough to maintain its fibrous morphology after calcination and to avoid the loss of filament shape; but no detailed study is available on this point. Furthermore, thermal treatment induces the integration of network modifiers within the silica network [62]. Also, as nitrates are often brought into glass systems through the use of calcium nitrate precursor, a calcination step is necessary to eliminate this toxic compound, whose thermal decomposition starts around 500 °C. It is also important not only to stabilise the glass but also not to exceed its crystallisation temperature so as not to lower its bioactivity. Calcination of 58S-containing fibre at 600 °C led to the production of inorganic XRD-amorphous fibres for example [80,84], while a wollastonite $CaSiO_3$ phase was detected after treatment of 58S-containing PAN fibres at 1000 °C [66]. Interestingly, this study also evidenced that XRD analysis can lack sensitivity to detect some crystalline phases into electrospun fibres, due to their possible nanometric size. Indeed, crystalline wollastonite could only be detected by HR-TEM and FFT diffraction patterns. This phenomenon should be taken into account when characterizing this type of material. So far in the literature, authors have most of the time limited the crystallisation study to XRD analysis.

The calcination step also leads to the reduction of fibre diameter through the elimination of polymers and the consolidation of the glass network upon heat treatment [75,80,84]. Similarly, it also influences fibre shrinkage in the longitudinal direction, as reported in greater detail in the review of Nagrath *et al.* [36]. Finally, heat treatment was correlated with the apparition of a core-shell structure after the calcination of calcium-containing silica xerogel/PVB fibres [104]. While the distribution of elements was homogeneous in the as-spun fibres, the phase separation occurring upon heat treatment at 1000 °C was suggested to result from the decomposition of organic species. The latter drives the silica towards the fibre surface and results in a SiO_2 shell. On the contrary, a calcium rich phase remains in the

core and forms $CaSiO_3$. This phenomenon was found to be dependent on the calcium to silicon ratio, temperature and the presence of other doping elements [104].

I.4. Applications of silicon-based fibres in Bone Tissue Engineering

Different biological evaluations of Si-based electrospun fibres have been presented throughout this first chapter in order to justify the selection of the studied materials as well as the methods used to synthesise them. This section I.4 is meant above all to emphasise the potential uses of silicon-based fibres for BTE. As a support, *Figure 7* gathers in broad lines all the cellular and *in vivo* studies of materials prepared with silica-based fibres. Most of them are developed in this section I.4 but previously mentioned studies are also included. In this figure, three classes of materials are distinguished: self-supported fibres (developed in section I.4.1), composite and biphasic materials of silicon-based fibres and either polymeric or inorganic phases (both detailed in section I.4.3). In section I.4.2, drug-delivery systems made of Si-based fibres are presented. However, they do not appear in *Figure 7* due to the absence of cellular or *in vivo* investigations in presence of the drugs.

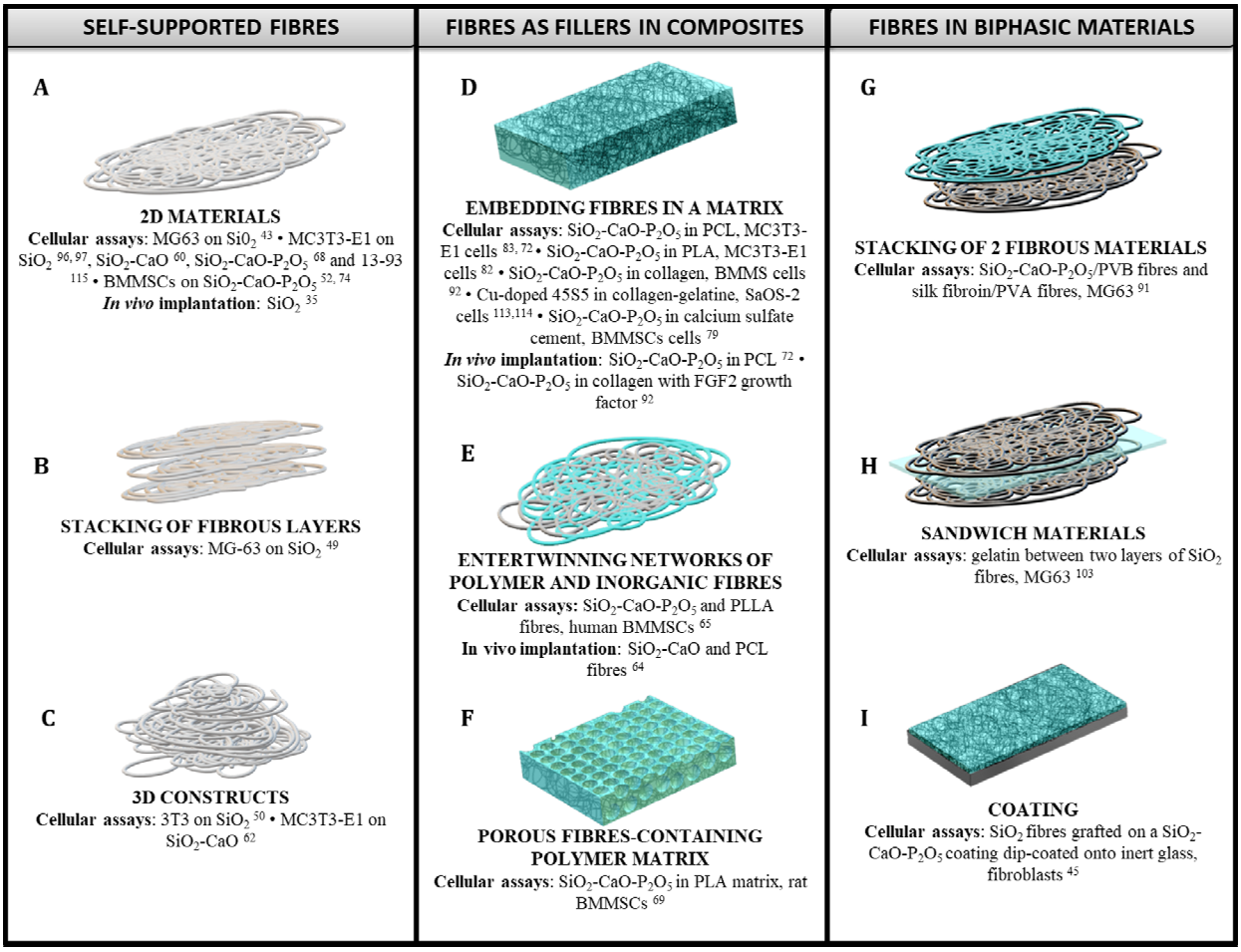

Figure 7. Different types of Si-based ceramic-containing materials studied in the field of BTE: cellular and *in vivo* studies. For the electrospun fibres, only the composition of the inorganic phase is given (polymer phase not specified)

I.4.1. Use of fibres as self-supported materials

In vivo implantation of electrospun silica xerogel-containing fibres was reported in 2011 by Jang *et al*. [35] (representation in *Figure 7.A*). Hybrid fibres were synthesised to be used as-spun in Guided Bone Regeneration (GBR). This technique aims at reconstructing damaged bone tissue through the use of a barrier membrane, both by improving regeneration of the new bone and by preventing in-growth of

fibrous connective tissue into the space required for the bone regeneration. After electrospinning, PLLA polymer was kept in the final fibres to improve the mechanical properties of these silicon-based hybrids. Sufficient mechanical properties matter in order to favour an easy handling of the materials during implantation as well as to withstand external forces *in vivo*. The fibres elastic modulus was improved with the content of silica xerogel. Similarly, the tensile strength of the filaments raised with the amount of silica xerogel and reached a maximum for PLLA-40% silica xerogel fibres but dropped drastically when the silica xerogel content reached 60 % [35]. Also, the use of an excessive concentration of silica xerogel had a deleterious effect on the ductile nature of PLLA which gradually switched to a brittle behaviour as the silica xerogel content increased. From a biological point of view, increasing the silica xerogel content in PLLA-SiO_2 hybrid membranes led to a gain in surface hydrophilicity, in silicon release and in ALP activity of MC3T3-E1 cells. The sample containing 40 wt.% of silica xerogel was compared to pure PLLA membranes for *in vivo* experiments, for which membranes were placed in rat calvarial defects [35]. Six weeks after implantation, the higher bone regeneration ability of the hybrid membranes compared to pure PLLA ones (*Figure 8*) was confirmed by both micro-CT 3D images of the defect and histological staining with Masson-trichrome and Haematoxylin-Eosin of the extracted bone tissue. In addition, no inflammatory response was revealed for either sample nor did soft tissue penetrate into the defect margin, proving the potential use of this material in GBR.

While the previously reported study used fibres in the form of a membrane, 3D materials can also be used. In this case, it is important to take material porosity into account. This aspect is indeed essential for cell in-growth as well as better cellular diffusion and exchange of essential nutrients throughout the structure. It has been demonstrated that stacking a few layers of fibrous silica membranes (*Figure 7.B*) in order to increase material three-dimensionality was not an efficient method of improving biological behaviour [49]. Indeed, layer-by-layer stacking of such porous material reduces the macroporosity that is commonly useful for cell infiltration and angiogenesis. In order to improve the infiltration of cells in the materials, Hoa-Yang Mi *et al*. modified the final macroscopic architecture of fibrous silica [50]. They fabricated, via the calcination of self-assembled silica xerogel-PVA electrospun fibres, super absorbable 3D silica sponges with a bulk density of 16 mg/cm^3, a surface area of 6.45 m^2/g and a large porosity (98 %). This self-assembled 3D structure (*Figure 7.C*) was obtained by adjusting the electrospinning solution parameters, mainly the PVA concentration and solution ageing. Indeed, while 2D structures (thickness not given in the original article) were obtained when 14% PVA-containing solutions were electrospun without ageing time, 3D structures were obtained when the ageing time was increased to three hours. The height of the structure reached about 10 cm after spinning for 2 h *(Figure 9.A)*. However, because the construct preferentially grows in the direction of the needle tip, the material doesn't become homogeneously thicker over its entire surface and takes the shape of a cone. The authors explained this three-dimensionality by the linkage formation between the TEOS and PVA occurring in the solution during ageing and in the electrospun fibres. This link leads to the formation of a highly electronegative siloxane shell among PVA molecules that causes electrostatic repulsion between the fibres and thus a loosely packed structure of deposited fibres. After calcination (800 °C, 3 h), light, soft and easily deformable silica sponges were obtained *(Figure 9.A.e)*. High viability and proliferation rates were obtained for 3T3 fibroblast cells cultured on these sponges [50]. As expected, cells were able to penetrate deeper into the 3D construct. Indeed, as they penetrated up to 148 µm in the silica membranes after 10 days, the maximum penetration depth was 243 µm in the silica sponges (*Figure 9.B*). Yet, it is noteworthy that this penetration depth remains low compared to the thickness of the whole material. Finally, 3D structures showed a higher viability of 3T3 fibroblast cells compared to silica 2D membranes. Another possible method of producing cotton wool-like fibres was reported and involves the addition of calcium in the silica sol [62] (*Figure 7.C*). This structure results from the modification of different solution parameters such as rheological properties and conductivity of the solutions, with instabilities during electrospinning leading to branching. Yet, no details are provided about the thickness of the obtained materials nor the infiltration of cells.

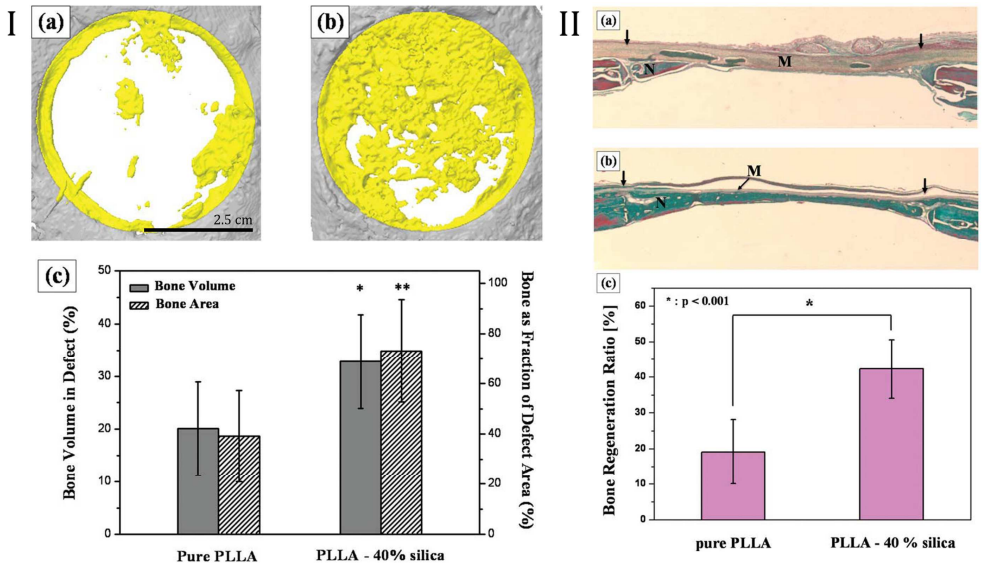

Figure 8. I) Micro computed tomography images of the rat calvarial defects, 6 weeks after they were covered with (a) pure PLLA membrane and (b) PLLA-40 % silica xerogel hybrid membrane. c) Regenerated bone volume 6 weeks after the membranes were implanted (*p < 0.005, **p < 0.001, n = 10). II) Optical micrographs of the stained (Masson-trichrome and haematoxylin-eosin) bone tissues 6 weeks after the membranes were implanted: (a) pure PLLA nanofibrous membrane and (b) PLLA-40% silica xerogel hybrid membrane. No scale bar indicated in the original article; (c) Bone regeneration rate (ratio of the new bone to the total defect area). Arrow: edges of the defects; N: new bone; M: membrane". Reproduced from [35]

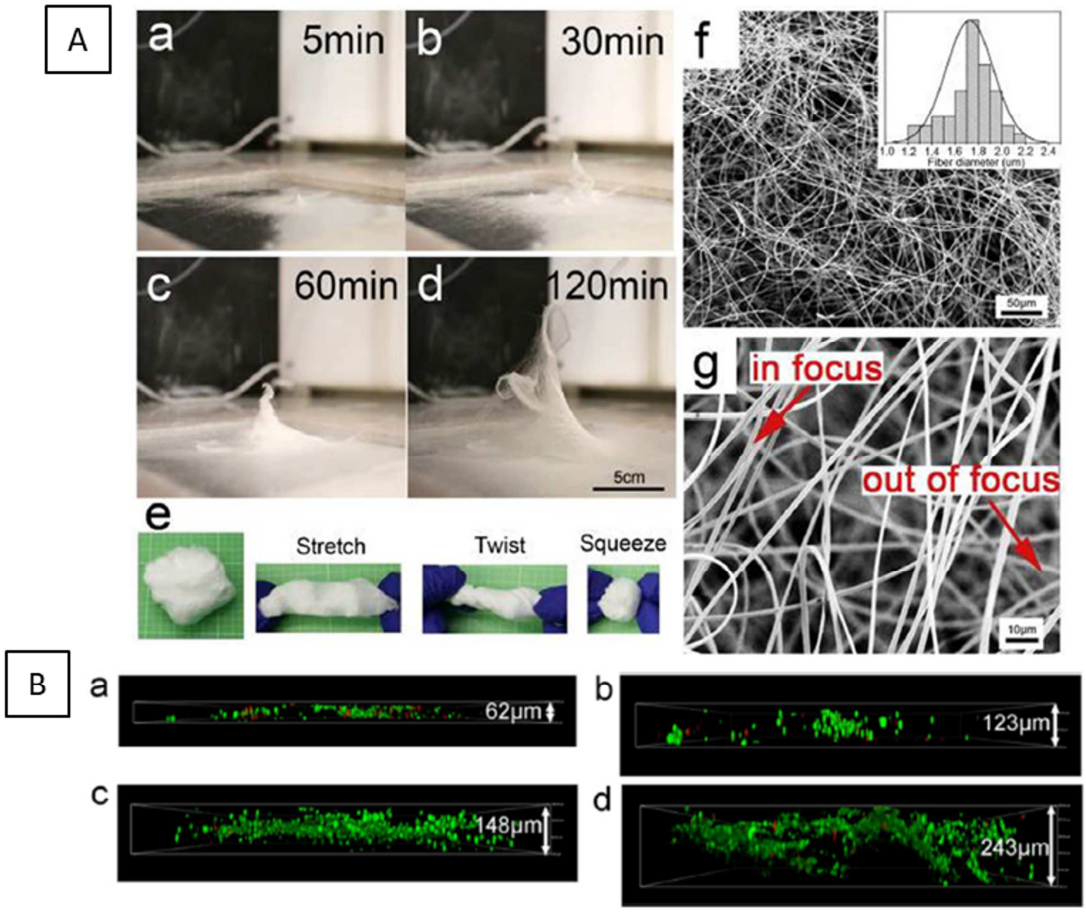

Figure 9. (A) (a-d) Electrospinning of TEOS/PVA sponge and 3D development with time; (e) deformation of silica sponge on a macroscopic level; (f-g) SEM images of the resulting fibres, with a fibre diameter distribution histogram as an insert in (f). (B) Confocal images of live/dead assay, showing the penetration depth of cells cultured on (a,c) silica membranes for 3 and 10 days respectively, and on (b,d) silica sponges for 3 and 10 days respectively. Reproduced from [50]

I.4.2. Applications in drug-loading/delivery systems

Bioactive glass based-fibres can be used as a carrier for antibiotics or biologically active proteins such as growth factors, cytokines or antibodies. These drug-delivery materials are promising for enhanced bone regeneration since they can direct cell activities through integrin-ligand interactions [80]. The regenerative capacity of an implanted material will then depend on the release specificities of proteins from the material. In addition, it is important that the release capacity of antibiotics should last for 5-10 days in order to be efficient [75].

As biologically active substances are sensitive to temperature, they can be introduced in the solution to be electrospun only when no heat treatment is necessary after electrospinning. Using this technique, delivery of levofloxacin (LFX) [105] and tetracycline hydrochloride (TCH) [106] was shown to be very fast as a plateau was reached within the first few hours of immersion in SBF. Also, an increased amount of silica content in the fibres was linked to faster drug delivery. Graphical comparison of these delivery rates is represented in *Figure 10*.

A frequent strategy to load these bioactive molecules is to create porosity on the fibres in which they can be hosted and be released. This porosity is achieved by using additional surfactant compounds or template additives. This method is thus compatible with the use of thermal treated filaments. Some systems displayed fast drug release, with a plateau in the delivery reached in 8 hours for ibuprofen [107] or in slightly more than 20 hours for gentamicin sulfate [108] (*Figure 10).* Better delivery control over time was reported with ibuprofen and gentamicin sulfate. For the former, P123 was used alone as a structure-directing agent and was responsible, after dissolution in ethanol, for the creation of 4-5 nm mesopores in sol-gel synthesised phosphosilicate-containing PLA fibres [67]. No burst release was observed in the first hours of immersion and controlled delivery was displayed over around 100-120 hours of release in SBF. Total delivery was therefore 55-65 %. The amount of drug delivered was also shown to be dependent on the quantity of bioactive glass loaded on the PLA-based fibres as a higher amount of glass led to an enhanced mesoporous structure (see *Figure 10*). Regarding gentamicin sulfate (GS) drug delivery system, a controlled release was obtained through the creation - after calcination of PVP and P123 contained in the as-electrospun bioactive glass fibres - of hexagonal ordered structure displaying mesoporous size of approximately 4 nm [75]. These fibres were subsequently loaded with GS and freeze-dried. Delivery was well-controlled as the matrix exhibited prolonged and gradual release of GS over 10 days, as displayed in *Figure 10*.

Another suggested method for improved drug-loading capacities is the creation of hollow fibres. It was expected that the space available for drug hosting would be enhanced, as well as interactions with a biological medium. However, burst deliveries were highlighted in both protocols proposed in the literature, either with BSA (Bovine Serum Albumin) [70] or gentamicin sulfate [78] (*Figure 10*).

This section reported different systems developed with a view to controlling the delivery of bioactive molecules from electrospun bioactive glasses. Even though controlling the delivery rate was shown to be difficult, a few systems – being characterised by fibres with mesopores at their surfaces - seem promising. Yet, even if cytotoxic assays were carried out on TCH drug loaded silica/PCL fibres [106], there were a lack of controls such as tissue culture plate and drug-free fibres. Actually, none of the aforementioned studies determined the influence of delivered molecules on the bioactivity of the materials with *in vitro* or *in vivo* studies, information that would be very relevant to confirm the suitability of such materials in tissue engineering applications.

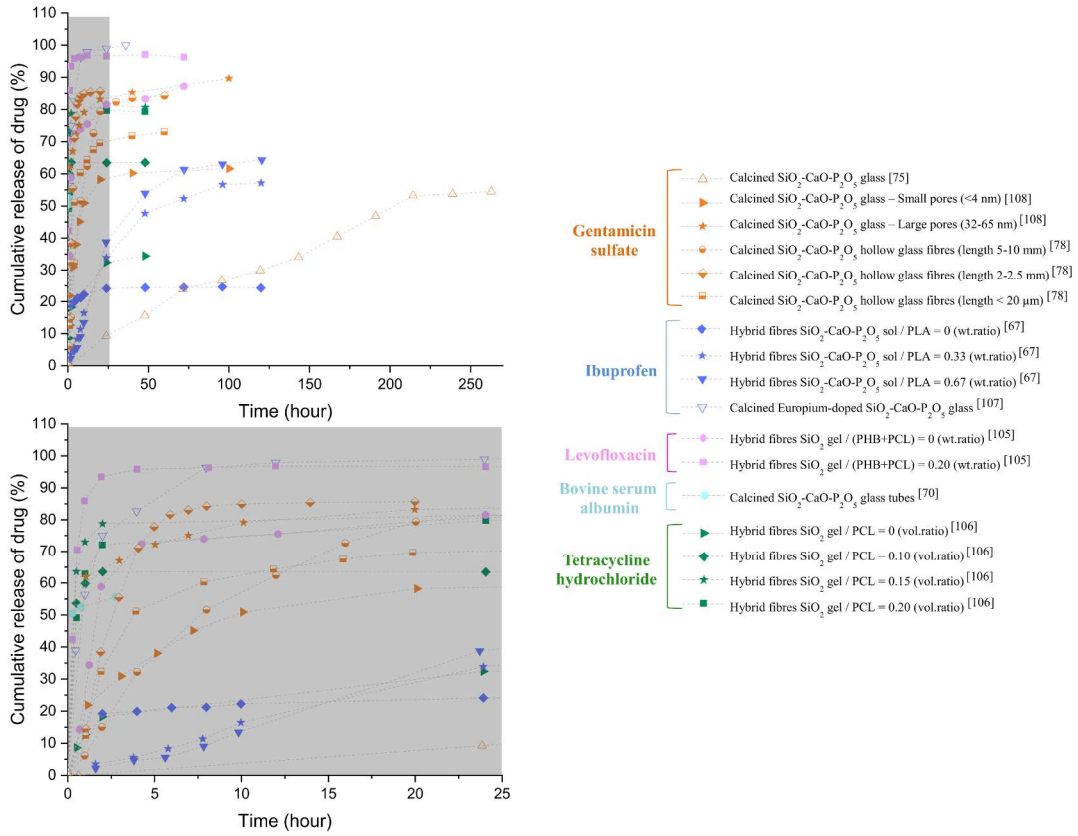

Figure 10. Comparison of literature results regarding cumulative releases of drugs loaded on silicon-based fibres. Grey area in the upper graph is magnified in the second one. Studied drugs are distinguished in the graph by their colours. For an easier reading, errors bars have not been plotted but can be found in the original articles [67,70,75,78,105–108]. It is also important to note that this graph is a comparison of cumulative release of drug in percentage of the amount of drug initially loaded on the fibres. This amount depends on the protocol used in each study.

I.4.3. Use of Si-based fibres in composite and biphasic materials

A large number of articles reports the use of *in situ* synthesised Si-based electrospun fibres in a final composite or biphasic system, where combining these inorganic fibres with polymeric matrices presents favourable conditions for degradability, biocompatibility and mechanical properties. Therefore, as outlined in the second and third columns of *Figure 7*, the polymer matrix can either be used in a bulk form to integrate the inorganic fibres, or can be shaped by electrospinning.

First of all, the addition of bioactive glass in the form of electrospun fibres instead of spherical particles to a PCL solid matrix was associated with an increase in ALP activity (by 55 % compared to glass-particles loaded PCL and by approximately 240 % compared to PCL-only matrices) [72]. Also, in this composite represented in *Figure 7.D*, the presence of the fibres increased the elastic modulus of the material, while a similar tensile strength to that of a filler-free PCL matrix was maintained. Besides, *in vivo* studies showed that the incorporation of bioactive glass fibres into the PCL matrix led to a thicker and higher amount of new bone formation into a calvarial bone defect [72]. Similarly, other materials combining both bioactive glass fibres and a polymeric matrix were studied, *i.e.* thin membranes of PCL-embedded bioactive glass fibres [83], dense sheets of PLA/bioactive glass fibres [82] and scaffolds of PLA/bioactive glass fibres in which open porous structure (porosity of around 83%) was created using NaCl particles as a porogen agent (*Figure 7.F*) [69]. In each case, cell attachment and proliferation were increased in comparison with purely polymeric matrices, as well as osteoblastic responses in terms of ALP expression (and other bone gene expression in the last cited example [69]). Finally, a composite combining two inorganic materials was reported. Bioactive glass fibres were incorporated within a calcium sulfate cement for bone healing applications (*Figure 7.D*) [79]. Improved mechanical properties as well as cell viability and the potential to induce osteogenic differentiation of human BMMSCs were endowed to these composites compared to both pure calcium sulfate cements and bioactive glass fibres. In

addition to bioactive ceramics, growth factors such as FGF2 fibroblast growth factor can further stimulate bone formation. Because FGF2 can sustainably be released from collagen, membranes of collagen-bioactive glass fibres (*Figure 11.A&B)* were supplemented with this growth factor [92]. When the membranes were implanted into rat calvarial defect, (3.6 ± 1.6)% of new bone formation was quantified in the blank control, while it reached (31.2 ± 5.9)%, (44.0 ± 4.8) and (59.3 ± 14.0) % in the case of collagen membranes, collagen/bioactive glass fibres membranes, and collagen/bioactive glass fibres/FGF2 membranes respectively [92], proving the beneficial effect of this bioactive molecule. New bone formation can be seen in *Figure 11.C,* which represents histological staining of the tissues 3 weeks after implantation. [92].

In the aforementioned composite scaffolds, the porosity was lost when embedding the fibres in a polymer solid matrix (*Figure 7.D*) [63–65]. Therefore, fully fibrous and porous structures with interconnected pores could be obtained by combining bioactive glass and polymers both in the form of electrospun filaments (*Figure 7.E*). The resulting composite materials were capable of providing soluble ions for the stimulation of osteogenic differentiation (confirmed by ALP, osteocalcin, osteonectin, collagen I and RUNX2 gene expressions) as well as a suitable platform for cell emplacement [71]. *In vivo*, this type of composite material permitted a better new bone formation compared to PCL-only fibres, and it also limited the degree of foreign body reactions [69]. The choice of polymer was important, as the acidic degradation products of PLGA [poly[lactic-co-glycolic acid)] inhibited apatite formation in SBF [63]. On a mechanical point of view, the addition of a PCL network intertwined with 70S30C fibres increased the maximum fracture strength of the glass material by a factor of 6, the strain to failure by 320 and the Young's modulus by 8 [64].

Combining polymer and bioactive fibres was also possible in the form of sandwich materials (*Figure 7.H*). These were composed of a layer of solvent casted gelatine stacked between two mesoporous silica fibrous scaffolds [103]. The incorporation of this hydrogel layer aims to improve the resemblance to the native extracellular matrix that naturally contains a glycosaminoglycan gel architecture along with a collagen fibrous network. Also, gelatine contains an integrin binding domain [Arg-Gly-Asp (RGD) attachment site] which is known to be involved in cell attachment. As mechanical stiffness can influence cell behaviour, two different sandwich materials were studied with the intermediate layer of gelatine either crosslinked with glutaraldehyde vapours or left uncrosslinked. The results revealed that both materials supported osteoblast adhesion, growth, proliferation and maturation. However, cell extension and infiltration were slightly favoured in uncrosslinked gelatine-based scaffolds. According to the authors, osteoblast-like cell infiltration and spreading were limited in the second scaffold by the reduction in porosity caused by crosslinking of the gelatine layer, thus creating a microenvironment confining most of the cells to the surface. Nevertheless, no data is provided in terms of the pore size distribution for each material, which would be useful in linking this result to the size of cells. In addition, the hydrogel behaviour of uncrosslinked gelatine creates a layer allowing for the diffusion of nutrients and leading to a higher infiltration of cells.

Finally, so as to be used at the interface with bone and a material with a different composition (i.e. a prosthetic implant or cartilage), other kinds of biphasic materials have been developed. PEO/silica composite fibres grafted on the surface of an inert glass substrate was evaluated for its use as a component of a bioactive coating (*Figure 7.I*) [45]. It was found that silica nanofibres embedded in the coating favoured surface hydrophilicity and fibroblast cells proliferation. Also, for the reconstruction of osteochondral defects, a biphasic matrix was developed by electrospinning 70S glass-containing PVB filaments, subsequently coated with electrospun silk fibroin-containing PVA filaments (*Figure 7.G*) [91]. Analyses confirmed that the bioactive glass fibrous side of the membrane favoured the maintenance of the osteoblastic phenotype of seeded cells, while the silk side favoured the maintenance of chondrogenetic phenotypes.

All in all, the combination of two different materials with one being inorganic Si-based electrospun fibres and the other being polymer most of the time is interesting as it contributes to improving the mechanical and biological properties compared to each material taken separately. In this section, most of the studied materials had homogeneous composition throughout their volume, but

biphasic materials intended to be used at the interface between bone and another material (synthetic or natural) were also reported.

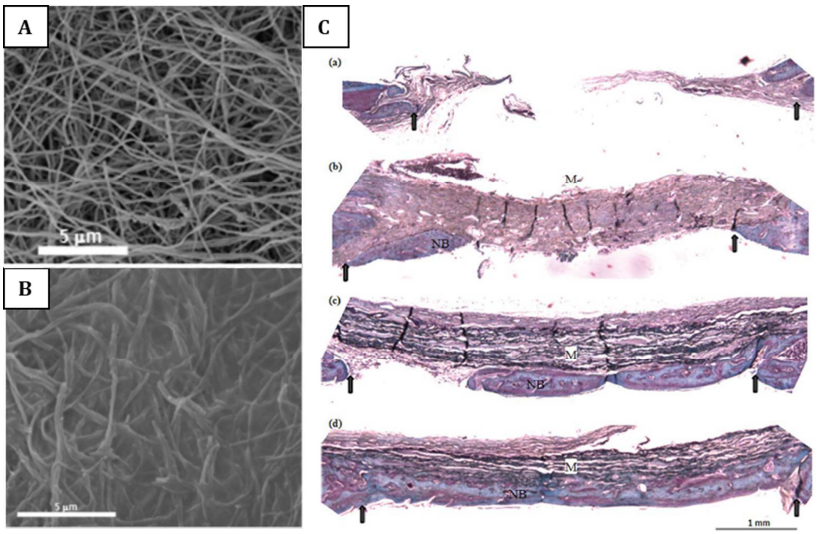

Figure 11. SEM observation of experimental membranes of (A) calcined bioactive glass fibres and (B) the composite made of calcined bioactive glass fibres embedded within a collagen matrix. (C) Optical microscope observation of histologically stained (H&E and Koeneff's bone & cartilage staining) tissues after 3 weeks of in vivo implantation in rat calvarium defects. (a) blank control and (b-d) membranes were used : (b) collagen, (c) collagen-BG, and (d) collagen-BG-FGF. Notations: « M » stands for membrane and « NB » for new bone. Arrows: edges of the defects. Adapted from [92]

I.5. MORE COMPLEX GLASS COMPOSITIONS, MORE CHALLENGES

Besides all the electrospun materials that have been detailed so far in this review - *i.e.* silica and bioactive glasses made of silicon, calcium and sometimes phosphorus - other compositions of phosphosilicate glasses were studied marginally in the literature for BTE application. The most well-known of these is 45S5 bioglass. 45S5 Bioglass® was developed by Lary Hench in the late 1960's with the aim of improving existing polymeric and metal implants which were prone to rejections through the creation of fibrous tissues that encapsulated the implanted material. The optimal composition $45SiO_2$–$24.5Na_2O$–$24.5CaO$–$6P_2O_5$ (wt %) was capable of not only creating a strong interface between the bone and the implant but also of genetically activating specific cell pathways [109] responsible for the stimulation of bone growth away from the bone-implant interface. Osteogenic properties are linked to the dissolution of ions from the glass, leading to the stimulation of osteogenic cells and production of bone matrix [16]. The original composition of 45S5 bioglass was FDA approved in 1985, and had been implanted in 1.5 million patients to repair bone and dental defects by 2016 [110]. The bioactivity of such glass can be improved by the creation of porous materials. Such features can be ascribed to the glass using sol-gel synthesis instead of melt-quenching. Nonetheless, to go even further into the creation of porosity, the formation of electrospun fibres is a promising challenge. Surprisingly, while this bioactive glass is largely studied for the formation of dense materials, there are only two articles detailing the electrospinning of 45S5 glass. The first one was published in 2014 by Deliormanli [111]. Although the process resulted in the production of fibres, crystallisation of sodium nitrate was observed at their surface. It is noteworthy that the inserted sodium precursor was sodium nitrate tetrahydrate ($Ca(NO_3)_2{\cdot}4H_2O$). A heat treatment at 700 °C permitted the elimination of the polymer and of the nitrates, present both inside the fibres and crystallised at their surface. However, one can wonder if the composition of the glass initially inserted in the electrospun solution is preserved after heat treatment - especially through the elimination of sodium nitrate crystals. EDS analysis of the glass was carried out but as there are no detailed percentages reported, no conclusion can be drawn on that point. With the addition of sodium in the composition, other crystalline phases that were not present in the

aforementioned Na-free glasses were obtained. Combeite $Na_{5.27}Ca_3Si_6O_{18}$ and clinophosinate $Na_3CaPSiO_7$ started to appear after calcination at 600 °C, and crystalline sodium silicate phosphate $Na_3Ca(SiO_3)(PO_4)$ from 700 °C. Hollow fibres of 45S5 (not totally amorphous either) were also used for drug delivery applications, but very fast releases within a few hours were evidenced [112]. In addition, bioactivity testing was very limited in both those foregoing articles. There is still a lack of similar investigations for electrospun *in situ* synthesised 45S5 glass to confirm its legitimacy for use in bone tissue engineering applications.

Cu-doped 45S5 fibres (composition 45 wt% SiO_2, 6 wt% P_2O_5, 23.5 wt% CaO, 1 wt% CuO, 24.5 wt% Na_2O) were fabricated by Esmaeel Sharifi *et al.* [113,114]. The addition of copper (through Cu(II) nitrate trihydrate precursor) in a collagen-gelatine hydrogel was expected to improve the materials angiogenesis and osteogenesis potentials. Compared to fibre-free hydrogels, Cu-doped 45S5-containing hydrogels displayed increased phenotypic markers that are ALP, osteonectin and osteopontin after 21 days of culture. However, no comparison with 45S5 fibres-containing composites was made to estimate the influence of copper added to the glass composition.

Deliormani also electrospun 13-93 glass, with the composition in mol%: 54.6% SiO_2 - 22.1% CaO - 7.9% K_2O - 7.7% MgO - 6.0% Na_2O - 1.7% P_2O_5 [115,116]. Magnesium and potassium precursors were also added in the form of nitrates - leading to the crystallisation of $NaNO_3$ on as-spun fibres, eliminated during thermal treatment. 13-93 glass is known for converting to hydroxyapatite-like material more slowly than 45S5 glass. This was confirmed by SBF testing, as carbonated apatite formation was 7 times faster during the immersion of 45S5 compared to that of 13-93 [115], when the same analysis conditions were used. The incorporation of Mg and K offers the advantage of reducing the glass ability to be crystallised during heat treatment: crystalline structure only started to appear after heat treatment at 680 °C, while crystallisation was much more obvious in 45S5 fibres even at 600 °C [111] and probably occurred at lower temperatures (data not provided). Unfortunately, the cellular study reported for these 13-93 glass fibres lacks controls [115] and no cellular assay was performed on composites created by electrospinning a PCL solution containing dispersed fibres of 13-93 glass [116].

Due to their low ability to crystallise and to their reactivity higher than 13-93, borosilicate glasses were also evaluated as electrospun fibres. The chosen system had a composition of $47SiO2–23B_2O_3–25CaO–5P_2O_5$ (mol%) [117] and tributyl borate was used as a boron precursor. It was demonstrated that the fibres were XRD-amorphous after treatment at 700 °C and that they induced apatite precipitation on their surface during SBF immersion. However, no reference controls were used during this SBF immersion to conclude on this higher reactivity and no cellular studies were reported.

Finally, Deliormanli reported the electrospinning of 13-93 with the substitution of silicon with either gallium or cerium [118]. Such glasses were expected to improve the antibacterial properties of the obtained materials, but it was ineffective as negative responses to gram positive (*Staphylococcus aureus*) and gram negative (*Escherichia coli*) bacteria were observed: agar plates were totally covered with the bacteria after 2 days and no inhibition zone was observed around the scaffold. On the contrary, when Ag-doped silica fibres were prepared [119], a maximum of 8 hours was necessary to annihilate *Escherichia coli* bacterium, while 48 hours were required to kill *Staphylococcus aureus*. Silver element does indeed exhibit inhibitory activity or an antimicrobial effect.

I.6. SUMMARY FOR SILICON-BASED ELECTROSPINNING

As outlined previously, silica and many different glass compositions can be successfully electrospun from solutions obtained by *in situ* sol-gel synthesis. They were shown to provide effective support for fibroblast and osteoblast cell growth and differentiation, and *in vivo* studies confirmed the potential use of such porous electrospun materials for BTE. Also, the fibrous morphology has been shown to enhance ALP expression of rat BMMSCs in comparison with smooth glass disks of the same composition. Optimising the final properties and morphologies of obtained fibres implies an important control of processing parameters, sol-gel composition and of carrying polymer if any. Drug-delivery systems could also be designed and some displayed gradual and appropriate release properties. Of all the silica-based fibres, the most commonly studied systems are SiO_2-CaO-P_2O_5 based. Unfortunately, promising materials with more

original compositions have been subject to sparse studies. For these materials, biological analysis requires further in-depth investigation. In particular, the well-known 45S5 bioglass that has already proven its superior properties in dense scaffolds could be a promising electrospun material. Also, comparing the biological responses of Si-based electrospun fibres is difficult as the number of biological studies is limited, and also because the materials are never tested in the same conditions (composition and concentration of the inorganic phase, type of cells, and so forth).

As explained above, the bioactivity of bioactive glass is due to solution-mediated dissolution of the material and surface reactions that lead to the formation of a carbonated hydroxyapatite layer. Working directly with calcium phosphate materials is also a possible method of creating such a layer with adequate biological properties, as will be detailed in the next chapter of this review.

II. ELECTROSPINNING OF CALCIUM PHOSPHATES

II.1. INTRODUCTION TO CALCIUM PHOSPHATES AND THEIR BIOACTIVITY

Because the inorganic phase of bone is naturally made of calcium phosphate (CaP), synthetic materials of CaP possess biocompatible properties, as well as osteoconductivity and osteoinductivity [120,121]. When in contact with biological media, the surface of implanted calcium phosphate materials undergo solution-mediated surface reactions which are partly responsible for new bone formation. This may imply not just the dissolution of the CaP material but also the adsorption of ions and proteins on its surface, generally leading to the formation of a carbonated hydroxyapatite. Macrophages, osteoblast, osteoclast-like cells and undifferentiated cells can not only adhere to the resulting surface but also proliferate, potentially differentiate and synthesise the organic phase of bone matrix which is essentially made of collagen. New bone is created after a mineralisation process [122,123]. A diagram representing the interactions between bioactive calcium phosphates and their surrounding biological environment is represented in *Figure 12*.

The most commonly studied crystalline forms of CaP to create biomaterials for BTE are stoichiometric hydroxyapatite (HAp, $Ca_{10}(PO_4)_6(OH)_2$) and tricalcium phosphate (TCP, $Ca_3(PO_4)_2$). TCP was found to stimulate bone formation by Alee in the 1920s, while the osteoconductive properties of hydroxyapatite were reported in the 1970-80s [124]. A mixture with different ratios of HAp and β-TCP (the rhomboedral polymorph of TCP) is also commonly used and called biphasic calcium phosphate BCP [125]. Other possible phases of calcium orthophosphates are listed in *Table 1*. Taking into account the aforementioned biological process of new bone formation, it is evident that an important feature of these calcium phosphate phases is their solubility and thus the speed of their resorption. Resorption is the process by which the material is absorbed into the body, either by cells or via solution-mediated dissolution [126]. As the solubility of each CaP phase is also dependent on temperature and pH, *Figure 13* gives the solubility isotherms of a few selected calcium phosphate phases at 37 °C, which is representative of the temperature conditions experienced in the body. Such solubility isotherms couldn't be found for calcium phosphate electrospun fibres. Similarly, study on their resorption rate in the presence of cells is lacking.

In short, different calcium phosphate phases are studied in the field of biomaterials, especially for the repair and regeneration of bones and teeth as well as for those implants designed to replace some of their missing parts. This is also the case for CaP electrospun fibres. It should be noted that, as for bioactive glasses, dissolution is also governed by the morphology and porosity of the material. Thus, electrospinning allows for the formation of fibres that are more prone to dissolution as opposed to bulk materials. As a reminder, this review is focused on the *in situ* synthesis of inorganic materials that are subjected to electrospinning. In this chapter, the production of calcium phosphate fibres is detailed in terms of chemical synthesis, spinnability, characterisation of obtained phases and first investigations of cellular viability on these biomaterials.

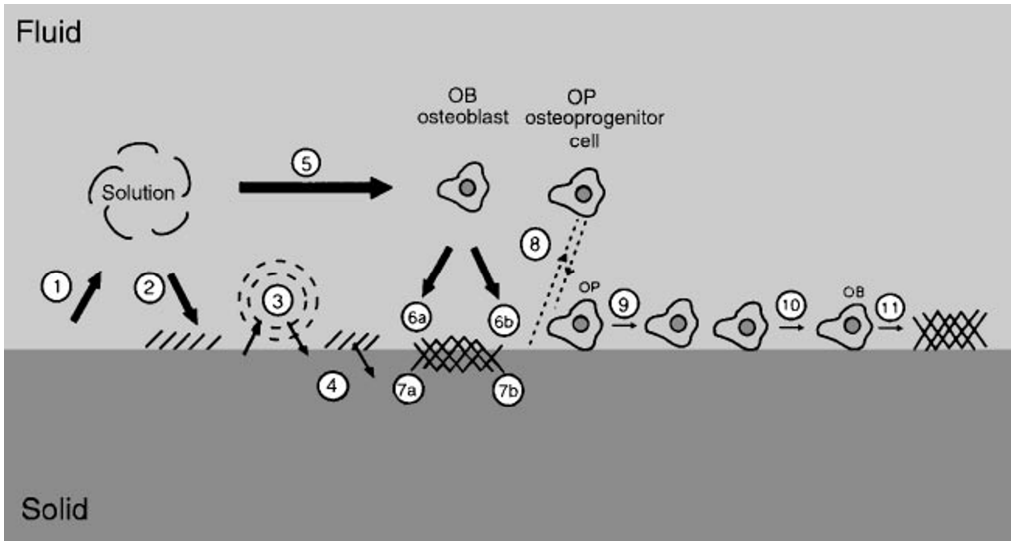

Figure 12. Schematic diagram representing the events that occur at the interface between CaP and the surrounding biological environment. The list does not imply a ranking in terms of time sequence or importance. (1) dissolution from the ceramic; (2) precipitation from solution onto the ceramic; (3) ion exchange and structural rearrangement at the ceramic surface; (4) interdiffusion from the surface into the ceramic; (5) solution-mediated effects on cellular activity; (6) deposition of either the mineral phase (a), or the organic phase (b), without integration into the ceramic surface; (7) deposition with integration into the ceramic; (8) chemotaxis to the ceramic surface; (9) cell attachment and proliferation; (10) cell differentiation; and (11) extracellular matrix formation. Figure and its legend reproduced from [123]

NAME	FORMULA	Ca/P MOLAR RATIO	pH STABILITY RANGE
Monobasic calcium phosphate monohydrate (MCPM)	$Ca(H_2PO_4)_2{\cdot}H_20$	0.5	0.0-2.0
Dicalcium phosphate anhydrous (DCPA), also called monetite	$CaHPO_4$	1.0	2.0-5.5 (>80 °C)
Dicalcium phosphate dihydrate (DCPD), also called brushite	$CaHPO_4{\cdot}2H_20$	1.0	2.0-6.0
Octacalcium phosphate (OCP)	$Ca_8(HPO_4)_2(PO_4)_4{\cdot}5H_20$	1.33	5.5-7.0
α-tricalcium phosphate (α-TCP)	$\alpha\text{-}Ca_3(PO_4)_2$	1.5	Precipitated from aqueous solutions only at T>1125 °C
β-tricalcium phosphate (β-TCP)	$\beta\text{-}Ca_3(PO_4)_2$	1.5	Precipitated from aqueous solutions only at T>800 °C
Amorphous calcium phosphate (ACP)	$Ca_xH_y(PO_4)_z{\cdot}nH_2O$, n = 3–4.5, 15%–20% H_2O	1.2-2.2	≈5-12
Calcium deficient hydroxyapatite (CaDHA, CDHA, CDHAp, precipitated HAp, pHA, pHAp)	$Ca_{10-x}(HPO_4)_x(PO_4)_{6-x}(OH)_{2-x}$ (0<x<2)	1.50-1.67	6.5-9.5
Hydroxyapatite (HAp, OHAp)	$Ca_{10}(PO_4)_6(OH)_2$	1.67	9.5-12.0
Tetracalcium phosphate (TTCP, TetCP)	$Ca_4(PO_4)_2O$	2.0	Precipitated from aqueous solutions only at T>1300 °C

Table 1. Selected CaP phases of interest for biomedical applications, their chemical formula, Ca/P ratios and pH stability range.

Highlighted in grey are the phases studied in the case of electrospinning of *in situ* synthesised CaP. Adapted from [126]

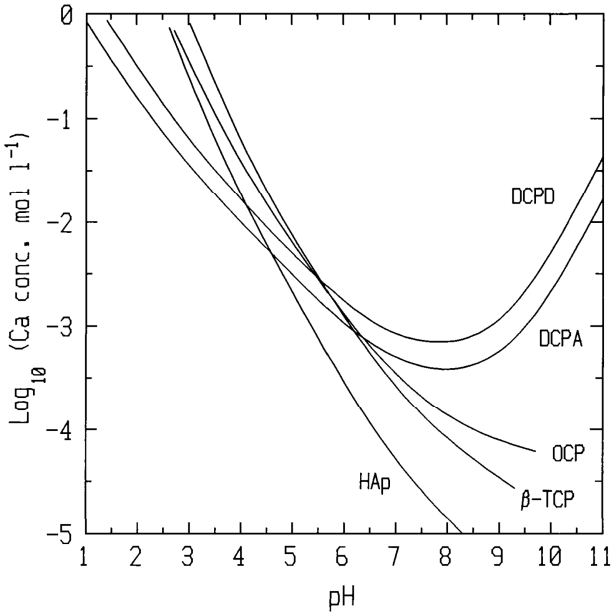

Figure 13. Solubility isotherms (37 °C) of few CaP phases in the system $Ca(OH)_2$-H_3PO_4-H_2O. Notations: DCPD: Dicalcium phosphate dihydrate; DCPA: Dicalcium phosphate anhydrous; OCP: Octacalcium phosphate; β-TCP: β-tricalcium phosphate; HAp: Hydroxyapatite. Reproduced from [127]

II.2. CALCIUM PHOSPHATES SYNTHESIS

Before presenting the crystalline phases obtained after electrospinning the *in situ* synthesised calcium phosphates, the general considerations for their synthesis are first presented in this section II.2, and also summarised in *Figure 14*. Different combinations of phosphorus and calcium precursors were studied for the synthesis of calcium phosphate fibres. In the following, the reactivity of these precursors with respect to the synthesis parameters is presented.

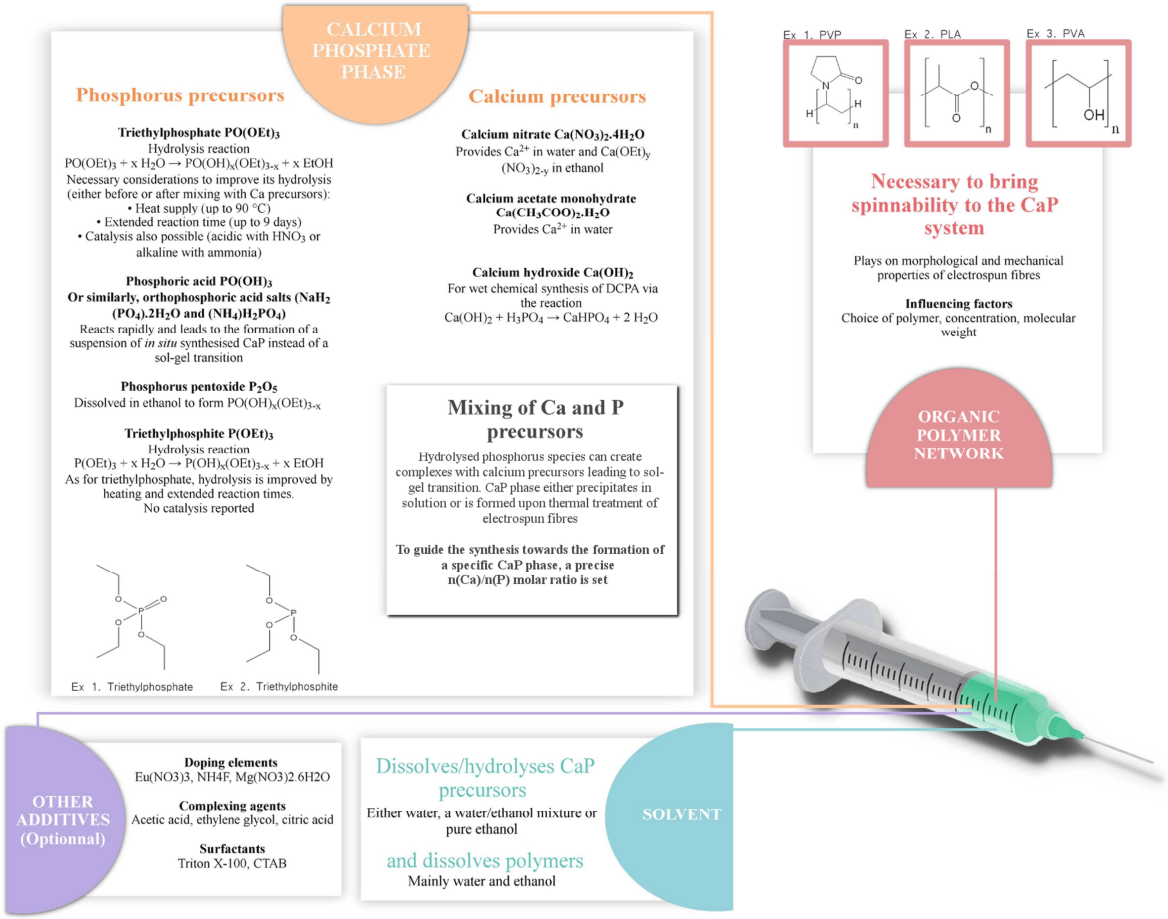

Figure 14. Considerations for the preparation of spinnable calcium phosphate solutions with adequate bioactive properties

II.2.1. Choice of phosphorus precursor

A well-known method for calcium phosphate synthesis is the wet precipitation method, with the neutralisation of the different acidities of orthophosphoric acid by calcium ions. Depending on the pH, different forms of the orthophosphate ions are predominantly present in solution: PO_4^{3-}, HPO_4^{2-}, $H_2PO_4^-$, or H_3PO_4. Therefore, different phases are obtained by the progressive replacement of acidic protons by calcium ions [13]. *Table 1* reports the pH stability range of different CaP phases. A calcium phosphate phase precipitates and can then be subjected, when needed, to thermal treatment to crystallise the desired phase. Sol-gel chemistry is another wet chemistry technique that can be carried out to prepare calcium phosphates. When combined with electrospinning, the sol-gel chemistry can be advantageous to the precipitation method since it doesn't lead to phase precipitation, implying a better chemical repartition into the electrospun fibres. Once more, this justifies the importance of the material *in situ* synthesis.

Using sol-gel synthesis, gel formation results from the hydrolysis and condensation of the phosphorus species present in the solution which is to be electrospun, following the same principle governing silicon species - as previously mentioned in this review. However, the commonly used phosphorus alkoxides present chemical inertia. The appropriate optimisation of the system is thus of primary importance to provide a certain chemical reactivity to the system. The most widely used phosphate precursor is triethylphosphate (TEP), $PO(OEt)_3$, a phosphate ester with a very low hydrolysis constant rate. This hydrolysis results from a nucleophilic substitution that replaces an alkoxide –OEt by a hydroxide –OH, leading to the formation of $PO(OH)_x(OEt)_{3-x}$ species. In water, hydrolysis proceeds via a SN_2 mechanism on the α-carbon atom of the alkoxy group of the ester [128]. Therefore, for the purpose of this hydrolysis, the solvents used contain reacting water, either pure or mixed with an organic solvent

[129–132]. Surprisingly, hydrolysis carried out in almost pure alcohol has also been reported [133–135]. In this case, we suppose that water is supplied by both impure ethanol, ambient humidity and by the water present in the calcium nitrate tetrahydrate used as a calcium precursor in the same solution where the phosphorus is added. However in most of these cases, a lack of detail regarding the synthesis prevents the calculation of a water to TEP molar ratio to further investigate the possibility of this hydrolysis happening. Nonetheless, triethylphosphate $PO(OEt)_3$ does not react under ambient conditions: a heat supply or an acidic or alkaline catalysis is necessary. Unsubstituted trialkyl phosphates display very little sensitivity to acid catalysis [136]. For this reason, alkaline catalysis can be used to obtain $PO(OH)(OEt)_2$ and subsequently acid catalysis is performed to hydrolyse di- and monoesters that hardly react at high pH [137]. Yet, in the papers referring to the electrospinning of TEP-derived calcium phosphates, acid [133] or alkaline [138] catalysis were used alone. Nitric acid was used in the former case, while ammonia was selected in the latter one. No details about the catalysis or proof of its efficiency were reported. It is briefly mentioned that a pH change from 7.5 to 6.5 proves the occurrence of TEP hydrolysis [139]. In the scope of this review, extended reaction times and heating of the precursor solution are the preferred methods of improving TEP reactivity. Indeed, before proceeding to electrospinning, a prolonged hydrolysis and/or reaction time with calcium precursor is always carried out: either of the phosphorus solution alone [131], of the mixture of phosphorus with calcium [6, 8–12, 16], or even after addition of the polymer [133,135,138]. Taking all the published papers together, this reaction time lasts for at least 24 hours but can reach up to 9 days [134]. In addition, the heat supply ranges from 30 °C to 90 °C.

Even though triethylphosphate is largely used, alternative phosphorus precursors are interesting species as they present a higher reactivity. Under ambient conditions, phosphoric acid H_3PO_4 (also written $PO(OH)_3$) reacts too fast in water. Therefore, as previously mentioned, syntheses reporting the use of phosphoric acid are not considered as sol-gel synthesis and lead to the formation of a suspension of *in situ* synthesised particles [141,142], explaining the short reaction times and absence of heating. Similarly, orthophosphoric acid salts were also employed. Specifically, monosodium phosphate dihydrate $NaH_2(PO_4).2H_2O$ [143] and ammonia biphosphate $(NH_4)H_2PO_4$ [130] which can both dissociate in solution, in DMSO (dimethyl sulfoxide) or water respectively, and provide ionic species for the synthesis of calcium phosphates. In addition, dissolving P_2O_5 into alcohols leads to the formation of different $PO(OH)_{3-x}(OR)_x$ species with chemical reactivities in between the one of phosphoric acid and triethylphosphate [137]. This precursor has thus been used for both *in situ* synthesis in the presence of ethanol and subsequent electrospinning after polymeric addition [144,145]. However, ethylene glycol as a stabilizer was necessary in one case to avoid precipitation in the solution by coordinating with calcium metal ions [145]. Another extensively used phosphorus precursor for the sol-gel synthesis of calcium phosphate is triethylphosphite (TEPI). Alkyl phosphites $P(OR)_3$ are hydrolysed much faster than alkyl phosphates $PO(OR)_3$. Indeed, trialkyl phosphites hydrolyse in alkali several hundred times faster than the corresponding phosphates, while in acid the phosphite hydrolyzes 10^{12} times as fast as the phosphates [136]. Using the same hydrolysis process that was previously suggested for triethylphosphate, hydrolysed triethylphosphite species are created as follows: $P(OC_2H_5)_3 + H_2O \rightarrow P(OC_2H_5)_{3-x}(OH)_x + x\ C_2H_5OH$ [146]. This TEPI precursor has been used for the purpose of electrospinning calcium phosphates [140,147–150]. As for syntheses with triethylphosphate, the ones with triethylphosphite involve hydrolysis of the precursor in water [140,147,148], a mixture of water and ethanol [150], or in ethanol alone [149]. In this last study where ethanol is the only solvent, water brought by the calcium nitrate tetrahydrate precursor can be sufficient for triethylphosphite to hydrolyse, as the water/phosphorus molar ratio is 6.7 and therefore above the stoichiometric ratio of 3. No acid- or alkaline-catalysis were used to increase TEPI reactivity.

Subsequently to hydrolysis, hydrolysed phosphorus species can then create complexes with calcium present in the system, leading to polymerisation and as a result to a sol-gel transition [151,152].

II.2.2. Selection of calcium source

For calcium phosphate synthesis, hydrolysed or dissociated phosphorous precursors are mixed with calcium species. Calcium nitrate tetrahydrate is by far the most common precursor [129,131–

135,138,140,142–145,147–150]. It provides Ca^{2+} calcium ions in water and $Ca(OEt)_y(NO_3)_{2-y}$ species in anhydrous ethanol, which will further interact with phosphorus species upon ageing to form Ca-P intermediates containing Ca-O-P bonds [152]. Possible reactions pathways between hydrolysed triethylphosphite and calcium nitrate in water- or ethanol-based solutions were suggested by Dean-Mo Lia *et al.* [152]. The advantages of calcium nitrate over the other precursors are its solubility and its ability to provide oxidizing agents (the nitrate anions) which facilitate the decomposition of organic species during heat treatment. Though, as previously explained, due to their toxicity, nitrates need to be eliminated at high temperature (700-800 °C) for the materials to be used in biological applications. Other calcium precursors were also selected, such as calcium acetate monohydrate which can produce calcium ions in water [139] and calcium hydroxide $Ca(OH)_2$. The latter was used during the wet chemical synthesis of DCPA ($CaHPO_4$), through the following reaction: $Ca(OH)_2 + H_3PO_4 \rightarrow CaHPO_4 + 2H_2O$ [141]. However, none of the reported works actually investigated the reaction of hydrolysed phosphorus species with calcium precursors. Franco *et al*. briefly mentioned that an incomplete reaction could be explained by a high gel conductivity due to the dissociation of the calcium nitrate that did not react [144].

II.2.3. Experimental considerations for the synthesis

Experimentally, in almost all cases, calcium and phosphorus precursors are first mixed and the solution is then aged. Next, a polymer is incorporated and the resulting mixture homogenised. The benefits of polymer incorporation with regard to electrospinning are detailed in the next section. Though, in terms of the synthesis, Tesik Chae *et al.* reported that better elemental repartition was observed when PLA was first mixed with calcium precursor before the addition of the phosphorus source [143]. This observation accounted for an initial complex formation between the calcium ions and PVA carbonyl groups which form nucleation sites that are well scattered in the material. Thus, a more uniform calcium phosphate formation is obtained compared to when phosphorus is added beforehand.

Also, an important consideration is how to trigger the formation of the desired calcium phosphate phase. Indeed, each phase has a specific dissolution rate and thus biological properties, as previously explained. As was also mentioned in section II.2.1, during the wet precipitation method, the pH of the solution is the main factor influencing the orientation of the synthesis towards a specific phase. However in all the sol-gel systems used for electrospinning, the pH was not studied and controlled by the researchers. It is supposed that the main influencing factor for this method of synthesis is the input value of calcium to phosphorus molar ratio. Intermediates containing both Ca and P in the sol are transformed into the desired CaP phases during the thermal treatment of the obtained fibres, when the organic species are decomposed. This is similar to dry synthesis, in which the precursors are mixed with a specific n(Ca)/n(P) molar ratio that conditions the formation of a specific phase which can be obtained during calcination. For all these reasons, the ratio between calcium and phosphorus precursors, set during the synthesis, is of prime importance.

Besides calcium and phosphorus, precursors of other elements (such as magnesium and fluorine) can be added during the material synthesis in order to incorporate desired elements into the calcium phosphate lattice and provide the materials with additional - mainly biological - properties. Both these aspects will be discussed with more details in sections II.4.1 and II.5.

Finally, ethylene glycol was used as a complexing agent during the synthesis of calcium phosphates as a stabiliser to avoid colloidal particles gathering as they are prone to precipitation and crystallisation [145].

II.3. FROM CALCIUM PHOSPHATE SOLUTION TO CaP FIBRES

II.3.1. Electrospinning and effects of solution and process parameters

As previously presented for SiO_2 fibres and bioactive glasses in the first chapter (I), polymer addition helps in improving the spinnability of the solutions. Most of the time, smooth fibres are obtained after electrospinning. However, adjusting the parameters can help in tailoring the final characteristics of the fibres, as presented for bioactive glasses in section I.3.1. The same trends are observed when adjusting electrospinning parameters for CaP materials as for SiO_2 or bioactive glasses.

When it comes to calcium phosphate materials, none of the published works with electrospinning could be performed without supplementing the solution with a polymer. Without a polymer, droplets instead of fibres were obtained [145,147,153]. This could be due to the lower ability of phosphorus to create a viscous gel and macromolecules as opposed to silicon-based sol-gel systems [137]. Actually, in the study of Yuanyuan *et al*. [145], while polymer-free calcium phosphate sol presented a viscosity of 25 mPa.s, uniform electrospinning could only be achieved when the viscosity was adjusted to a minimum of 63 mPa.s by adding 2% of PVP. It was also reported that beaded filaments or webs instead of individual electrospun fibres were formed when the viscosity was low [140,147,153]. For instance, smooth fibres could be obtained from a PVA-CaP sol solution with a viscosity value of about 1.4 Pa.s (see *Figure 15.I.a*), while beads were obtained for a viscosity of around 0.1 Pa.s (*Figure 15.I.b*) [153]. Similarly in the same study but using a PVA with a different molecular mass, smooth filaments were obtained for a viscosity of 2.6 Pa.s (*Figure 15.I.c*) while a value of 0.8 Pa.s led to the formation of fused webs (*Figure 15.I.d*).

For calcium phosphates, the most commonly used polymer is by far PVP [132–135,138,140,142,144,145] as it is soluble not only in water but also in ethanol, the two most commonly used solvents for the synthesis of CaP. Other sparsely used polymers are PAN [131], PVA [132,147,148,153], PLA [141,143], PLA/Polyethylene glycol PEG [143], gelatine [149], PVB [150] and PEO [139]. Increase in solution viscosity was directly linked to a raise of polymer concentration [145], polymer molecular weight [147,153] and had a direct influence on fibre diameter [145]. However, while achieving a high level of viscosity is beneficial for the purpose of electrospinning, an intimate mixing of the CaP sol and polymer macromolecules is only possible at limited viscosity [153]. Consequently, a compromise has to be found in terms of viscosity in order to allow a uniform elemental repartition of elements along the fibres (viscosity as low as possible), and a good spinnability of the solution (moderate to high values of viscosity).

The electrospinning process itself can also be optimised to tailor the fibre morphology by varying the process parameters, such as the tip-to-collector distance, spinning voltage or relative humidity [145]. For instance, it was possible to obtain CaP microribbons instead of nanofibres by increasing the PVP concentration (from 8.7 to 9.8 wt%), the feeding rate (from 0.5 to 0.75 mL/h), the voltage (from 8 to 10 kV) and the needle to collector distance (from 16 to 16.5 cm) during electrospinning (see *Figure 15.II*) [130]. In their study, Touny and Bhaduri created porosity by Water Induced Pore Formation (WIPF) resulting from a cement forming reaction of $Ca(OH)_2$ with phosphoric acid [141] (see *Figure 15.III*). This reaction creates water as a by-product as well as heat, which improves solvent evaporation during electrospinning. As water is not a solvent for PLA (the polymer used in that case), it creates pores through the evaporation of unmixed droplets. The feeding rate, spinning voltage and calcium phosphate content play a role in water and heat formation as well as solvent evaporation, making it possible to tailor the resulting porosity.

Furthermore, it was possible to supplement the calcium phosphate solution with additives - in addition to polymers - in order to ease the electrospinning process. The presence of citric acid in the solution helped to reach adequate conductivity for electrospinning [148]. Its use also ensured that the fibrous structure was maintained both before and after the heat treatment of the as-spun fibres that displayed moisture instability [148]. Acetic acid was used as a complexing agent to endow better stability to the electrospinning process [142]. Indeed, the aim was to chelate the conductive metal ions that are responsible for the effective ionic strength of the solutions, which destabilises the electrospinning process. This acid however modified the crystalline phases obtained after calcination (this will be discussed later in section II.4.2.). Similarly, little is said about the reasons that prompted the use of triton X-100 (t-Octylphenoxypolyethoxyethanol) as a surfactant, but it was suggested that this facilitated the spinnability and stabilisation of the electrospun jet [143]. Finally, the production rate could be increased via needle-less electrospinning (NLE) also known as free liquid surface electrospinning [158]. In the corresponding

method, the solution which is to undergo electrospinning is loaded into a bath with a rotating electrode. Numerous fibres are created directly and ejected to the collector from the surface of the electrode.

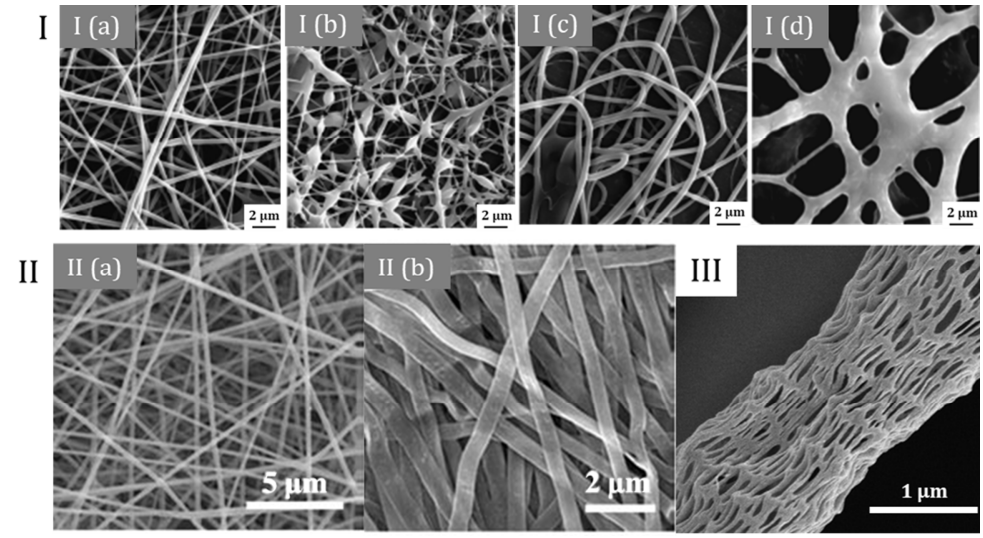

Figure 15. Examples of the effects of solution properties and electrospinning process on the morphologies of electrospun materials. (I) Different viscosities of PVA-CaP sols led to the formation of (a) smooth filaments and (b) beaded filaments for viscosity values of 1.4 and 0.1 Pa.s respectively (PVA molecular weight: 67 500 g/mol); (c) smooth filaments and (d) fused webs for viscosity values of 2.6 and 0.8 Pa.s respectively (PVA molecular weight: 155 000 g/mol). Adapted from [153]. (II) Adjusting electrospinning parameters led to the formation of either Europium-doped hydroxyapatite (a) filaments or (b) microribbons. Adapted from [130]. (III) Porous fibres of $CaHPO_4$ and PLA resulting from WIPF (Water Induced Pore Formation). Reproduced from [141]

II.3.2. Thermal treatment

Post-treatments of as-spun fibres are usually necessary to eliminate the carrying polymer and thus obtain pure inorganic fibres. Nevertheless, this step is principally necessary to crystallise the CaP phases from the calcium and phosphorus intermediates formed by sol-gel, as discussed in the next section (II.4). In addition, controlling the thermal treatment can increase their crystallinity [148]. On the contrary, dicalcium phosphate anhydrous is obtained at low temperature and therefore in that case, no calcination is required [141,143]. Also, the degradation of this phase into calcium pyrophosphate ($Ca_2P_2O_7$) - an undesired toxic element - occurs at around 320-340 °C [13]. Furthermore, drying the fibres at 85 °C for 5 hours was shown to be beneficial in maintaining the initial morphology of the electrospun fibres, whereas those filaments merged into connected fibre webs when dried at room temperature for 24 hours [140]. Different effects result from thermal treatment and include the loss of fibrous morphology when electrospun fibres present uneven structures [153], the formation of micropores at the fibres surface [153] and a shrinkage of fibre diameter [130,133,140,145,150].

II.4. CRYSTALLINE PHASES OF CALCIUM PHOSPHATE FIBRES

As previously discussed, the differences in each calcium phosphate phase - in terms of chemical composition or crystallinity – impact on their dissolution behaviours and as a result on their bioresorption rate and bioactivity [120]. In the literature, *in vitro* evaluation of *in situ* synthesised and subsequently electrospun CaP material is very poorly reported, while no *in vivo* study could be found. However, different CaP phases can be obtained and are presented in this section, to give an initial insight into the potential synthesis and processability of calcium phosphate nanofibres. Three paragraphs are developed below; each of them is dedicated to one of the main (and desired) phases composing the final material: hydroxyapatite, β-tricalcium phosphate or dicalcium phosphate anhydrous. A summary of the obtained phases in respect to the synthesis conditions is presented in *Table 2*.

It is assumed that the input value of Ca/P atomic ratio in the sol-gel system orientates the formation of a preferred CaP phase during thermal treatment. *Table 1* gives the Ca/P ratios of different phases of calcium phosphate. Stoichiometric hydroxyapatite $Ca_{10}(PO_4)_6(OH)_2$ for instance has a Ca/P molar ratio of 1.67, while it is 1.50 for β-TCP $Ca_3(PO_4)_2$. This is the reason why different calcium to phosphorus values are chosen for calcium phosphate sol-gel synthesis, depending on which crystalline phase is desired after the heat treatment of the as-spun fibres. Nonetheless, obtaining a single-phase calcium phosphate is very challenging.

II.4.1. Hydroxyapatite

In a few studies, the Ca/P molar ratio was set to 1.67 with the aim of obtaining a stoichiometric hydroxyapatite $Ca_{10}(PO_4)_6(OH)_2$. It was shown that XRD amorphous calcium phosphates were not only obtained as-spun [129,145] but also after treatment at 400 °C [140] or even 500 °C [144]. Crystallisation usually began around 500–600 °C [140,144,149] and increased with the rise in temperature. Crystallisation of pure hydroxyapatite was reported by M. Streckova *et al*. [148] after sintering electrospun fibres at 800 °C.

However, undesired crystalline phases could also appear beside hydroxyapatite upon sintering due to different factors such as change in pH, ageing time, as well as the order of addition of the precursors [122] and the temperature and the atmosphere of the thermal treatment. Another common event disturbing the stoichiometric hydroxyapatite lattice is the substitution of ions, such as PO_4^{3-} and HO^- by CO_3^{2-} that may lead to the apparition of new phases (β-TCP, CaO) after calcination. In the case of *in situ* synthesis and electrospinning of CaP, no reasons are given for the apparition of additional undesired phases besides HA in the published papers and probably a lack of analysis can be noticed, but more details about the stability and apparition of new phases during the synthesis of bulk hydroxyapatite are available in the literature [13,127].

For instance Zang *et al.* did indeed evidence the carbonation of calcium phosphate by FTIR in as-spun fibres, through the presence of vibration modes of CO_3^{2-} at 1427 and 870 cm^{-1} [133]. XRD analysis confirmed the phase separation of stoichiometric hydroxyapatite and calcium oxide after treatment at 800 °C. Similary, Jung-Hee Lee and Young-Jin Kim state that they obtained hydroxyapatite after the treatment of amorphous fibres at both 600 and 800 °C [149]. However, the presence of the diffraction peak at 37 °(2θ) (XRD analysis with a copper anticathode) seems to support the formation of a supplementary CaO phase, which is consistent with the carbonation of apatite evidenced by FTIR at lower temperature. The apparition of β-TCP after treatment of amorphous fibres at 600 °C was also reported [140], as well as the formation of both β-TCP and CaO after calcination of fibres at a temperature comprised between 600 and 800 °C [132,144]. It was also reported that the choice of the polymer also affects the nature of obtained CaP phases while composition of the CaP sol is kept identical [154]. Yet, no investigation on the influencing factor was made to understand this phenomenon.

Obtaining a single-phase hydroxyapatite thus represents a challenging task, and undesired phases such as β-TCP and CaO can crystallise during heat treatment. Actually, because a polymer is necessarily added in the CaP solution to be electrospun, the calcination step performed on the filaments leads to the formation of carbonates that enter the hydroxyapatite lattice. New phases can then appear by decomposition of the resulting carbonated HAp upon treatment [13]. An adequate characterisation of the obtained material is thus required to evidence the presence of a carbonated phase, which can be detected by FTIR but not by XRD. Furthermore, while β-TCP is a biocompatible phase and is sometimes required to optimise the solubility of CaP materials, the presence of CaO has to be avoided due to its strongly alkaline pH which could be detrimental to osteoblastic cells [155].

Adding doping elements to the apatite lattice can also be beneficial in obtaining materials with additional biological or optical properties. Doping a hydroxyapatite phase with Europium using $Eu(NO_3)_3$ enabled photoluminescent fibres to be obtained (see the II.5. “applications” section for more details) without disturbing the apatite lattice [130]. The same outcome was noted with the incorporation of fluorine (using NH_4F) within the apatite lattice to form $Ca_{10}(PO_4)_6(OH)_{2-2x}F_{2x}$, where x = 0.25 [150]. Contraction of the lattice along the a-axis direction while the c-axis remained unchanged was consistent

with the literature and confirmed fluorine positioning in the hydroxyl site. In contrast, doping fibres with magnesium using magnesium nitrate hexahydrate ($Mg(NO_3)_2{\cdot}6H_2O$) resulted in the formation of Mg-whitlokite ($(Ca_{18}Mg_2H_2(PO_4)_{14}$) and traces of MgO after heat treatment instead of doped-hydroxyapatite [148]. Fluorine-doped apatitic fibres were expected to have high stability properties, to stimulate bone cell responses and improve mineralisation and bone formation but no biological assays were reported [150]. Applications of europium and magnesium doped CaP fibres will be further detailed in their own dedicated section (II.5.1 and II.5.2 respectively).

II.4.2. Tricalcium Phosphate

Tricalcium phosphates $Ca_3(PO_4)_2$ are calcium phosphate phases distinguishable by their allotropic forms. The rhomboedral polymorph of TCP is called β-TCP and has been used clinically as a bone filler and artificial tooth root and skull [135]. Its synthesis, physico-chemical properties and *in vivo* behaviour have been reviewed recently [156]. For its synthesis in electrospun solutions, a Ca/P molar ratio equals to 1.50 is experimentally set.

As previously outlined for stoichiometric hydroxyapatite, obtaining pure β-TCP fibres can be challenging. Indeed, for a fixed Ca/P ratio of 1.50, different phases besides or instead of β-TCP were obtained after annealing as-spun fibres [142]: CaO, α-TCP (the high temperature polymorph of TCP) and other CaDHA. The amount of each phase was shown to be dependent on the type of heating apparatus (convection oven or microwave oven, both of which display different heating/cooling rates), on the dwelling time and on the presence or absence of acetic acid which is used as a chelating agent to stabilise the electrospinning process. Although β-TCP starts forming at 800 °C [13], it is usually heated at high temperatures around 1100 °C for better stability and density [157]. However, a loss of fibrous structure was evidenced when β-TCP/PVP-based fibres were annealed above 1000 °C. On the contrary when using PAN-based fibres, sintering of the material at 1100 °C under N_2 atmosphere is compatible with a conservation of fibrous morphology [131]. As a result, carbon nanofibres decorated with β-TCP nanoparticles were obtained. Formation of an apparently pure β-TCP phase crystallised during thermal treatment was confirmed by HR-TEM, SAED pattern and XRD. It was decided not to go into too much detail on these materials in this review, due to the uneven repartition of the ceramic phase in the fibres, but readers are redirected to the original papers for further details on their biological evaluation [131].

II.4.3. Dicalcium phosphate anhydrous

Dicalcium phosphate anhydrous (DCPA) $CaHPO_4$ is a calcium phosphate with a higher solubility than HAp and β-TCP (*Figure 13*). This phase was reported to enhance bone healing during *in vivo* testing of rabbit calvaria defects [158]. Also called monetite, this material was electrospun following an *in situ* synthesis in the presence of a spinnable polymer. A reaction of calcium nitrate tetrahydrate and sodium phosphate monobasic dihydrate was carried out at pH 4 in a mixture of organic solvents [143]. In another study, DCPA was also synthesised via an *in situ* cement forming reaction, but it was suggested that unreacted calcium hydroxide $Ca(OH)_2$ may be found in the final material [141]. In both these articles reporting the formation of DCPA electrospun fibres, no thermal treatment was required to induce monetite crystallisation. In actual fact this phase decomposes at low temperatures to form calcium pyrophosphate, a reason why thermal treatment should be avoided. However, the presence of polymers in the solution during monetite synthesis highly limits its crystallisation. It is suggested that polymer molecular chains hinder the transportation of precursor ions during nucleation and crystal growth. EDX mapping also evidenced the lack of homogeneity in phosphorus and calcium repartition in the prepared fibres.

II.4.4. Conclusion on the crystallinity of electrospun CaP fibres

Even though it has been reported that it is possible to prepare fibres of hydroxyapatite, β-tricalcium phosphate and dicalcium phosphate anhydrous deriving from an *in situ* reaction and further

electrospinning, obtaining single-phase materials is a challenging task. These aforementioned studies prove the importance of precisely controlling both the environment of the precursors during CaP synthesis and the conditions for heat treatment so as to initiate crystallisation of the desired calcium phosphate phase. While undesired crystallised phases can result from the substitution of some ions in the CaP lattice, controlling these substitutions can allow for the preparation of new materials with advanced properties. This was the expected result when synthesised CaP was doped with europium [130], magnesium [148] or fluorine [150]. After thermal treatments, electrospun fibres are made of calcium phosphates crystallites with sizes up to 100 nm [132,133,142–144,150,154] and spherical [130,131,133] or polygonal [150] shapes. Also, the size of the crystallites increases with the temperature of the thermal treatment [132,133,144,154]. When comparing fibres treated at 600 and 800 °C, the size ratio can even reach a value of 17 [154]. Applications of these CaP doped-fibres will be presented in the following section.

CaP precursors and doping elements (if any)	Ca/P molar ratio	Polymer	Solvents	Other additives	Synthesis conditions before electrospinning	Thermal treatments and CaP phases evidenced by XRD analysis	Ref
$Ca(NO_3)_2 \bullet 4H_2O$ Triethylphosphate	1.67	Not specified	Distilled water 2-methoxyethanol		• Separate solutions of precursors mixed for 2-3 h • Ageing 48 h at 80-90 °C • Solvent evaporation • Mixing 10 h with the polymer	• Drying for 1 h at 150 °C • Then treated for 2 h at 350 °C (2 °C/min) followed by: - 1 h at 500 °C → HAp, CaO, $CaHPO_4$, β-TCP - 1 h at 600 °C → HAp, trace of β-TCP	[129]
$Ca(NO_3)_2 \bullet 4H_2O$ P_2O_5	1.67	PVP (1,300,000 g/mol)	Ethanol	With or without ethylene glycol as stabiliser	• Separate solutions of precursors mixed for 10 min • Polymer addition and stirring for 24 h	• Drying for 24 h → XRD amorphous • Then 3 h at 350 °C (1 °C/min) and 1 h at 600 °C (10 °C/min) → HAp	[145]
$Ca(NO_3)_2 \bullet 4H_2O$ Triethylphosphite	1.67	PVP (1,300,000 g/mol)	Water Ethanol		• Separate solutions of precursors mixed for 15 min and aged 2 h at 45 °C • Mixing with PVP solution	• Drying for 24 h at RT or for 5 h at 85 °C) • Then annealing for 10 min at: - 400 °C → Amorphous - 500 °C → Beginning of crystallisation - 600 °C → HAp + β-TCP	[140]
$Ca(NO_3)_2 \bullet 4H_2O$ P_2O_5	1.67	PVP (1,300,000 g/mol)	Water Ethanol		• Separate solutions of precursors mixed for 24 h • Mixing with PVP solution	• Drying for 24 h and treated at 350 °C for 2 h (2 °C/min) • Then, treated for 30 min (10 °C/min) at: - 500 °C → Amorphous - 600 °C → HAp - 700 °C → HAp + β-TCP + CaO	[144]
$Ca(NO_3)_2 \bullet 4H_2O$ Triethylphosphite	1.67	Gelatin	Ethanol Water TFE		• Separate solutions of precursors mixed for 24 h at 40 °C, then aged at 60 °C for 6 h • Solvent evaporation for 1 h • Mixing with gelatin solution, 12 h	• Treated for 1 h at 200 °C • Then, post treatment for 1 h at: - 400 °C → Amorphous - 600 °C → HAp + CaO - 800 °C → HAp + CaO	[149]
$Ca(NO_3)_2 \bullet 4H_2O$ Triethylphosphate	1.67	PVP (1,300,000 g/mol)	Water		• Separate solutions of precursors mixed for 24 h • Mixing with polymer solution	• Drying for 24 h at 60 °C and treatment at 350 °C for 2 h (1 °C/min) • Then, post treatment for 1 h (10 °C/min) at: - 600 °C → HAp - 800 °C → HAp + β-TCP + CaO	[132]

CaP precursors and doping elements (if any)	Ca/P molar ratio	Polymer	Solvents	Other additives	Synthesis conditions before electrospinning	Thermal treatments and CaP phases evidenced by XRD analysis	Ref
$Ca(NO_3)_2 \bullet 4H_2O$ Triethylphosphite	1.67	PVA (85,000-124,000 g/mol)	Water	Citric acid	• Separate solutions of precursors mixed for 2 h at RT • Addition of citric acid, ageing for 8 h at 80 °C • Mixing with PVA solution	• Drying for 30 min at 80 °C • Then, post treatment for 6 h (10 °C/min) at: - 600 °C → HAp - 800 °C → HAp	[148]
$Ca(NO_3)_2 \bullet 4H_2O$ Triethylphosphite $Mg(NO_3)_2 \bullet 6H_2O$						• Drying for 30 min at 80 °C • Then, post treatment for 6 h (10 °C/min) at: - 600 °C → poorly crystallised whitlockite ($Ca_{18}Mg_2H_2(PO_4)_{14}$) - 800 °C → whitlockite, MgO	
$Ca(NO_3)_2 \bullet 4H_2O$ Triethylphosphate	1.67	PVP (40,000 g/mol)	Ethanol		• Precursors are mixed in ethanol for 3 h and aged for 48 h at 80 °C • Mixing with PVP solution for 24 h	• Treatment at 300 °C for 1 h (5 °C/min) • Then, post treatment for 1 h (5 °C/min) at: - 600 °C → HAp, CaO - 800 °C → HAp, CaO	[133]
$Ca(NO_3)_2 \bullet 4H_2O$ $(NH_4)H_2PO_4$ $Eu(NO_3)_3$	1.67	PVP (1,300,000 g/mol)	Water Ethanol pH is stabilised at 2-3 adding HNO_3	Citric acid CTAB (N-cetyltrimethylammonium bromide)	• Separate solutions of precursors are mixed with citric acid solution • Addition of CTAB • Addition of PVP, mixing for 3 h	• As-spun → Amorphous • Then, post treatment for 3 h (1 °C/min) at: - 500 °C → Amorphous - 600 °C → Eu-doped HAp - 700 °C → Eu-doped HAp - 800 °C → Eu-doped HAp + weak trace of CaO	[130]
$Ca(NO_3)_2 \bullet 4H_2O$ Triethylphosphite NH_4F	1.67	PVB	Ethanol Water		• Separate solutions of precursors are stirred for 24 h and then aged for 10 days • Vortexed with PVB solution and stirring for 24 h	• Treated for 2 h at 700 °C (1 °C/min) → Fluorinated HAp	[150]

CaP precursors and doping elements (if any)	Ca/P molar ratio	Polymer	Solvents	Other additives	Synthesis conditions before electrospinning	Thermal treatments and CaP phases evidenced by XRD analysis	Ref
$Ca(NO_3)_2•4H_2O$ Triethylphosphite	1.67	Gelatin	Ethanol TFE Water		• Separate solutions of precursors are mixed for 24 h at 40 °C and aged for 6 h at 60 °C • Solvent evaporation for 1 h • Mixing with polymer solution	• Treated for 2 h at 200 °C (1 °C/min) • Then, post treatment for 6 h (1 °C/min) at: - 600 °C → Mainly amorphous - 700 °C → HAp + β-TCP - 800 °C → HAp + β-TCP	[154]
		PVP (1,300,000 g/mol)	Ethanol Water			• Treated for 2 h at 350 °C (1 °C/min) • Then, post treatment for 6 h (1 °C/min) at: - 600 °C → HAp + CaO - 700 °C → HAp + CaO - 800 °C → HAp	
$Ca(NO_3)_2•4H_2O$ Phosphoric acid	1.50	PVP (360,000 g/mol)	Ethanol Water	With or without acetic acid	• Separate solutions of precursors are mixed • Addition of PVP	• Treatment at 950 °C for 1.5 h, without acid: β-TCP, HAp, α-TCP • Or treatment at 1050 °C - With acid → CaDHA, α-TCP, CaO - Without acid → β-TCP, α-TCP, CaO	[142]
$Ca(NO_3)_2•4H_2O$ Triethylphosphate	1.50	PAN (100,000 g/mol)	Water DMF		• Ca precursor is added in a solution of hydrolysed TEP, stirring for 120 h at RT • Addition of PAN solution, stirring for 6 h at RT	• Treatment at 260 °C for 30 min • Then, heating at 1100 °C for 2 h in N_2 → β-TCP	[131]
$Ca(NO_3)_2•4H_2O$ $NaH_2(PO_4)•2H_2O$	1.65	PLA PEG (20,000 g/mol)	THF DMF DMSO	Triton X-100	• Calcium precursor is dissolved in the PLA solution • Mixing with the $NaH_2(PO_4)•2H_2O$ solution, stirring for 24 h • Synthesis is performed at pH 4 • Mixing with PEG solution for 6 h • Addition of Triton X-100 solution	• Washing with deionised water by vacuum filtration and freeze drying in a lyophilizer → DCPA, weakly crystallised	[143]
$Ca(OH)_2$ H_3PO_4	Not given	PLA (114,000 g/mol)	Water DMF Chloroform	$NaHCO_3$	• Mixing H_3PO_4 and $NaHCO_3$ with water • Addition of $Ca(OH)_2$ • Mixing with PLA solution	• Drying at RT → very poorly crystallised DCPA, possible trace of $Ca(OH)_2$	[141]

Table 2. Overview of CaP phases obtained in relation to solutions compositions and thermal treatments carried out on electrospun fibres. Phases reported are the ones detected in XRD diffractograms. Ca/P molar ratios are the one set experimentally for the synthesis.

II.5. APPLICATIONS OF CaP FIBRES IN BONE TISSUE ENGINEERING

Although several studies report the production of calcium phosphate nanofibres, their characterisation is quite limited and in particular, their biological application properties have been poorly investigated. In the following will be presented the assessment of their potential application as drug carriers, followed by investigations into the *in vitro* biocompatibility of CaP nanofibres and CaP nanofibrous coatings.

II.5.1. CaP fibres as drug carriers

The first reported application of CaP electrospun fibres was their use as drug carriers to control and extend drug release time in the body. The aim was to deliver therapeutic drugs directly to the targeted cells or tissues as well as maintaining the optimum concentration for delivering an efficient therapeutic effect [130]. Just like bioactive glasses, hydroxyapatite based-fibres can present the appropriate surface properties for such applications. First of all, they can display the mesoporosity necessary for hosting the medicine, but the –OH group at their surface can also bind directly to the drugs. Indeed, the hydroxyl group reacts with appropriate drug functional groups without spoiling their molecular structure [130]. Diffusion, resorption of calcium phosphate and ionic exchanges between the medium and the fibres are the main mechanisms leading to the release of medicines from calcium phosphate nanocarriers.

It is in this scope that fibres consisting in apatitic interconnected grains of approximately 24 to 40 nm were created [133], as presented in *Figure 16.II*. The porosity created by narrow intervals between those sintered grains was assumed to be capable of hosting the studied protein, BSA (Bovine Serum Albumin); but the size of the porosity is not mentioned. When protein-adsorbed HAp fibres were dispersed in PBS, BSA was initially released at a relatively large rate and accumulative release reaches around 70% within the first 6 days (*Figure 16.I*), which is a suitable timescale for drug release purposes. During this step, no difference was observed between the samples with distinct HAp sizes (which depend directly on the CaP sol concentration in the electrospun solution as well as on the sintering temperature). Then, sustained release at a steady and slow rate continued until day 18. During this last stage, higher released amounts were evidenced for samples containing more CaP sol and calcined at lower temperatures. However, no statistical error bars are drawn, rendering the analysis difficult regarding the influence of these parameters.

Another study investigated hydroxyapatite-based nanofibres and microribbons as drug carriers of Ibuprofen, a nonsteroidal analgesic and anti-inflammatory drug commonly used as a drug model [130]. The drug was loaded in mesopores created at the fibre/ribbon surface (pore size close to 14 nm) through the thermal removal of CTAB (Cetyltrimethylammonium bromide) micelles. In this case, a burst release was evidenced as the entire content of the loaded drug was released after 24 hours. However, an interesting aspect of this research is the doping of nanofibres and microribbons with europium, which provides red photoluminescence that can help in evaluating the efficiency of drug release. Indeed, the presence of ibuprofen in the fibres quenches the luminescence of Eu^{3+}, leading to a decrease in emission intensity. When ibuprofen is released, the quenching effect is weakened and results in an increase in emission intensity. Although the relation between the cumulative released amount of drug (determined via ibuprofen's absorbance) and photoluminescent emission intensity is not linear, both values can be correlated by a monotonic function, as illustrated in *Figure 17.* After optimisation, this fluorescent effect could be useful for tracking the drug-release process.

Similarly to Si-based filaments, fibres of CaP produced for drug delivery purpose have not been biologically tested. Thus, no conclusion on the beneficial or detrimental effect of the delivered drug on cell activity can be drawn.

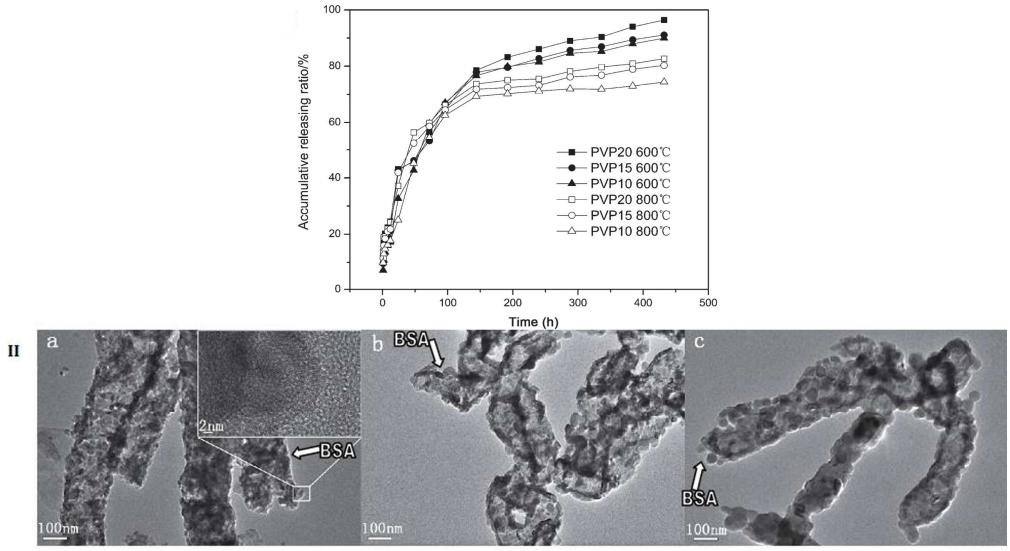

Figure 16. I- Cumulative release curve of BSA from HA fibres. PVP concentration remained constant in all electrospun solutions (25 w/v%). PVP20, PVP15 and PVP10 contained respectively 20, 15 and 10 wt% of HAp precursor based on the weight of PVP. II- FESEM images of some HAp fibres: PVP10 treated at (a) 600 and (b) 800 °C; (c) PVP20 treated at 800 °C. Arrows indicate examples of possible BSA loading sites. Adapted from [133]

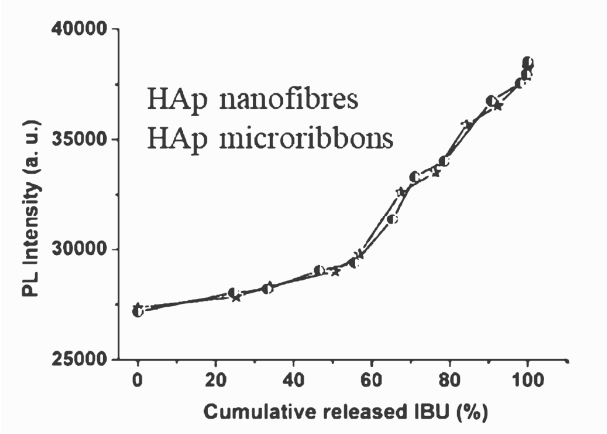

Figure 17. Photoluminescent emission intensity of Eu^{3+} in IBU-HAp nanofibres and microribbons, as a function of cumulative amount of released ibuprofen. Reproduced from [130]

II.5.2. First *in vitro* investigations of CaP electrospun fibres

Only few biological studies have been reported for the characterisation of calcium phosphate electrospun fibres. Two acellular assessments were made on CaP materials in simulated body fluid (SFB) [132,149]. But because the layers formed on the immersed materials were not characterised at all in these studies, results are not reviewed here as it would be hard to draw a conclusion on such poor investigations. In actual facts, only two articles in the literature report the *in vitro* cellular assessment of CaP electrospun fibres, while no *in vivo* study could be found. *In vitro* investigations of HAp fibres demonstrated that these ceramic fibres favoured the proliferation of mouse calvaria osteoblasts (MC3T3-E1) compared to tissue culture plate (*Figure 18*).

M. Streckova *et al*. created for their part calcium phosphate fibrous coatings (1-2 µm) on the surface of Ti–6Al–4V titanium alloy [148]. Also called TA6V, this alloy is used extensively in the field of orthopaedics and dental applications. Titanium presents good biocompatibility, resistance to corrosion and mechanical strength. However, Ti and its alloys lack bioactivity and osseointegration. For these reasons, coatings can be applied to their surface to act as a biological active layer that will favour implant fixation at the implantation site. In addition, magnesium, which is naturally present in bone composition,

was used as a doping element with a view to improving the biocompatibility of these HAp coatings. As shown in *Figure 19*, the coatings doped with magnesium exhibited a lower porosity compared to undoped hydroxyapatite fibres. Also, coated samples treated at 600 °C presented slightly lower biocompatibility compared to nude untreated TA6V substrates, based on proliferation assay (MTS) and live-dead fluorescent staining (*Figure 20*). Nonetheless, the addition of magnesium did not permit an enhancement of the biocompatibility of the CaP coatings. Though, after 10 days of culture, the density of viable cells was significantly enhanced on all samples and no dead cells were seen. In contrast, a strong cytotoxicity of samples calcined at 800 °C was demonstrated by both MTS proliferation assay and live/dead imaging, regardless of the culture time and the chemical composition (HAp or Mg-whitlokite). It is suggested that this cytotoxicity is caused by the formation of needle-like particles of rutile resulting from the titanium oxidation at 800 °C. In this article [148], samples calcined at 600 °C present good preliminary results in terms of biological compatibility, even though the latter remains lower than the one of bare untreated TA6V substrates. A further in-depth investigation would now be necessary, such as an examination of the osteoinductivity of the coatings.

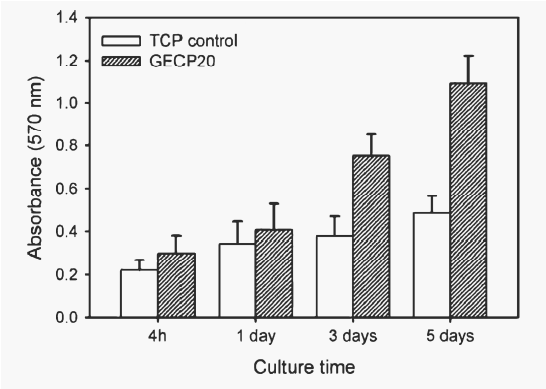

Figure 18. Viability of MC3T3-E1 cells cultured onto HAp ceramic fibres (named "GECP20") as a function of time. Reproduced from [149]

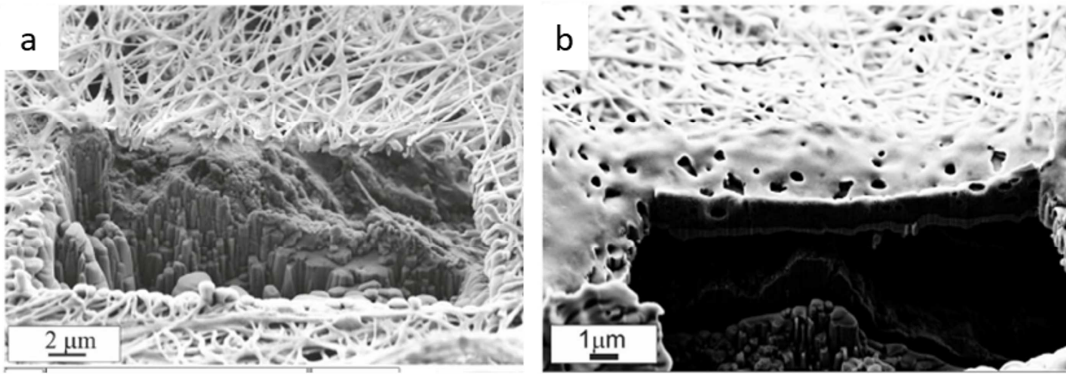

Figure 19. SEM/FIB observation of bioactive coatings of a) HAp and b) Mg doped calcium phosphate after thermal treatment at 600 °C. Reproduced from [148]

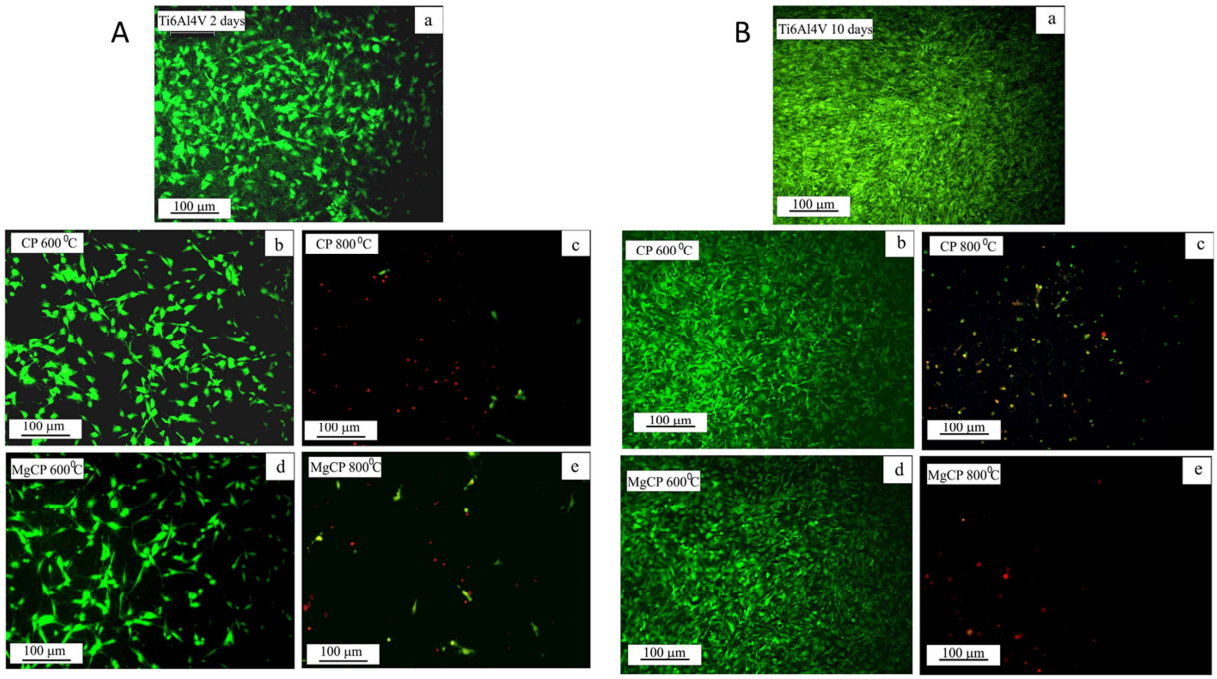

Figure 20. Morphology and density of osteoblastic cells after A) 2 and B) 10 days of culture. Cell culture was made on a) Pure TA6V substrates; CaP coated TA6V substrates calcined at b) 600 °C and c) 800 °C; Mg-CaP coated TA6V substrates calcined at d) 600 °C and e) 800 °C. Reproduced from [148]

II.6. SUMMARY FOR CALCIUM PHOSPHATES ELECTROSPINNING

Calcium phosphates are promising materials for the preparation of electrospun bone tissue engineering scaffolds. Nonetheless, the synthesis of a single-phase calcium phosphate is quite challenging and unexpected phases can present adverse effects on cells. After *in situ* synthesis, the shaping of such materials in nanofibres was documented by a few researchers, however biological investigations into these materials are terribly lacking, as they are limited to only two *in vitro* studies. Therefore, efforts should be put in the obtaining of pure calcium phosphate phases (such as hydroxyapatite and β-tricalcium phosphate), and characterisations should be further investigated, both on a composition and biological point of view.

CONCLUDING DISCUSSION AND FUTURE TRENDS

Positioning of the electrospinning technique

When designing materials for BTE applications, some specific requirements in terms of scaffolds structures have to be considered. In particular, the optimal pore size for cell migration in bone scaffolds has been estimated at 100-500 µm [159], provided that the pore geometry permits the entry of the cells. There is however a lack of consensus on this value, as other authors report the best pore size to be 100-350 µm [160] or even 10-400 µm [161]. Beside these large pores, the presence of pores close to the micrometre scale plays a complementary role : it ensures the flow of nutrients, the evacuation of cell wastes and can also favour the angiogenesis of the materials [160,162]. The largest porosity is also responsible for an enhanced specific surface area, and results in an increased adsorption of proteins [163]. Moreover, an interconnectivity of the porosity is an essential requirement for the movement of cells, nutrients and wastes through the scaffolds [164]. As already reported in this review, the fibrillary collagen naturally present in the bone ECM displays diameters of a few hundred of nanometres [165]. Mimicking this nanoscale morphology serves as a tool to improve the cellular responses. Indeed, while large porosity

is ideal for cell migration and vascularization, nano-sized substrates act as protein, cells and mineral binding architecture [161,166].

Different techniques can be used to create 3D materials with porous structures, including solvent casting and particulate leaching, gas foaming, or freeze drying [164,165,167]. Yet, none of these techniques can play on the nano-architecture of the scaffolds. Nanofibers of polymers can be prepared by phase separation or self-assembly [166], however, these methods only apply to some specific polymers and only short strands of nanofibers can be obtained. Also, the low amount of fibres created by self-assembly is not suitable for mass production. Therefore, the electrospinning method stands out as it enables the production of long and continuous nanofibers with large surface area. The experimental setup is simple, low cost and suitable for a large scale production. A wide range of materials can be shaped by this technique and as detailed in this review, it is compatible with an *in situ* synthesis of bioceramics. Compared to the suspension of pre-synthesised nanoparticles, this *in situ* synthesis brings about a more homogenous repartition of the inorganic phase within the electrospun fibres, avoiding as such aggregation of the particles and inhomogeneous properties. With the electrospinning method, fibres display diameters of submicron sizes. As detailed previously, fibres diameters can be adapted by adjusting the synthesis and electrospinning parameters (such as the sol ageing time, the sol and polymer concentrations, the flow rate or the voltage applied). The porosity naturally created between electrospun fibres is usually well interconnected but the pore size ranges from several to tens of micrometres [166]. This size is suitable for the flow of nutrient; even so it prevents the penetration of cells into the scaffolds. For this reason, the electrospinning method may be more adapted to create bioactive coatings on inert implants, as the infiltration of cells is not required. Comparatively, additive manufacturing techniques are well adapted for tailoring the pore size of engineering scaffolds, and large dimensions can be reached. Nonetheless, these methods are mostly not compatible with the obtaining of nanofibers, because the resolution is generally higher than a few tens of microns [168]. The more advanced additive manufacturing techniques are the two-photon polymerization and the electro-writing electrospinning [169]. With the first method, the resolution usually reaches around 100-200 nm but the necessity for photo-curable resins limits the diversity of materials being adapted to this process. Another well-resolved technique is the electro-writing electrospinning, where the electrospinning process is combined with a displacement of the collector along the X, Y and Z axis, so as to precisely localise the deposition of the filament [169]. In that case, the resolution is of several micrometres.

Taking into account all of these available methods for producing BTE scaffolds, obtaining both sub-micron filaments mimicking the collagen structure of the bone ECM and adequate porosity appears challenging. Therefore, combining two methods such as electro-writing and electrospinning could be considered so as to create scaffolds with tailored porosity, yet with the surface of the scaffolds displaying submicron filaments that are favourable to cell adhesion, proliferation and differentiation.

Bioactive ceramics versus resorbable polymers

The biodegradability of a BTE scaffold enables its gradual replacement with the new bone. Therefore, the degradation rate of the scaffold should be controlled, and degraded residues should be nontoxic [164]. Polymer materials have been extensively investigated for their use as bone regenerative scaffolds. While natural polymers provide bio-functional molecules that guarantee their bioactivity, they can yet generate immunogenic responses or microbial contamination [161,170]. On the other hand, synthetic polymers present tunable properties in terms of degradation rate for instance. But even though they can be biocompatible, they present a reduced bioactivity, a lack of cells recognition sites and of osteoconductivity [165,170]. On the contrary, the bioactive properties of some bioceramics – such as bioactive glasses and calcium phosphates – result from their ability to produce, via solution-mediated surface reaction, a carbonated hydroxyapatite layer on their surface. This layer is necessary for a bond with bone tissue to occur. Some bioceramics can also trigger osteoconductivity and osteoinductivity [164,171]. In this review paper, the supplementation of polymer materials with bioactive ceramics has indeed evidenced an improvement in their ability to regenerate bone tissue *in vivo*: by comparing either polymer-only with polymer-bioactive ceramic electrospun fibres [35], polymer matrices with and without

electrospun bioactive glasses embedded in them [72,92], or finally by considering mats composed of electrospun PCL fibres either alone or intertwined with an electrospun network of bioactive glass [64].

In spite of their bioactivity, bioceramics are inadequate for load bearing applications due to their inherent brittleness (feature of hard materials with small elongation to failure) [161,171]. This property limits their use on their own, but combining them with polymers can counterbalance their reduced mechanical properties. When combining the *in situ* synthesis of the inorganic phase and a subsequent electrospinning, purely inorganic fibres can be obtained after polymer calcination or by polymer-free synthesis. These inorganic fibres are characterised by tensile strengths below or equal to 0.1 MPa, Young modulus of a few mega Pascals [50,62,64], and a compressive strength of 0.15 MPa [62]. When the polymer was kept in the hybrid fibres, these properties were improved (tensile strength of a few mega Pascals [35,43,61,67,87,91,105,106], Young modulus of several tens [35,87,91,106] to more than 100 MPa of mega Pascals [43,87,105] and a compressive strength lower than 1 MPa [67]) but still low compared to natural bone. In actual facts, the best mechanical properties could be obtained when purely inorganic fibres were inserted into matrices of polymer (tensile strength of 10 MPa, Young modulus of 0.2 GPa [72]) or of calcium sulfate cement. In that case, the Young modulus and the compressive strength varied between 0.4 and 0.82 GPa and between 17 and 30 MPa, respectively, depending on the amount of fibrous filler [79]. These values are close to the mechanical features of cancellous bone, which are: a tensile strength of 7.4 MPa, a compressive strength of 4-12 MPa and a Young modulus of 0.02-0.5 GPa [172].

A major challenge in bone tissue engineering is to develop a scaffold material that is mechanically strong and yet biodegradable. This review has confirmed, on a biological point of view, the interest of shaping bioceramics into nano- or micro-fibres through electrospinning. However, to counteract their lack of mechanical resistance, future research should focus on the development of composite materials, where the matrix embedding the fibres presents mechanical strength as well as biodegradable properties, in order to expose gradually the bioactive fibres to the surrounding area. Also, the fibres could be contained into or deposited on the surface of a mechanically strong 3D printed grid with adequate porous feature to enable cell migration. Finally, these inorganic fibres could also be deposited on orthopedic implants so as to beneficiate from the strength of the bioinert metal (such as TA6V).

Calcium phosphates versus Si-based materials

Both bioactive glasses and calcium phosphates are bioactive materials, as they can improve bone cell growth and enhance bone tissue formation [173]. As the formation of a carbonated hydroxyapatite layer at their surface is solution-mediated, controlling their dissolution rate is critical for tissue regeneration. While hydroxyapatite possesses a high chemical stability that restricts its dissolution *in vivo*, β-tricalcium phosphate is characterized by an adversely resorbability rate [173]. As detailed in this review paper, the electrospinning of these two phases have been considered in the literature. However, a strong lack in biological evaluation, both *in vitro* and *in vivo* has been noticed and should be looked at in the future. Also, a common strategy to obtain intermediate properties of dissolution in bulk materials is based on the preparation of biphasic calcium phosphate, a mixture of HAp and β-TCP, whose dissolution can be tailored by the ratio set between the two phases. This ratio would likely be hard to control if the two phases were to be *in situ* synthesised into the same electrospun fibre. Thus, alternatively, the two materials could be prepared in two different solutions that would be simultaneously electrospun to create one biphasic electrospun mat. Though, materials prepared from biphasic calcium phosphates exhibit rather two different kinetics of resorption (the one of HAp and the one of β-TCP) than one intermediate rate. Therefore, the use of bioactive glasses is interesting in the sense that its composition can be easily adapted to adjust its dissolution behaviour. Indeed, as the concentration of the network former decreases in the glass, its solubility increases. In this review, this tendency has also been reported on electrospun fibres [68]. Bioglass 45S5, which contains 46.1 mol% of silica, is known to have to most stimulatory effect on bone cell function. Also, when implanted in bone, bioglass has been shown to accelerate bone growth three times more than HAp [173]. The electrospinning of this material after *in situ* synthesis is really sparsely reported, and limitations on the obtaining of a homogeneous glass network were evidenced [111]. Future studies could therefore address these limits. Besides the well-studied SiO_2-CaO and SiO_2-

$CaO\text{-}P_2O_5$ systems, other more complex compositions have been reported to produce electrospun fibres, including the glass 13-93 - for its ability to keep its amorphous structure at higher temperature than 45S5 [115] - or Ag-doped silica, for its antibacterial potential [119]. Yet, only preliminary results were available on these materials. Also, it is worth mentioning that none of the reported studies compared CaP and Si-based materials on a biological point of view.

Moreover, this review brought to light the difficulty in controlling the synthesis of these two types of ceramics. Regarding calcium phosphates, obtaining pure phases of either HAp, β-TCP or DCPA is challenging. For instance calcium oxide, which is indirectly toxic to cells, often appears in the final fibres. This phase results from the strong tendency of calcium phosphate to incorporate other ions into its lattice [173] in combination with the high thermal treatment imposed to the fibres after electrospinning. This treatment is nevertheless necessary to crystallise the desired CaP phase and to eliminate the toxic nitrate ions brought by the calcium nitrate precursor, which is extensively used in the reported studies. Regarding bioactive glasses, the deviations in composition with respect to the expected glass network are due to a loss of phosphorus during the synthesis/electrospinning process [87], as well as a tendency of the glass to crystallise upon heat treatment [66,111]. For these glasses, the thermal treatment also favours the entry of calcium, if any, in the glass network. All in all, for both kinds of materials, efforts should be put into the optimisation of their synthesis in order to obtain fibres of the expected composition. We can for instance imagine using other precursors to avoid bringing nitrates that only decompose at high temperature, as previously mentioned in a few articles [63,64,139,141].

Finally, beside the use of bioactive ceramics, mesoporosity could be provided to the electrospun fibres in a way to host bioactive molecules and use them as drug delivery systems. Interesting drug release kinetics throughout several days have indeed been reported for bioactive glass [67,75] or HAp [133] fibres, while burst released were evidenced when using hollow fibres [70,78]. Nonetheless, a strong lack of biological evaluation regarding the impact of the released drugs on cell behaviour is noticed, and should be addressed in the future.

LIST OF ABBREVIATIONS

ALP: Alkaline phosphatase
BCP: Biphasic calcium phosphate
BMMSC: Bone marrow mesenchymal stem cell
BSA: Bovine serum albumin
BTE: Bone tissue engineering
CaDHA: Calcium deficient hydroxyapatite
CaP: Calcium phosphate
CHA or HCA: Carbonated hydroxyapatite
CTAB: N-cetyltrimethylammonium bromide
DCPA: Dicalcium phosphate anhydrous
DCPD: Dicalcium phosphate dihydrate
DMSO: Dimethyl sulfoxide
ECM: Extracellular matrix
FGF: Fibroblast growth factor
GBR: Guided bone regeneration
GPTEOS: 3-glycidyloxypropyltriethoxysilane
GPTMOS or GPTMS:
3-glycidyloxypropyltrimethoxysilane
GS: Gentamicin sulfate
HAp: Hydroxyapatite
hEnSC: human endometrial stem cell
LFX: Levofloxacin
MCPM:
Monobasic calcium phosphate monohydrate
MEK: Methylethylketone
NLE: Needle less electrospinning
OCP: Octacalcium phosphate
PAN: Polyacrylonitrile
PBS: Phosphate buffered saline
PCL: Polycaprolactone
PEG: Polyethylene glycol
PEO: Polyethylene oxide
PHB: Polyhydroxybutyrate
PLA: Polylactic acid
PLGA: Poly(lactic-co-glycolic acid)
PLLA: Poly(L-lactic acid)
PMMA: Poly(methyl methacrylate)
PVA: Polyvinyl alcohol
PVB: Polyvinylbutyral
PVP: Polyvinyl pyrrolidone
SBF: Simulated body fluid
TCH: Tetracycline hydrochloride
TCP: Tricalcium phosphate
TEOS: Tetraethylorthosilicate
TEP: Triethylphosphate
TEPI: Triethylphosphite

TMOS: Tetramethoxysilane
TTCP: Tetracalcium phosphate
WIPF: Water induced pore formation

ACKNOWLEDGEMENTS

The authors would like to thank the French National Research Agency for the financial support (project ANR-17-CE19-0004-03). The authors are grateful to Mr. David Lewis and Mr. Gauthier Chambon for their attentive review of this article and to Ms. Nina Attik for her pertinent scientific advice.

AUTHOR DISCLOSURE STATEMENT

No competing financial interests exist.

REFERENCES

[1] A.R. Amini, C.T. Laurencin, S.P. Nukavarapu, Bone Tissue Engineering: Recent Advances and Challenges, Crit. Rev. Biomed. Eng. 40 (2012) 363–408.

[2] M. Dang, L. Saunders, X. Niu, Y. Fan, P.X. Ma, Biomimetic delivery of signals for bone tissue engineering, Bone Res. 6 (2018).

[3] P. Bajaj, R.M. Schweller, A. Khademhosseini, J.L. West, R. Bashir, 3D biofabrication strategies for tissue engineering and regenerative medicine, Annu. Rev. Biomed. Eng. 16 (2014) 247–276.

[4] H. Ma, C. Feng, J. Chang, C. Wu, 3D-printed bioceramic scaffolds: From bone tissue engineering to tumor therapy, Acta Biomater. 79 (2018) 37–59.

[5] G. Pocock, C.D. Richards, Human Physiology : The Basis of medicine, Oxford Core Texts, 2006.

[6] M.M. Giraud Guille, N. Nassif, F.M. Fernandes, Collagen-based materials for tissue repair, from bio-inspired to biomimetic, in: Mater. Des. Inspired by Nat. Funct. through Inn. Archit., The Royal Society of Chemistry, 2013.

[7] U. Cheema, M. Ananta, V. Mudera, Collagen: applications of a natural polymer in regenerative medicine, in: D. Eberli (Ed.), Regen. Med. Tissue Eng. - Cells Biomater., IntechOpen, 2011.

[8] A.K. Nair, A. Gautieri, S.-W. Chang, M.J. Buehler, Molecular mechanics of mineralized collagen fibrils in bone, Nat. Commun. 4 (2013).

[9] S.C. Cowin, L. Cardoso, Blood and interstitial flow in the hierarchical pore space architecture of bone tissue, J. Biomech. 48 (2015) 842–854.

[10] Z. Ramakrishna, S.; Fujihara, K.; Teo, W.E.; Ma, An introduction to electrospinning and nanofibers, World Scientific Publishing Co., 2005. doi:10.1142/9789812567611_0003.

[11] T.B. Brown, P.D. Dalton, D.W. Hutmacher, Melt electrospinning today: an opportune time for an emerging polymer process, Prog. Polym. Sci. 56 (2016) 116–166. doi:https://doi.org/10.1016/j.progpolymsci.2016.01.001.

[12] B. Alberts, A. Johnson, J. Lewis, D. Morgan, M. Raff, K. Roberts, P. Walter, Biologie moléculaire de la cellule, 6ème éditi, Lavoisier Médecine Sciences, 2017.

[13] P. Ducheyne, K. Healy, D.W. Hutmacher, D.W. Grainger, C.J. Kirkpatrick, eds., Comprehensive Biomaterials II - 2nd Edition, Elsevier, 2017.

[14] J. Jeong, J.H. Kim, J.H. Shim, N.S. Hwang, C.Y. Heo, Bioactive calcium phosphate materials and applications in bone regeneration, Biomater. Res. 23 (2019).

[15] J.S. Al-Sanabani, A.A. Madfa, F.A. Al-Sanabani, Application of calcium phosphate materials in dentistry, Int. J. Biomater. (2013).

[16] J.R. Jones, Review of bioactive glass: from Hench to hybrids, Acta Biomater. 9 (2013) 4457–4486. doi:10.1016/j.actbio.2012.08.023.

[17] P. Wutticharoenmongkol, N. Sanchavanakit, P. Pavasant, P. Supaphol, Preparation and characterization of novel bone scaffolds based on electrospun polycaprolactone fibers filled with nanoparticles, Macromol. Biosci. 6 (2006) 70–77. doi:10.1002/mabi.200500150.

[18] Z. Cao, D. Wang, L. Lyu, Y. Gong, Y. Li, Fabrication and characterization of PCL/CaCO3 electrospun composite membrane for bone repair, RSC Adv. 6 (2016) 10641–10649. doi:10.1039/c5ra22548e.

[19] K. Fujihara, M. Kotaki, S. Ramakrishna, Guided bone regeneration membrane made of polycaprolactone/calcium carbonate composite nano-fibers, Biomaterials. 26 (2005) 4139–4147. doi:10.1016/j.biomaterials.2004.09.014.

[20] D.M. Reffitt, N. Ogston, R. Jugdaohsingh, H.F.. Cheung, B.A.. Evans, R.P.. Thompson, J.. Powell, G.. Hampson, Orthosilicic acid stimulates collagen type 1 synthesis and osteoblastic differentiation in human osteoblast-like cells in vitro, Bone. 32 (2003) 127–135.

[21] T. Wakita, A. Obata, G. Poologasundarampillai, J.R. Jones, T. Kasuga, Preparation of electrospun siloxane-poly(lactic acid)-vaterite hybrid fibrous membranes for guided bone regeneration, Compos. Sci. Technol. 70 (2010) 1889–1893. doi:10.1016/j.compscitech.2010.05.014.

[22] A. Obata, T. Hotta, T. Wakita, Y. Ota, T. Kasuga, Electrospun microfiber meshes of silicon-doped vaterite/poly(lactic acid) hybrid for guided bone regeneration, Acta Biomater. 6 (2010) 1248–1257. doi:10.1016/j.actbio.2009.11.013.

[23] N. Takeuchi, M. Machigashira, D. Yamashita, Y. Shirakata, T. Kasuga, K. Nogushi, S. Ban, Cellular compatibility of a gamma-irradiated modified siloxane-poly(lactic acid)-calcium carbonate hybrid membrane for guided bone regeneration, Dent. Mater. J. 30 (2011) 730–738. doi:10.4012/dmj.2011-075.

[24] T. Kasuga, A. Obata, H. Maeda, Y. Ota, X. Yao, K. Oribe, Siloxane-poly(lactic acid)-vaterite composites with 3D cotton-like structure, J. Mater. Sci. Mater. Med. 23 (2012) 2349–2357. doi:10.1007/s10856-012-4607-5.

[25] D. Lee, H. Maeda, A. Obata, K. Inukai, K. Kato, T. Kasuga, Aluminum silicate nanotube modification of cotton-like siloxane-poly(L- lactic acid)-vaterite composites, Adv. Mater. Sci. Eng. 2013 (2013). doi:10.1155/2013/169721.

[26] A. Obata, H. Ozasa, T. Kasuga, J.R. Jones, Cotton wool-like poly(lactic acid)/vaterite composite scaffolds releasing soluble silica for bone tissue engineering, J. Mater. Sci. Mater. Med. 24 (2013) 1649–1658. doi:10.1007/s10856-013-4930-5.

[27] S. Naghieh, E. Foroozmehr, M. Badrossamay, M. Kharaziha, Combinational processing of 3D printing and electrospinning of hierarchical poly(lactic acid)/gelatin-forsterite scaffolds as a biocomposite: Mechanical and biological assessment, Mater. Des. 133 (2017) 128–135. doi:10.1016/j.matdes.2017.07.051.

[28] M. Kharaziha, M.H. Fathi, H. Edris, Effects of surface modification on the mechanical and structural properties of nanofibrous poly(ε-caprolactone)/forsterite scaffold for tissue engineering applications, Mater. Sci. Eng. C. 33 (2013) 4512–4519. doi:10.1016/j.msec.2013.07.002.

[29] M. Kharaziha, M.H. Fathi, H. Edris, Development of novel aligned nanofibrous composite membranes for guided bone regeneration, J. Mech. Behav. Biomed. Mater. 24 (2013) 9–20. doi:10.1016/j.jmbbm.2013.03.025.

[30] A. Suryavanshi, K. Khanna, K.R. Sindhu, J. Bellare, R. Srivastava, Magnesium oxide nanoparticle-loaded polycaprolactone composite electrospun fiber scaffolds for bone-soft tissue engineering applications: In-vitro and in-vivo evaluation, Biomed. Mater. 12 (2017) 55011. doi:10.1088/1748-605X/aa792b.

[31] H. Zhou, M. Nabiyouni, B. Lin, S.B. Bhaduri, Fabrication of novel poly(lactic acid)/amorphous magnesium phosphate bionanocomposite fibers for tissue engineering applications via electrospinning, Mater. Sci. Eng. C. 33 (2013) 2302–2310. doi:10.1016/j.msec.2013.01.058.

[32] S. Wang, R. Castro, X. An, C. Song, Y. Luo, M. Shen, H. Tomás, M. Zhu, X. Shi, Electrospun laponite-doped poly(lactic-co-glycolic acid) nanofibers for osteogenic differentiation of human mesenchymal stem cells, J. Mater. Chem. 22 (2012) 23357. doi:10.1039/c2jm34249a.

[33] A.K. Gaharwar, S. Mukundan, E. Karaca, A. Dolatshahi-Pirouz, A. Patel, K. Rangarajan, S.M. Mihaila, G. Iviglia, H. Zhang, A. Khademhosseini, Nanoclay-enriched poly(ε-caprolactone) electrospun scaffolds for osteogenic differentiation of human mesenchymal stem cells, Tissue Eng. Part A. 20 (2014) 2088–2101. doi:10.1089/ten.tea.2013.0281.

[34] G. Nitya, G.T. Nair, U. Mony, K.P. Chennazhi, S. V. Nair, In vitro evaluation of electrospun PCL/nanoclay composite scaffold for bone tissue engineering, J. Mater. Sci. Mater. Med. 23 (2012) 1749–1761. doi:10.1007/s10856-012-4647-x.

[35] T.S. Jang, E.J. Lee, J.H. Jo, J.M. Jeon, M.Y. Kim, H.E. Kim, Y.H. Koh, Fibrous membrane of nano-hybrid poly-L-lactic acid/silica xerogel for guided bone regeneration, J. Biomed. Mater. Res. - Part B Appl. Biomater. 100 B (2012) 321–330. doi:10.1002/jbm.b.31952.

[36] M. Nagrath, A. Alhalawani, A. Rahimnejad Yazdi, M.R. Towler, Bioactive glass fiber fabrication via a combination of sol-gel process with electro-spinning technique, Mater. Sci. Eng. C. 101 (2019) 521–538. doi:10.1016/j.msec.2019.04.003.

[37] L.M. Jurkić, I. Cepanec, S. Kraljević Pavelić, K. Pavelić, Biological and therapeutic effects of ortho-silicic acid and some ortho-silicic acid-releasing compounds: New perspectives for therapy, Nutr. Metab. (Lond). 10 (2013).

[38] R. Jugdaohsingh, Silicon and bone health, J. Nutr. Health Aging. 11 (2007) 99–110.

[39] K. Szurkowska, J. Kolmas, Hydroxyapatites enriched in silicon – Bioceramic materials for biomedical and pharmaceutical applications, Prog. Nat. Sci. Mater. Int. 27 (2017) 401–409.

[40] M. Jokinen, T. Peltola, S. Veittola, H. Rahiala, J.B. Rosenholm, Adjustable biodegradation for ceramic fibres derived from silica sols.pdf, 20 (2000) 1739–1748.

[41] T. Peltola, M. Jokinen, S. Veittola, H. Rahiala, A. Yli-Urpo, Influence of sol and stage of spinnability on in vitro bioactivity and dissolution of sol-gel-derived SiO2 fibers, Biomaterials. 22 (2001) 589–598. doi:10.1016/S0142-9612(00)00219-2.

[42] S. Sakai, Y. Yamada, T. Yamaguchi, K. Kawakami, Prospective use of electrospun ultra-fine silicate fibers for bone tissue engineering, Biotechnol. J. 1 (2006) 958–962. doi:10.1002/biot.200600054.

[43] Y. Ding, Q. Yao, W. Li, D.W. Schubert, A.R. Boccaccini, J.A. Roether, The evaluation of physical properties and in vitro cell behavior of PHB/PCL/sol-gel derived silica hybrid scaffolds and PHB/PCL/fumed silica composite scaffolds, 136 (2015) 93–98.

[44] G. Toskas, C. Cherif, R.D. Hund, E. Laourine, B. Mahltig, A. Fahmi, C. Heinemann, T. Hanke, Chitosan(PEO)/silica hybrid nanofibers as a potential biomaterial for bone regeneration, Carbohydr. Polym. 94 (2013) 713–722. doi:10.1016/j.carbpol.2013.01.068.

[45] I. Das, G. De, L. Hupa, P.K. Vallittu, Porous SiO2 nanofiber grafted novel bioactive glass-ceramic coating: A structural scaffold for uniform apatite precipitation and oriented cell proliferation on inert implant, Mater. Sci. Eng. C. 62 (2016) 206–214. doi:10.1016/j.msec.2016.01.053.

[46] A.M. Buckley, M. Greenblatt, The sol-gel preparation of silica gels, J. Chem. Educ. 71 (1994) 599.

doi:10.1021/ed071p599.

[47] S.H. Xia, S.H. Teng, P. Wang, Synthesis of bioactive polyvinyl alcohol/silica hybrid fibers for bone regeneration, Mater. Lett. 213 (2018) 181–184. doi:10.1016/j.matlet.2017.11.084.

[48] Z. Ma, G. Dong, C. Lv, J. Qiu, Core-shell glass fibers with high bioactivity and good flexibility, Mater. Lett. 88 (2012) 136–139. doi:10.1016/j.matlet.2012.08.045.

[49] R. Ravichandran, S. Gandhi, D. Sundaramurthi, S. Sethuraman, U.M. Krishnan, Hierarchical mesoporous silica nanofibers as multifunctional scaffolds for bone tissue regeneration, J. Biomater. Sci. Polym. Ed. 24 (2013) 1988–2005. doi:10.1080/09205063.2013.816930.

[50] H.Y. Mi, X. Jing, B.N. Napiwocki, Z.T. Li, L.S. Turng, H.X. Huang, Fabrication of fibrous silica sponges by self-assembly electrospinning and their application in tissue engineering for three-dimensional tissue regeneration, Chem. Eng. J. 331 (2018) 652–662. doi:10.1016/j.cej.2017.09.020.

[51] C.R. Silva, C. Airoldi, Acid and base catalysts in the hybrid silica sol-gel process, J. Colloid Interface Sci. 195 (1997) 381–387. doi:10.1006/jcis.1997.5159.

[52] H.W. Kim, H.E. Kim, J.C. Knowles, Production and potential of bioactive glass nanofibers as a next-generation biomaterial, Adv. Funct. Mater. 16 (2006) 1529–1535. doi:10.1002/adfm.200500750.

[53] G. Kaur, Bioactive glasses - Potential biomaterials for future therapy, Series in, Springer, 2017. http://linkinghub.elsevier.com/retrieve/pii/B9781845692049500120.

[54] W. Höland, G.H. Beall, Glass-Ceramics, in: Handb. Adv. Ceram. Mater. Appl. Process. Prop. Second Ed., 2013: pp. 371–381.

[55] A.R. Boccaccini, D.S. Brauer, L. Hupa, eds., Bioactive Glasses - Fundamentals, technology and applications, Royal Society of Chemistry, 2017.

[56] L. Linati, G. Lusvardi, G. Malavasi, L. Menabue, M.C. Menziani, P. Mustarelli, A. Pedone, S. Ulderico, Medium-range order in phospho-silicate bioactive glasses: Insights from MAS-NMR spectra, chemical durability experiments and molecular dynamics simulations, J. Non. Cryst. Solids. 354 (2008) 84–89. doi:https://doi.org/10.1016/j.jnoncrysol.2007.06.076.

[57] A. Tilocca, A.N. Cormack, N.H. de Leeuw, The structure of bioactive silicate glasses: new insight from molecular dynamics simulations, Chem. Mater. 19 (2007) 95–103. doi:https://doi.org/10.1021/cm061631g.

[58] R.A. McCauley, Corrosion of Ceramic Materials - Third Edition, CRC Press, 2016.

[59] A. Hoppe, N.S. Güldal, A.R. Boccaccini, A review of the biological response to ionic dissolution products from bioactive glasses and glass-ceramics, Biomaterials. 32 (2011) 2757–2774. doi:10.1016/j.biomaterials.2011.01.004.

[60] Y.J. Seol, K.H. Kim, M.K. Young, A.K. In, S.H. Rhee, Bioactivity, pre-osteoblastic cell responses, and osteoconductivity evaluations of the electrospun non-woven SiO2-CaO gel fabrics, J. Biomed. Mater. Res. - Part B Appl. Biomater. 90 B (2009) 679–687. doi:10.1002/jbm.b.31334.

[61] C. Gao, Q. Gao, Y. Li, M.N. Rahaman, A. Teramoto, K. Abe, In vitro evaluation of electrospun gelatin-bioactive glass hybrid scaffolds for bone regeneration, J. Appl. Polym. Sci. 127 (2013) 2588–2599. doi:10.1002/app.37946.

[62] G. Poologasundarampillai, D. Wang, S. Li, J. Nakamura, R. Bradley, P.D. Lee, M.M. Stevens, D.S. McPhail, T. Kasuga, J.R. Jones, Cotton-wool-like bioactive glasses for bone regeneration, Acta Biomater. 10 (2014) 3733–3746. doi:10.1016/j.actbio.2014.05.020.

[63] I.A. Kim, S.H. Rhee, Effects of poly(lactic-co-glycolic acid) (PLGA) degradability on the apatite-forming capacity of electrospun PLGA/SiO2-CaO nonwoven composite fabrics, J. Biomed. Mater. Res. - Part B Appl. Biomater. 93 (2010) 218–226. doi:10.1002/jbm.b.31578.

[64] Y. Seol, K. Kim, I.A. Kim, S. Rhee, Osteoconductive and degradable electrospun nonwoven poly (e-caprolactone)/CaO-SiO2 gel composite fabric, J. Biomed. Mater. Res. - Part A. 94A (2010) 649–659. doi:10.1002/jbm.a.32738.

[65] M. Shamsi, M. Karimi, M. Ghollasi, N. Nezafati, M. Shahrousvand, M. Kamali, A. Salimi, In vitro proliferation and differentiation of human bone marrow mesenchymal stem cells into osteoblasts on nanocomposite scaffolds based on bioactive glass (64SiO2-31CaO-5P2O5)-poly-L-lactic acid nanofibers fabricated by electrospinning method, Mater. Sci. Eng. C. 78 (2017) 114–123. doi:10.1016/j.msec.2017.02.165.

[66] X. Jia, T. Tang, D. Cheng, C. Zhang, R. Zhang, Q. Cai, X. Yang, Micro-structural evolution and biomineralization behavior of carbon nanofiber/bioactive glass composites induced by precursor aging time, Colloids Surfaces B Biointerfaces. 136 (2015) 585–593. doi:10.1016/j.colsurfb.2015.09.062.

[67] X. Han, D. Wang, X. Chen, H. Lin, F. Qu, One-pot synthesis of macro-mesoporous bioactive glasses/polylactic acid for bone tissue engineering, Mater. Sci. Eng. C. 43 (2014) 367–374. doi:10.1016/j.msec.2014.07.042.

[68] Q. Yang, G. Sui, Y.Z. Shi, S. Duan, J.Q. Bao, Q. Cai, X.P. Yang, Osteocompatibility characterization of polyacrylonitrile carbon nanofibers containing bioactive glass nanoparticles, Carbon N. Y. 56 (2013) 288–295. doi:10.1016/j.carbon.2013.01.014.

[69] J. Kim, G. Jin, H. Yu, S. Choi, H. Kim, I.B. Wall, Providing osteogenesis conditions to mesenchymal stem cells using bioactive nanocomposite bone scaffolds, Mater. Sci. Eng. C. 32 (2012) 2545–2551. doi:10.1016/j.msec.2012.07.038.

[70] J. Xie, E.R. Blough, C.H. Wang, Submicron bioactive glass tubes for bone tissue engineering, Acta Biomater. 8 (2012) 811–819. doi:10.1016/j.actbio.2011.09.009.

[71] K.T. Noh, H.Y. Lee, U.S. Shin, H.W. Kim, Composite nanofiber of bioactive glass nanofiller incorporated poly(lactic acid) for bone regeneration, Mater. Lett. 64 (2010) 802–805. doi:10.1016/j.matlet.2010.01.014.

[72] J.H. Jo, E.J. Lee, D.S. Shin, H.E. Kim, H.W. Kim, Y.H. Koh, J.H. Jang, In vitro/in vivo biocompatibility and mechanical properties of bioactive glass nanofiber and poly(ε-caprolactone) composite materials, J. Biomed. Mater. Res. - Part B Appl. Biomater. 91 (2009) 213–220. doi:10.1002/jbm.b.31392.

[73] F. Hsu, M. Lu, R. Weng, H. Lin, Hierarchically biomimetic scaffold of a collagen–mesoporous bioactive glass nanofiber composite for bone tissue engineering, Biomed. Mater. 10 (2015) 25007. doi:10.1088/1748-6041/10/2/025007.

[74] X.R. Zhang, X.Q. Hu, X.L. Jia, L.K. Yang, Q.Y. Meng, Y.Y. Shi, Z.Z. Zhang, Q. Cai, Y.F. Ao, X.P. Yang, Cell studies of hybridized carbon nanofibers containing bioactive glass nanoparticles using bone mesenchymal stromal cells, Sci. Rep. 6 (2016) 1–14. doi:10.1038/srep38685.

[75] F.Y. Hsu, R.C. Weng, H.M. Lin, Y.H. Lin, M.R. Lu, J.L. Yu, H.W. Hsu, A biomimetic extracellular matrix composed of mesoporous bioactive glass as a bone graft material, Microporous Mesoporous Mater. 212 (2015) 56–65. doi:10.1016/j.micromeso.2015.03.027.

[76] C. Zhang, D. Cheng, T. Tang, X. Jia, Q. Cai, X. Yang, Nanoporous structured carbon nanofiber-bioactive glass composites for skeletal tissue regeneration, J. Mater. Chem. B. 3 (2015) 5300–5309. doi:10.1039/C5TB00921A.

[77] B. Han, X. Zhang, H. Liu, X. Deng, Q. Cai, X. Jia, X. Yang, Y. Wei, G. Li, Improved bioactivity of PAN-based carbon nanofibers decorated with bioglass nanoparticles, J. Biomater. Sci. Polym. Ed. 25 (2014) 341–353. doi:10.1080/09205063.2013.861169.

[78] B.Y. Hong, X. Chen, X. Jing, H. Fan, Z. Gu, Fabrication and drug delivery of ultrathin mesoporous bioactive glass hollow fibers, Adv. Funct. Mater. 20 (2010) 1503–1510.

doi:10.1002/adfm.200901627.

[79] M. Shams, N. Nezafati, D. Poormoghadam, S. Zavareh, A. Zamanian, A. Salimi, Synthesis and characterization of electrospun bioactive glass nanofibers-reinforced calcium sulfate bone cement and its cell biological response, Ceram. Int. 46 (2020) 10029–10039. doi:10.1016/j.ceramint.2019.12.270.

[80] Y. Li, B. Li, G. Xu, Z. Ahmad, Z. Ren, Y. Dong, X. Li, W. Weng, G. Han, A feasible approach toward bioactive glass nanofibers with tunable protein release kinetics for bone scaffolds, Colloids Surfaces B Biointerfaces. 122 (2014) 785–791. doi:10.1016/j.colsurfb.2014.08.022.

[81] H.-W. Kim, J.H. Song, H.E. Kim, Bioactive glass nanofiber–collagen nanocomposite as a novel bone regeneration matrix, J. Biomed. Mater. Res. - Part A. 79 (2006) 698–705. doi:10.1002/jbm.a.30848.

[82] H.W. Kim, H.H. Lee, G.S. Chun, Bioactivity and osteoblast responses of novel biomedical nanocomposites of bioactive glass nanofiber filled poly(lactic acid), J. Biomed. Mater. Res. - Part A. 85 (2008) 651–663. doi:10.1002/jbm.a.31339.

[83] H.H. Lee, H.S. Yu, J.H. Jang, H.W. Kim, Bioactivity improvement of poly(e-caprolactone) membrane with the addition of nanofibrous bioactive glass, Acta Biomater. 4 (2008) 622–629. doi:10.1016/j.actbio.2007.10.013.

[84] W. Xia, D. Zhang, J. Chang, Fabrication and in vitro biomineralization of bioactive glass (BG) nanofibres, Nanotechnology. 18 (2007) 135601. doi:10.1088/0957-4484/18/13/135601.

[85] Z. Ghaffarian, A. Faghihimani, A. Doostmohammadi, M.R. Saeri, Fabrication, characterization and process parameters optimization of electrospun 58S bioactive glass submicron fibers, Adv. Ceram. Prog. 1 (2015) 16–21.

[86] L. Wu, Y. Dou, K. Lin, W. Zhai, W. Cui, J. Chang, Hierarchically structured nanocrystalline hydroxyapatite assembled hollow fibers as a promising protein delivery system., Chem. Commun. (Camb). 47 (2011) 11674–6. doi:10.1039/c1cc14709a.

[87] Y. Ding, W. Li, T. Müller, D.W. Schubert, A.R. Boccaccini, Q. Yao, J.A. Roether, Electrospun polyhydroxybutyrate/poly(ϵ-caprolactone)/58S sol-gel bioactive glass hybrid scaffolds with highly improved osteogenic potential for bone tissue engineering, ACS Appl. Mater. Interfaces. 8 (2016) 17098–17108. doi:10.1021/acsami.6b03997.

[88] B.A. Allo, A.S. Rizkalla, K. Mequanint, Synthesis and electrospinning of ε-polycaprolactone-bioactive glass hybrid biomaterials via a sol-gel process, Langmuir. 26 (2010) 18340–18348. doi:10.1021/la102845k.

[89] D. Cheng, R. Xie, T. Tang, X. Jia, Q. Cai, X. Yang, Regulating micro-structure and biomineralization of electrospun PVP-based hybridized carbon nanofibers containing bioglass nanoparticles via aging time, RSC Adv. 6 (2016) 3870–3881. doi:10.1039/C5RA23337B.

[90] G. Toskas, C. Cherif, R.D. Hund, E. Laourine, A. Fahmi, B. Mahltig, Inorganic/organic (SiO2)/PEO hybrid electrospun nanofibers produced from a modified sol and their surface modification possibilities, ACS Appl. Mater. Interfaces. 3 (2011) 3673–3681. doi:10.1021/am200858s.

[91] J. Christakiran M, P.J.T. Reardon, R. Konwarh, J.C. Knowles, B.B. Mandal, Mimicking hierarchical complexity of the osteochondral interface using electrospun silk-bioactive glass composites, ACS Appl. Mater. Interfaces. 9 (2017) 8000–8013. doi:10.1021/acsami.6b16590.

[92] K.S. Hong, E.C. Kim, S.H. Bang, C.H. Chung, Y. Il Lee, J.K. Hyun, H.H. Lee, J.H. Jang, T. Il Kim, H.W. Kim, Bone regeneration by bioactive hybrid membrane containing FGF2 within rat calvarium, J. Biomed. Mater. Res. - Part A. 94 (2010) 1187–1194. doi:10.1002/jbm.a.32799.

[93] K. Geltmeyer, Jozefien; Van der Schueren, Lien; Goethals, Frederik; De Clerck, Optimum sol viscosity for stable electrospinning of silica nanofibres, J. Sol-Gel Sci. Technol. 67 (2013) 188–195.

[94] S. Sakai, T. Yamaguchi, R.A. Putra, R. Watanabe, M. Kawabe, M. Taya, K. Kawakami, Controlling

apatite microparticles formation by calcining electrospun sol-gel derived ultrafine silica fibers, J. Sol-Gel Sci. Technol. 61 (2012) 374–380. doi:10.1007/s10971-011-2637-y.

[95] T. Yamaguchi, S. Sakai, R. Watanabe, T. Tarao, K. Kawakami, Heat treatment of electrospun silicate fiber substrates enhances cellular adhesion and proliferation, J. Biosci. Bioeng. 109 (2010) 304–306. doi:10.1016/j.jbiosc.2009.08.482.

[96] M. Hwang, Y.-K. Lee, B.-S. Lim, S.-H. Rhee, Osteoblast-like cell behaviors on non-woven silica fabric, Key Eng. Mater. 309–311 (2006) 469–472. doi:10.4028/www.scientific.net/kem.309-311.469.

[97] Y.M. Kang, K.H. Kim, Y.J. Seol, S.H. Rhee, Evaluations of osteogenic and osteoconductive properties of a non-woven silica gel fabric made by the electrospinning method, Acta Biomater. 5 (2009) 462–469. doi:10.1016/j.actbio.2008.07.004.

[98] S.-H. Rhee, Y.-K. Lee, B.-S. Lim, Bioactive non-woven silica fabric made through electro-spinning method, Key Eng. Mater. 309–311 (2006) 465–468. doi:10.4028/www.scientific.net/kem.309-311.465.

[99] J.H. Yu, S. V. Fridrikh, G.C. Rutledge, The role of elasticity in the formation of electrospun fibers, Polymer (Guildf). 47 (2006) 4789–4797. doi:10.1016/j.polymer.2006.04.050.

[100] B. Song, L. Wu, C. Wu, J. Chang, Preparation of hollow bioactive glass nanofibers by a facile electrospinning method, Biomed. Glas. 1 (2015) 136–139. doi:10.1515/bglass-2015-0013.

[101] X.H. Li, C.L. Shao, Y.C. Liu, A simple method for controllable preparation of polymer nanotubes via a single capillary electrospinning, Langmuir. 23 (2007) 10920–10923. doi:10.1021/la701806f.

[102] W. Wang, J. Zhou, S. Zhang, J. Song, H. Duan, M. Zhou, C. Gong, Z. Bao, B. Lu, X. Li, W. Lan, E. Xie, A novel method to fabricate silica nanotubes based on phase separation effect, J. Mater. Chem. 20 (2010) 9068–9072. doi:10.1039/c0jm02120b.

[103] R. Ravichandran, D. Sundaramurthi, S. Gandhi, S. Sethuraman, U.M. Krishnan, Bioinspired hybrid mesoporous silica-gelatin sandwich construct for bone tissue engineering, Microporous Mesoporous Mater. 187 (2014) 53–62. doi:10.1016/j.micromeso.2013.12.018.

[104] Z. Du, L. Guo, T. Zheng, Q. Cai, X. Yang, Formation of core-shell structured calcium silicate fiber via sol-gel electrospinning and controlled calcination, Ceram. Int. 45 (2019) 23975–23983. doi:10.1016/j.ceramint.2019.08.099.

[105] Y. Ding, W. Li, A. Correia, Y. Yang, K. Zheng, D. Liu, D.W. Schubert, A.R. Boccaccini, H.A. Santos, J.A. Roether, Electrospun polyhydroxybutyrate/poly(ϵ-caprolactone)/sol-gel-derived silica hybrid scaffolds with drug releasing function for bone tissue engineering applications, ACS Appl. Mater. Interfaces. 10 (2018) 14540–14548. doi:10.1021/acsami.8b02656.

[106] K.-H. Shin, Y.-H. Koh, H.-E. Kim, Synthesis and characterization of drug-loaded poly(ε -caprolactone)/silica hybrid nanofibrous scaffolds, J. Nanomater. 2013 (2013). doi:10.1155/2013/351810.

[107] S. Huang, X. Kang, Z. Cheng, Y. Jia, J. Lin, Electrospinning preparation and drug delivery properties of Eu3+/Tb3+ doped mesoporous bioactive glass nanofibers, J. Colloid Interface Sci. 387 (2012) 285–291. doi:10.1016/j.jcis.2012.08.004.

[108] B.Y. Hong, X. Chen, X. Jing, H. Fan, B. Guo, Z. Gu, X. Zhang, Preparation, bioactivity, and drug release of hierarchical nanoporous bioactive glass ultrathin fibers, Adv. Mater. 22 (2010) 754–758. doi:10.1002/adma.200901656.

[109] F. Baino, S. Hamzehlou, S. Kargozar, Bioactive glasses: where are we and where are we going ?, J. Funct. Biomater. 9 (2018). doi:10.3390/jfb9010025.

[110] J.R. Jones, D.S. Brauer, D.C. Greenspan, S. Consulting, B. Court, S. Augustine, Bioglass and bioactive glasses and their impact on healthcare, Int. J. Appl. Glas. Sci. 7 (2016) 423–434. doi:10.1111/ijag.12252.

[111] A.M. Deliormanli, Preparation and in vitro characterization of electrospun 45S5 bioactive glass nanofibers, Ceram. Int. 41 (2014) 417–425. doi:10.1016/j.ceramint.2014.08.086.

[112] D. Durgalakshmi, S. Balakumar, Phase separation induced shell thickness variations in electrospun hollow Bioglass 45S5 fiber mats for drug delivery applications, Phys. Chem. Chem. Phys. 17 (2015) 15316–15323. doi:10.1039/C5CP01738F.

[113] E. Sharifi, M. Azami, A.M. Kajbafzadeh, F. Moztarzadeh, R. Faridi-Majidi, A. Shamousi, R. Karimi, J. Ai, Preparation of a biomimetic composite scaffold from gelatin/collagen and bioactive glass fibers for bone tissue engineering, Mater. Sci. Eng. C. 59 (2016) 533–541. doi:10.1016/j.msec.2015.09.037.

[114] E. Sharifi, S. Ebrahimi-Barough, M. Panahi, M. Azami, A. Ai, Z. Barabadi, A.M. Kajbafzadeh, J. Ai, In vitro evaluation of human endometrial stem cell-derived osteoblast-like cells' behavior on gelatin/collagen/bioglass nanofibers' scaffolds, J. Biomed. Mater. Res. - Part A. 104 (2016) 2210–2219. doi:10.1002/jbm.a.35748.

[115] A.M. Deliormanli, Preparation, in vitro mineralization and osteoblast cell response of electrospun 13-93 bioactive glass nanofibers, Mater. Sci. Eng. C. 53 (2015) 262–271. doi:10.1016/j.msec.2015.04.037.

[116] R. Konyalı, A.M. Deliormanlı, Preparation and mineralization of 13-93 bioactive glass-containing electrospun poly-epsilon-caprolactone composite nanofibrous mats, J. Thermoplast. Compos. Mater. (2019). doi:10.1177/0892705718772889.

[117] C. Gao, Q. Gao, X. Bao, Y. Li, A. Teramoto, K. Abe, Preparation and in vitro bioactivity of novel mesoporous borosilicate bioactive glass nanofibers, J. Am. Ceram. Soc. 94 (2011) 2841–2845. doi:10.1111/j.1551-2916.2011.04434.x.

[118] A.M. Deliormanlı, Electrospun cerium and gallium-containing silicate based 13-93 bioactive glass fibers for biomedical applications, Ceram. Int. 42 (2016) 897–906. doi:10.1016/j.ceramint.2015.09.016.

[119] H. He, J. Wang, Q. Gao, M. Chang, Z. Ren, X. Zhang, X. Li, W. Weng, G. Han, Ag-silica composite nanotube with controlled wall structures for biomedical applications, Colloids Surfaces B Biointerfaces. 111 (2013) 693–698. doi:10.1016/j.colsurfb.2013.07.015.

[120] R.L. Reis, S. Weiner, Learning from nature how to design new implantable biomaterials: from biomineralization fundamentals to biomimetic materials and processing routes., Dordrecht Kluwer Academic Publishers - NATO science series, 2005. https://books.google.com/books?id=dfI-AAAAQBAJ&pgis=1.

[121] J. Lu, H. Yu, C. Chen, Biological properties of calcium phosphate biomaterials for bone repair: a review, RSC Adv. 8 (2018) 2015–2033. doi:10.1039/C7RA11278E.

[122] C. Combes, C. Rey, Biomatériaux à base de phosphates de calcium, Tech. l'ingénieur. (2013).

[123] P. Ducheyne, Q. Qiu, Bioactive ceramics: the effect of surface reactivity on bone formation and bone cell function, Biomaterials. 20 (1999) 2287–2303.

[124] K. de Groot, Calcium phosphate ceramics: their current status, in: J. Boretos, M. Eden (Eds.), Contemp. Biomater., Noves Publications, 1984: pp. 477–492.

[125] G. Daculsi, Biphasic calcium phosphate concept applied to artificial bone, implant coating and injectable bone substitute, Biomaterials. 19 (1998) 1473–1478.

[126] N. Eliaz, N. Metoki, Calcium phosphate bioceramics: a review of their history, structure, properties, coating technologies and biomedical applications, Materials (Basel). 10 (2017) 334.

[127] J.C. Elliott, Studies in Inorganic Chemistry, Volume 18, Elsevier science, Amsterdam, The Netherlands, 1994.

[128] V.E. Bel'skii, Kinetics of the hydrolysis of phosphate esters, Russ. Chem. Rev. 46 (1977) 828.

[129] Y. Wu, L.L. Hench, J. Du, K.-L. Choy, J. Guo, Preparation of hydroxyapatite fibers by electrospinning technique, J. Am. Ceram. Soc. 87 (2005) 1988–1991. doi:10.1111/j.1151-2916.2004.tb06351.x.

[130] Z. Hou, P. Yang, H. Lian, L. Wang, C. Zhang, C. Li, R. Chai, Z. Cheng, J. Lin, Multifunctional hydroxyapatite nanofibers and microbelts as drug carriers, Chem. A Eur. J. 15 (2009) 6973–6982. doi:10.1002/chem.200900269.

[131] H. Liu, Q. Cai, P. Lian, Z. Fang, S. Duan, The biological properties of carbon nanofibers decorated with β-tricalcium phosphate nanoparticles, Carbon N. Y. 48 (2010) 2266–2272. doi:10.1016/j.carbon.2010.02.042.

[132] R. Faridi-Majidi, N. Nezafati, M. Pazouki, S. Hesaraki, The effect of synthesis parameters on morphology and diameter of electrospun hydroxyapatite nanofibers, J. Aust. Ceram. Soc. 53 (2017) 225–233. doi:10.1007/s41779-017-0028-8.

[133] C. Zhang, H. Li, Z. Guo, B. Xue, C. Zhou, Fabrication of hydroxyapatite nanofiber via electrospinning as a carrier for protein, J. Nanosci. Nanotechnol. 17 (2017) 1018–1024. doi:10.1166/jnn.2017.12620.

[134] T.R. Tadjiev, S. Chun, H. Kim, I. Kang, S. Kim, Preparation and characterization of calcium metaphosphate nanofibers via electrospinning, Key Eng. Mater. 330–332 (2007) 207–210. doi:10.4028/www.scientific.net/KEM.330-332.207.

[135] T.R. Tadjiev, S. Chun, H. Kim, I.K. Kang, S. Kim, Preparation and characterization of beta-tricalcium phosphate nanofibers via electrospinning, ASBM7 Adv. Biomater. VII. 342–343 (2007) 817–820. doi:10.4028/www.scientific.net/KEM.330-332.207.

[136] F.H. Westheimer, S. Huang, F. Covitz, Rates and mechanisms of hydrolysis of esters of phosphorus acid, J. Am. Chem. Soc. 110 (1988) 181–185. doi:10.1021/ja00209a029.

[137] J. Livage, P. Barboux, M.T. Vandenborre, C. Schmutz, F. Taulelle, Sol-gel synthesis of phosphates, J. Non. Cryst. Solids. 147&148 (1992) 18–23.

[138] X. Song, F. Ling, H. Li, Z. Gao, X. Chen, Tuned morphological electrospun hydroxyapatite nanofibers via pH, J. Bionic Eng. 9 (2012) 478–483. doi:10.1016/S1672-6529(11)60143-1.

[139] K. Starbova, E. Krumov, D. Karashanova, N. Starbov, Polyoxyethylene assisted electrospinning of nanofibers from calcium phosphate sol solution, J. Optoelectron. Adv. Mater. 11 (2009) 1319–1322.

[140] Y. Ding, X. Yuan, J. Zhao, W. Guo, X. Wang, Formation of ultrafine apatite fibers by sol-gel/electrospinning, Chem. Res. Chinese. U. 23 (2007) 366–369. doi:10.1016/j.1andurbplan.2006.10.0I2.

[141] A.H. Touny, S.B. Bhaduri, A reactive electrospinning approach for nanoporous PLA/monetite nanocomposite fibers, Mater. Sci. Eng. C. 30 (2010) 1304–1312. doi:10.1016/j.msec.2010.07.015.

[142] G. Cadafalch Gazquez, H. Chen, L. Moroni, B.A. Boukamp, J.E. ten Elshof, β-Tricalcium phosphate nanofiber scaffolds with fine unidirectional grains, Mater. Lett. 208 (2017) 118–121. doi:10.1016/j.matlet.2017.05.038.

[143] T. Chae, H. Yang, F. Ko, T. Troczynski, Bio-inspired dicalcium phosphate anhydrate/poly(lactic acid) nanocomposite fibrous scaffolds for hard tissue regeneration: In situ synthesis and electrospinning, J. Biomed. Mater. Res. - Part A. 102 (2014) 514–522. doi:10.1002/jbm.a.34715.

[144] P.Q. Franco, C.F.C. João, J.C. Silva, J.P. Borges, Electrospun hydroxyapatite fibers from a simple sol-gel system, Mater. Lett. 67 (2012) 233–236. doi:10.1016/j.matlet.2011.09.090.

[145] Z. Yuanyuan, L. Yike, L. Qian, L. Zhongjun, Size control of electrospun hydroxyapatite nanofibers by sol-gel system, J. Nanomater. 13 (2013) 6581–6587. doi:10.1166/jnn.2013.7738.

[146] D. Liu, T. Troczynski, D. Hakimi, Effect of hydrolysis on the phase evolution of water-based sol-gel hydroxyapatite and its application to bioactive coatings, J. Mater. Sci. Mater. Med. 13 (2002) 657–665.

[147] X. Dai, S. Shivkumar, Electrospinning of hydroxyapatite fibrous mats, Mater. Lett. 61 (2007) 2735–2738. doi:10.1016/j.matlet.2006.07.195.

[148] M. Streckova, T. Sopcak, R. Stulajterova, M. Giretova, L. Medvecky, A. Kovalcikova, Needle-less electrospinning employed for calcium and magnesium phosphate coatings on titanium substrates, Surf. Coat. Technol. 340 (2018) 177–189. doi:10.1016/j.surfcoat.2018.02.063.

[149] J.H. Lee, Y.J. Kim, Hydroxyapatite nanofibers fabricated through electrospinning and sol-gel process, Ceram. Int. 40 (2014) 3361–3369. doi:10.1016/j.ceramint.2013.09.096.

[150] H.W. Kim, H.E. Kim, Nanofiber generation of hydroxyapatite and fluor-hydroxyapatite bioceramics, J. Biomed. Mater. Res. - Part B Appl. Biomater. 77 (2006) 323–328. doi:10.1002/jbm.b.30376.

[151] A. Beganskien, O. Dudko, R. Sirutkaitis, R. Giraitis, Water based sol-gel synthesis of hydroxyapatite, Mater. Sci. 9 (2003) 383–386.

[152] D. Liu, T. Troczynski, W.J. Tseng, Water-based sol-gel synthesis of hydroxyapatite: process development, Biomaterials. 22 (2001) 1721–1730.

[153] X. Dai, S. Shivkumar, Electrospinning of PVA-calcium phosphate sol precursors for the production of fibrous hydroxyapatite, J. Am. Ceram. Soc. 90 (2007) 1412–1419. doi:10.1111/j.1551-2916.2007.01569.x.

[154] T. Sebastian, T.R. Preisker, L. Gorjan, T. Graule, C.G. Aneziris, F.J. Clemens, Synthesis of hydroxyapatite fibers using electrospinning: A study of phase evolution based on polymer matrix, J. Eur. Ceram. Soc. 40 (2020) 2489–2496. doi:10.1016/j.jeurceramsoc.2020.01.070.

[155] L.-L. Tseng, C.-M. Ho, W.-Z. Liang, Y.-D. Hsieh, C.-R. Jan, Comparison of efficacies of different bone substitutes adhered to osteoblasts with and without extracellular matrix proteins, J. Dent. Sci. 8 (2013) 399–404.

[156] M. Bohner, B.L.G. Santoni, N. Döbelin, β-tricalcium phosphate for bone substitution: synthesis and properties, Acta Biomater. (2020). doi:10.1016/j.actbio.2020.06.022.

[157] E. Champion, Sintering of calcium phosphate bioceramics, Acta Biomater. 9 (2013) 5855–5875.

[158] F. Tamimi, J. Torres, C. Kathan, R. Baca, C. Clement, L. Blanco, E. Lopez Cabarcos, Bone regeneration in rabbit calvaria with novel monetite granules, J. Biomater. Res. Part A. 87 (2008) 980–985. doi:0.1002/jbm.a.31842.

[159] D.P. Bhattarai, L.E. Aguilar, C.H. Park, C.S. Kim, A review on properties of natural and synthetic based electrospun fibrous materials for bone tissue engineering, Membranes (Basel). 8 (2018). doi:10.3390/membranes8030062.

[160] K. Whang, D.R. Elenz, E.K. Nam, D.C. Tsai, C.H. Thomas, G.W. Nuber, F.H. Glorieux, R. Travers, S.M. Sprague, K.E. Healy, Engineering bone regeneration with bioabsorbable scaffolds with novel microarchitecture, Tissue Eng. 5 (1999) 35–51. doi:10.1089/ten.1999.5.35.

[161] J.R. Porter, T.T. Ruckh, K.C. Popat, Bone tissue engineering: A review in bone biomimetics and drug delivery strategies, Biotechnol. Prog. 25 (2009) 1539–1560. doi:10.1002/btpr.246.

[162] J. Soulié, Synthèse par voie sol-gel et réactivité in vitro de verres bioactifs dopés, mésostructurés et macrostructurés. Caractérisation par micro-faisceaux d'ions, Université Clermont II - Blaise Pascal, 2011.

[163] S. Samavedi, A.R. Whittington, A.S. Goldstein, Calcium phosphate ceramics in bone tissue engineering: A review of properties and their influence on cell behavior, Acta Biomater. 9 (2013) 8037–8045. doi:10.1016/j.actbio.2013.06.014.

[164] S. Chahal, A. Kumar, F.S.J. Hussian, Development of biomimetic electrospun polymeric biomaterials for bone tissue engineering. A review, J. Biomater. Sci. Polym. Ed. 30 (2019) 1308–1355. doi:10.1080/09205063.2019.1630699.

[165] P. Chocholata, V. Kulda, V. Babuska, Fabrication of scaffolds for bone-tissue regeneration, Materials (Basel). 12 (2019). doi:10.3390/ma12040568.

[166] G. Chiara, F. Letizia, F. Lorenzo, S. Edoardo, S. Diego, S. Stefano, B. Eriberto, Z. Barbara, Nanostructured biomaterials for tissue engineered bone tissue reconstruction, Int. J. Mol. Sci. 13 (2012) 737–757. doi:10.3390/ijms13010737.

[167] L. Roseti, V. Parisi, M. Petretta, C. Cavallo, G. Desando, I. Bartolotti, B. Grigolo, Scaffolds for Bone Tissue Engineering: State of the art and new perspectives, Mater. Sci. Eng. C. 78 (2017) 1246–1262. doi:10.1016/j.msec.2017.05.017.

[168] A. Wubneh, E.K. Tsekoura, C. Ayranci, H. Uludağ, Current state of fabrication technologies and materials for bone tissue engineering, Acta Biomater. 80 (2018). doi:10.1016/j.actbio.2018.09.031.

[169] L. Bourdon, J. Maurin, K. Gritsch, A. Brioude, V. Salles, Improvements in resolution of additive manufacturing: advances in two-photon polymerization and direct-writing electrospinning techniques, ACS Biomater. Sci. Eng. 4 (2018) 3927–3938. doi:10.1021/acsbiomaterials.8b00810.

[170] F. Donnaloja, E. Jacchetti, M. Soncini, M.T. Raimondi, Natural and synthetic polymers for bone scaffolds optimization, Polymers (Basel). 12 (2020). doi:10.3390/POLYM12040905.

[171] Q. Chen, C. Zhu, G.A. Thouas, Progress and challenges in biomaterials used for bone tissue engineering: bioactive glasses and elastomeric composites, Prog. Biomater. 1 (2012). doi:10.1186/2194-0517-1-2.

[172] M.I. Sabir, X. Xu, L. Li, A review on biodegradable polymeric materials for bone tissue engineering applications, J. Mater. Sci. 44 (2009) 5713–5724. doi:10.1007/s10853-009-3770-7.

[173] A. El-Ghannam, Bone reconstruction: From bioceramics to tissue engineering, Expert Rev. Med. Devices. 2 (2005) 87–101. doi:10.1586/17434440.2.1.87.